



Calhoun: The NPS Institutional Archive
DSpace Repository

Theses and Dissertations

1. Thesis and Dissertation Collection, all items

1972

Statistical study of sound speed in the inhomogenous upper ocean

Fitzgerald, James Richard

Monterey, California. Naval Postgraduate School

<http://hdl.handle.net/10945/16369>

This publication is a work of the U.S. Government as defined in Title 17, United States Code, Section 101. Copyright protection is not available for this work in the United States.

Downloaded from NPS Archive: Calhoun



Calhoun is the Naval Postgraduate School's public access digital repository for research materials and institutional publications created by the NPS community. Calhoun is named for Professor of Mathematics Guy K. Calhoun, NPS's first appointed -- and published -- scholarly author.

Dudley Knox Library / Naval Postgraduate School
411 Dyer Road / 1 University Circle
Monterey, California USA 93943

<http://www.nps.edu/library>

STATISTICAL STUDY OF SOUND SPEED
IN THE INHOMOGENEOUS UPPER OCEAN

James Richard Fitzgerald

NAVAL POSTGRADUATE SCHOOL

Monterey, California



THESIS

STATISTICAL STUDY OF SOUND SPEED
IN THE INHOMOGENEOUS UPPER OCEAN

by

James Richard Fitzgerald

Thesis Advisor:

H. Medwin

December 1972

Approved for public release; distribution unlimited.

T149567

LIBRARY
NAVAL POSTGRADUATE SCHOOL
MONTEREY, CALIF. 93940

Statistical Study of Sound Speed
in the Inhomogeneous Upper Ocean

by

James Richard Fitzgerald
Lieutenant Commander, United States Navy
B.S. B.A., University of Florida, 1962

Submitted in partial fulfillment of the
requirements for the degree of

MASTER OF SCIENCE IN ENGINEERING ACOUSTICS

from the
NAVAL POSTGRADUATE SCHOOL
December 1972

ABSTRACT

The statistics of the fluctuations of the in-situ speed of sound in the upper ocean have been studied by analyzing the instantaneous phase difference of the output of two hydrophones separated by one meter for sounds of frequency 15 to 151 kHz. The experiment was conducted at 11 ft in water of depth 60 ft in low sea states at night. Comparison of the speed calculated from the time averaged phase difference, with the speed given by velocimeter or empirical relations, yielded differential speeds which deviate by 1 m/sec to 8 m/sec from the accepted values, for frequencies less than 100 kHz. Correlation and spectral analysis of the sound phase and ocean height fluctuations has shown the close relation between these two parameters. There is strong evidence of the presence and importance of bubbles in all of the results, particularly of a large population resonant in the frequency range 56.3 to 71.1 kHz (radius 50 to 60 microns). Evidence is presented to suggest that bubbles appear at the surface during internal wave activity at lower depths and that for sound frequencies near the bubble resonances the sound phase is strongly modulated by, and in phase with, the ocean wave height.

TABLE OF CONTENTS

I.	INTRODUCTION-----	5
II.	INSTRUMENTATION-----	7
III.	OCEANOGRAPHIC COMPONENTS-----	11
IV.	EXPERIMENTAL SETUP-----	12
V.	DATA REDUCTION-----	14
VI.	COMPUTATIONAL METHOD-----	17
VII.	DISPERSION THEORY-----	19
VIII.	EXPERIMENTAL RESULTS-----	22
	A. DIFFERENTIAL SPEED OF SOUND-----	25
	B. OTHER STATISTICAL ANALYSES-----	31
	1. Probability Density Functions-----	31
	2. Correlation Functions-----	32
	3. Spectral Analysis-----	37
IX.	SUMMARY AND CONCLUSIONS-----	83
	APPENDIX A: PRESENTATION OF DATA-----	85
	COMPUTER PROGRAM 1-----	92
	COMPUTER PROGRAM 2-----	97
	COMPUTER PROGRAM 3-----	102
	COMPUTER PROGRAM 4-----	115
	BIBLIOGRAPHY-----	126
	INITIAL DISTRIBUTION LIST-----	127
	FORM DD 1473-----	129

ACKNOWLEDGMENTS

The writer wishes to express his gratitude to Professor Herman Medwin, of the Department of Physics and Chemistry, Naval Post-graduate School, for his guidance and assistance in this research work. Special thanks are also due to Mr. William Smith of NPS for his help in the construction and acquisition of equipment, and Dr. John C. Calhoun, formerly of NPS, for his assistance in computer programs 1, 2 and 3.

The writer also wishes to express thanks to the personnel of the U.S. Navy Undersea Research and Development Center for their support.

This thesis serves also as a technical report to Naval Ships systems Command (Code PMS 302) which provided the major part of the financial support for the facilities, technician, and computer services required for this research.

I. INTRODUCTION

The objective of this research was to measure acoustic phase shifts over a one meter path in order to study the statistics of the variation of sound speed with frequency and time in the upper layer of the ocean.

The sources of the dispersion of sound speed are bubbles of various radii. Motion of these bubbles and of other inhomogenieties cause the temporal fluctuations of phase.

Study of the dispersive behavior is important because in the top tens of meters of the ocean, the speed of sound at military frequencies differs both from the value given by velocimeters (which operate in the megahertz range) and that given by the various accepted empirical formulas. Study of the fluctuations is necessary in order to reveal the oceanographic origins and dependencies of the temporal variations in sonar surface duct propagation.

The bubble problem has been treated theoretically by Meyer and Skudrzyk (1950), Devin (1959) and Albers (1960). The experimental study of wind generated bubbles has been conducted in the laboratory by Glotov (1962) and at sea by Buxcey et al (1965) and Medwin (1970). Most recently Rautmann (1971) measured the magnitude of dispersion and fluctuation of sound speed in the surface layer of the ocean.

Change in the speed of sound with frequency in sea water is attributable in general either to molecular relaxation or bubbles since no other frequency dependent mechanisms

are known to exist at the frequencies of this study. The magnitude of the molecular relaxation can be shown to be negligible as compared to the bubble effects (a frequency shift from 20 to 70 kHz results in a Δc of only approximately 0.3 m/sec).

The research was conducted using the U.S. Naval Undersea Research and Development Center (NUC) Oceanographic Research Tower in Mission Bay, San Diego, as a test platform.

II. INSTRUMENTATION

An aluminum pipe frame of height six feet and length twelve feet was used to mount the transducers and hydrophones (Figure 1). To prevent displacement of the hydrophones, the frame wires were put under tension by spring loaded mounts. To minimize reflections from the frame caused by side-lobes of the transducers, the frame was pulse-echo checked; various segments of the frame were covered with acoustic absorbent rubber (SOAB) so that the echo was down 35 dB below the direct signal.

Opposite to the open end of the frame, at the center, and pointing in the X-direction, an USNRD F33 unidirectional transducer was mounted. On the acoustic axis of this transducer, two Atlantic Research LC-10 hydrophones were placed. The first LC-10 was mounted 82.3 cm from the source and the second was mounted 81.3 cm beyond the first.

The transmitting instrumentation (Figure 2) consisted of a General Radio Coherent Decade Frequency Synthesizer, type 1162-A, generating a stable sinusoidal voltage output of two volts rms and variable in frequency. The signal was amplified by a Hewlett Packard Power Amplifier, 467A, to 18 volts rms and then impressed across the transducer.

The receiving instrumentation (Figure 2) consisted of LC-10 #1 with a flat ($-108 \text{ dB} \pm 2 \text{ dB re 1 volt/microbar}$) receiving response from 15 kHz to 150 kHz, and LC-10 #2 with a flat ($-110 \text{ dB} \pm 3 \text{ dB re 1 volt/microbar}$) receiving response from 15 kHz to 150 kHz. The signals were then amplified 30 dB by an NUS

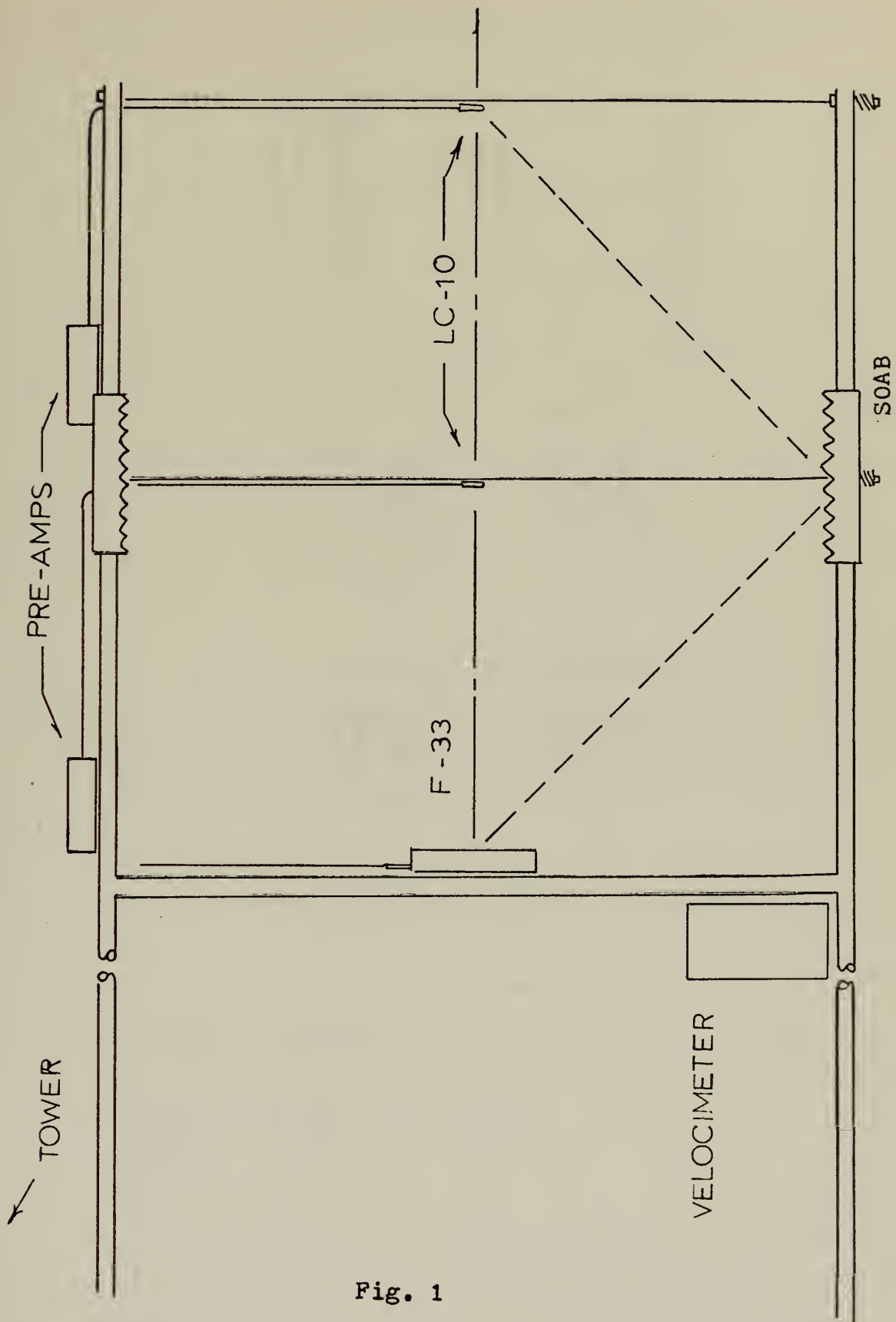


Fig. 1

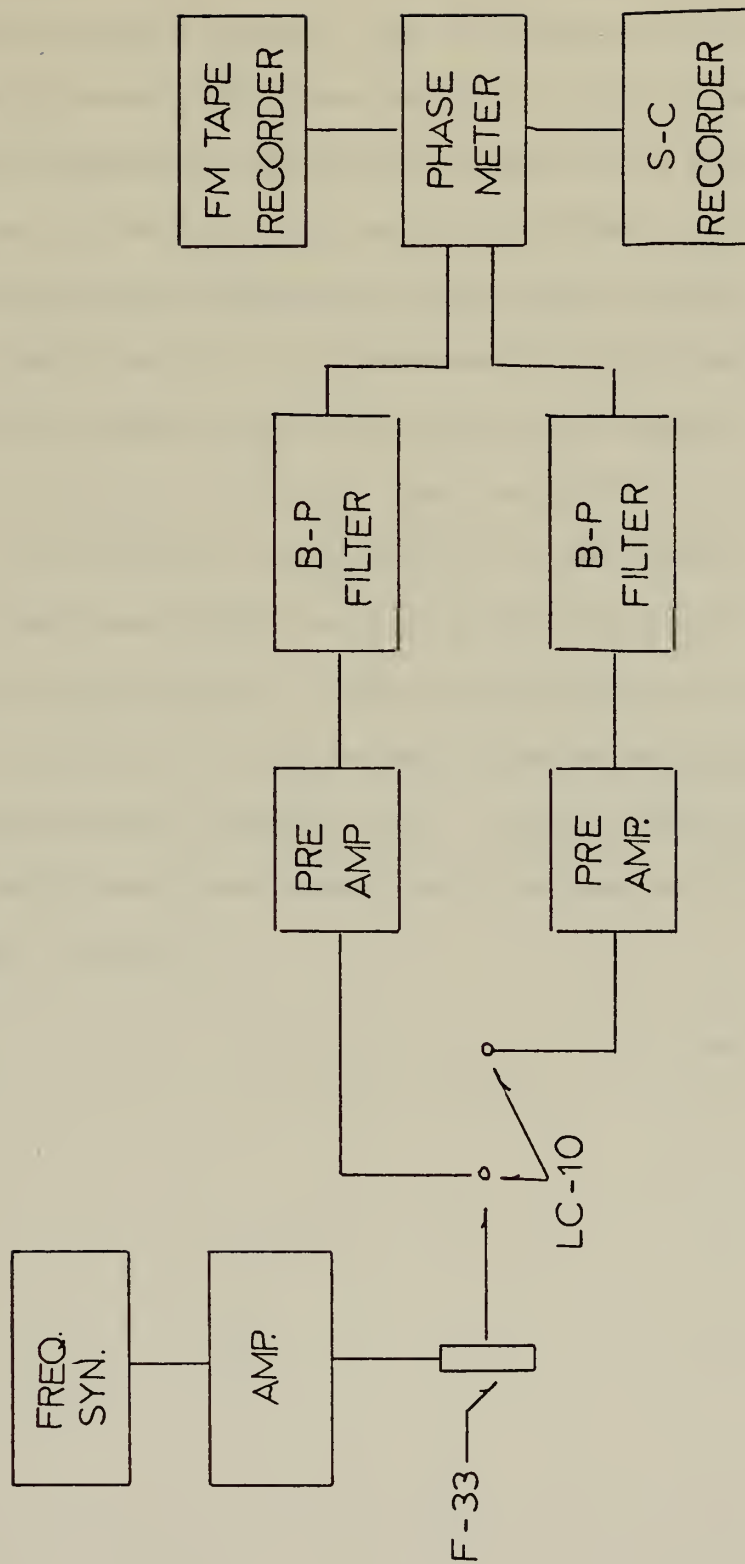


Fig. 2

pre-amplifier model 2010-030 before passing through 150 feet of waterproof shielded cable. Both signals were then bandpass filtered by a digitally tuned variable Krohn-Hite model 3322 Filter set with the center frequency equal to the transmitted frequency \pm 300 Hz. The filtered signals were then fed into a Dranetz model 305 Phase Meter. The phasemeter measured the phase angle between the two ac voltages at the same frequency and provided a dc voltage output proportional to the difference of the phase angles at 10 mV per degree. The dc voltage was simultaneously FM recorded on a Precision Instrument model 6200, eight track magnetic tape recorder at 3.75 i.p.s. and on a Brush model 220 strip chart recorder, at 10 mV per division and 1 mm per second.

The ocean wave height was measured utilizing the installed NUC Baylor wave height gauge. The wave height gauge was mounted a distance of 6 feet from the acoustic source and at an angle of 60 degrees from the acoustic axis. The dc voltage output was FM recorded with each phase record and simultaneously recorded on the strip chart recorder.

III. OCEANOGRAPHIC COMPONENTS

Field measurements were simultaneously taken to determine the fluctuations of temperature, salinity, water particle velocity and wave height to obtain a better understanding of the acoustic-ocean interaction (theses by CDR J. Gossner, LT M. Whittemore, LT W. Frigge and LT R. Krapole, March 1973).

Unfortunately much of this information is unavailable at this time. However, the time-varying ocean wave height, (NUC Baylor Gauge), the sound velocimeter output, (Ramsey Probe), and temperature (Ramsey Probe) were simultaneously recorded during the phase study. The average value of salinity ($33.8^{\circ}/\text{oo}$) measured that afternoon was used for the C calculations on the assumption that changes in salinity would have a minimal effect on C.

IV. EXPERIMENTAL SETUP

The frequency of the continuous wave signal applied to the transducer was adjusted by means of the frequency synthesizer until a phase angle of approximately 20 degrees was obtained. This value was selected to prevent the possibility of the phase going negative and changing the integral number of wave lengths between the hydrophones. Since the phase meter compares the signal at input B with respect to the signal at input A, and cannot detect integral numbers of wave lengths difference between the two signals, the displayed phase determines the fractional wave length by which signal B leads signal A. This means an integral number of wave lengths plus a fractional part fits into the separation distance between the two hydrophones. Increasing the frequency will change the phase by 360 degrees or step the integral number of wave lengths by one.

Because it was desired to study the statistics of the speed of sound as a function of frequency over a range most likely to contain resonant bubbles, the frequency range from 15-150 kHz was examined. The 81.3 cm separation between the two hydrophones caused the number of wave lengths within the spacing to be incremented by one approximately every two kHz.

In order to exclude possible errors in the results due to non-stationarity in the medium, it was necessary to examine the total frequency range in as short a period of time as possible. The frequency range was examined in steps of four kHz, and the

time variable phase difference and wave height were recorded between the hydrophones for four minutes at each frequency.

All the readings were taken within three consecutive hours, from 1900 to 2200 hours on June 5, 1972 at an initial transducer depth of 3.4 meters, and final depth of 2.8 meters. The tide during this period was falling at a rate of 0.5 ft/hr, with low water at approximately 2330.

V. DATA REDUCTION

Thirty-four four minute individual physical records make up the analog recorded sound phase and wave height data. One approach used was to digitize the analog data and use a computer to carry out the statistical and spectral analysis.

The recorded data were digitized using the NPS CDC 5000 and SDS 9300 computers. The initial sampling frequency was 50 Hz giving a Nyquist frequency of 25 Hz. The sampling interval was 0.02 seconds. The 7 track digital tape was then processed to remove spurious signals (Figure 3), scaled, and converted using the IBM 360/67 from 7 track octal to 9 track hexadecimal for use by the IBM 360/67, (computer program 1).

The samples generated, however, by using the 50 Hz sampling rate provided too much data to analyze to the degree of resolution required in any reasonable processing time on the IBM 360. It was then determined to reduce the rate to 6.25 Hz, a sampling interval of 0.16 seconds, and frequency resolution of 0.0244 Hz. This yielded 10 degrees of freedom. This also reduced the amount of each physical record that could be analyzed from 3 minutes 50 seconds to 3 minutes 40 seconds.

A second approach was essential in order to obtain statistics of the average and standard deviation which would be a measure of the microstructure rather than of the microstructure plus the internal wave. To minimize the effect of internal waves each record was analyzed in 30.72 second increments. Each increment



Raw (bottom) and filtered (top) signals (note: Amplitude scales are not equal)

Figure 3

consisted of 1536 samples for which instantaneous values of the velocity of sound were calculated and the means and standard deviation were determined. Similarly the mean value and standard deviation of the phase were computed, (computer program 2).

The speed of the coherent component was also calculated using the mean value of the phase and compared to the mean value of the speed. The point being made is that, if the mean of the entire physical record had been used, the large variance would have been relative to a mean value strongly influenced by the passage of any internal waves and not due to the microstructure of the medium as desired. The mean speed and the mean coherent speed of sound were then compared with the 30 second average values given by a Ramsey Velocimeter and those calculated by empirical formulas using the salinity, depth, and 30 second averages of the temperature.

For selected frequency runs, the temporal autocorrelations and power spectra, in dB re degrees, or dB re cm, of the phase and wave height were computed and plotted using a maximum time lag of 40.96 seconds. The temporal cross-correlation was also computed. From this the cross spectrum, coherence, and cross spectral phase angle were computed, (computer programs 3 and 4). The selected frequencies for which these were calculated were determined by first calculating and plotting the dispersion curve (Figure 4), and then selecting those frequencies of interest from the results.

VI. COMPUTATIONAL METHOD

The computational method for determination of the speed of sound using the phase difference was the same as that used by Rautmann (Dec. 1971) and is included here for information.

Since a continuous wave method was used, the signal received by the first hydrophone can be written as:

$$y_A = a \sin (\omega t)$$

and the signal received by the second hydrophone is:

$$y_B = b \sin (\omega t - kx)$$

where

$$k = \text{the wave number} = \frac{\omega}{C} = \frac{2\pi f}{C}$$

f = the frequency of the applied signal

C = the phase wave velocity

x = the separation between the hydrophones.

Since we compare the two signals with respect to phase by using the digital phase meter we have to find values for which

$$kx = \psi$$

where ψ is the total phase difference between the two signals due to an integral number of wave lengths and a fraction of the wave length. This is written as:

$$kx = (2\pi)n + \phi_r \qquad n = \text{an integer}$$

$$kx = \frac{\omega}{C} x = (2\pi)n + \phi_r \qquad \phi_r \text{ in radians}$$

$$C = \frac{\omega x}{(2\pi)n + \phi_r} .$$

The final result is:

$$C = \frac{fx}{n + \frac{\phi}{360}} \quad \text{where } \phi \text{ is in degrees.}$$

The integer n can be pre-estimated by calculating C from Wilson's equation using the known values of the temperature and salinity.

Therefore the instantaneous speed of sound may be obtained by using the measured frequency separation and whole number of wavelengths at which a residual phase difference is noted.

The value for the speed of sound of the coherent component is defined to be:

$$C_{\text{coh}} = \frac{fx}{n + \frac{\langle \phi \rangle}{360}} \quad \text{where } \langle \phi \rangle \text{ is the mean value of the phase.}$$

VII. DISPERSION THEORY

The following equation relates bubble size to the speed of sound and therefore shows the dispersion for a bubble population of unique radius R .

$$C = \left[\frac{1}{C_o} + \frac{3C_o}{2\omega^2} \frac{U(R)dR}{R^2} \frac{\left[\left(\frac{\omega_o}{\omega} \right)^2 - 1 \right]}{\left[\left(\frac{\omega_o}{\omega} \right)^2 - 1 \right] + \delta^2 \left(\frac{\omega_o}{\omega} \right)^2} \right]^{-1}$$

C_o = nondispersive sound speed

ω = sound frequency

$[U(R)dR]$ = fractional air to water volume for the increment between R and $R + dR$

ω_o = resonant frequency of bubble of radius R

δ = damping constant of bubble of radius R .

A typical dispersion (differential sound speed) curve is shown below. A graph of the variance of C due to a fluctuation of the number of bubbles for a single size bubble as studied by Professor P.C.C. Wang (personal communication) would be M-shaped. In addition, a constant number of bubbles of changing radius (say, due to changing pressure) would create a variance of C which should peak at the mean resonant frequency f_o , as shown by the dashed curve.

A mixed bubble population would have the same equation summed over all of the bubble radii. The various concentrations of bubbles of different resonant frequencies in the ocean would cause combinations of graphs such as shown on the following page. The

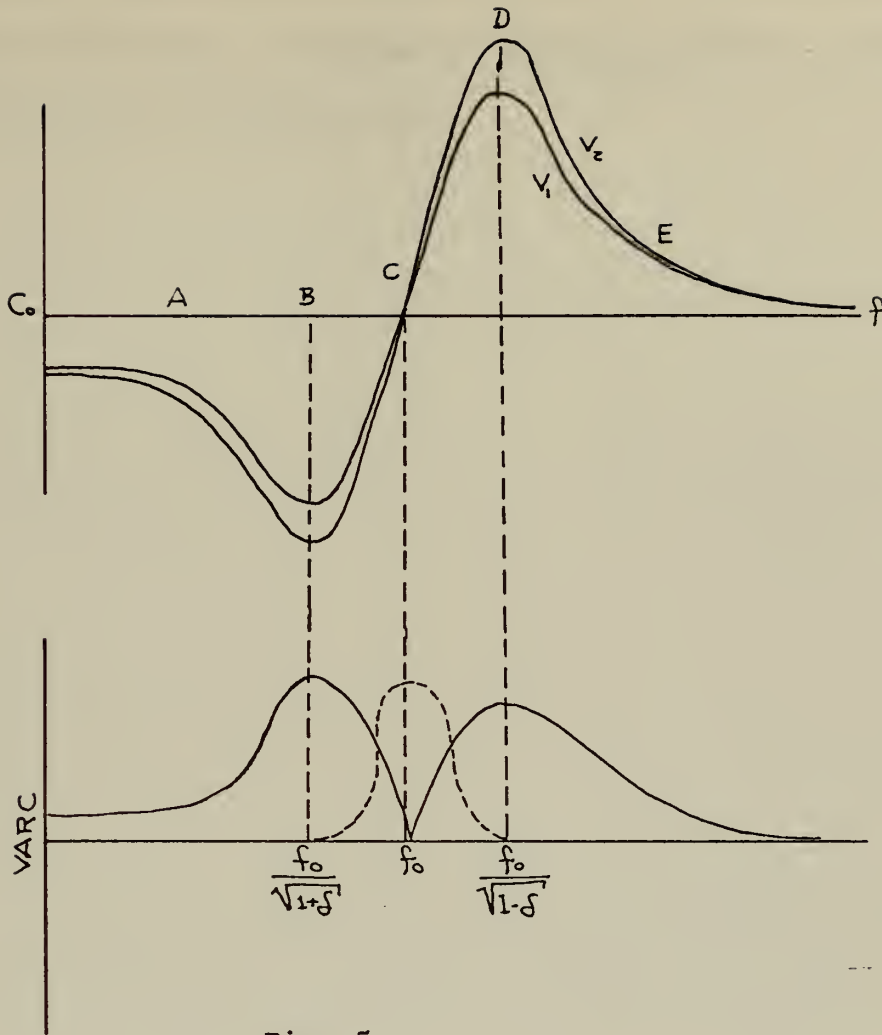


Fig. 5

where f_0 = mean resonance frequency of bubble

V_1 = small bubble density

V_2 = large bubble density

δ = damping constant of bubble

Var C = variance of speed of sound due to fluctuation of the number of bubbles

Five distinctive regions of the simple case shown are identified for future use:

Region A: low variance, small negative differential speed

Region B: maximum variance, maximum negative differential speed

Region C: large variance, minimum differential speed

Region D: large variance, maximum positive differential speed

Region E: low variance, small positive differential speed.

differential sound speed and the variance of the sound speed are studied as functions of frequency in order to deduce the bubble concentrations of various sizes.

VIII. EXPERIMENTAL RESULTS

The frequency run was conducted at a depth of 3.4 meters at 1900 decreasing to 2.8 meters by 2200. The run covered a total frequency range of 15 kHz to 151 kHz in steps of approximately 4 kHz.

Continuous direct recordings of temperature and sound velocity were taken throughout the frequency run by a Ramsey Velocimeter. Because of the internal wave presence, Ramsey velocities and temperatures were averaged over 31 second segments for comparison with the speed of sound measured by the phase method in the same interval. During that same interval, calculations of the empirical values of the speed of sound were done using both the generally accepted Wilson's equation [1] and the more recently proposed Leroy's equation [2]. Both methods yielded results within 0.1 m/sec over the range of physical parameters of the experiment (see Table I).

Wilson's equation was used in the following form:

$$\begin{aligned} C = & 1449.14000 + 4.57210(T) - 0.04453T^2 - 0.00026T^3 \\ & + 0.00001T^4 + 1.39799(S-35.0) + 0.00169(S-35.0)^2 \\ & + 0.06240 + (S-35.0)(-0.01244T). \end{aligned}$$

Leroy's equation was used in the following form:

$$\begin{aligned} C = & 1492.9000 + 3(T-10.0) - 0.00600(T-10.0)^2 - 0.04000 \\ & (T-18.0)^2 + 1.20000(S-35.0) - 0.01000(T-18.0)(S-35.0) \\ & + Z/61.0 + 0.1RHO^2 + 0.00020RHO^2(T-18.0)^2 + 0.10000RHO \\ & (\theta/90.0) + 2.0/(10.0)^7(T)(T-10.0)^4 \end{aligned}$$

where in the equations:

C = speed of sound in meters per second

T = temperature in degrees centigrade

S = salinity in parts per thousand

D = Z = depth in meters

θ = latitude

$\text{RHO} = Z/1000$.

The Leroy equation bubble free values were used as the reference for the differential speed of sound curve (Figure 4). The multi-peaked differential sound speed curve suggests several different bubble concentrations of different resonant frequencies. Therefore, the curve was studied and the following frequencies were selected for analysis:

TABLE II: Selected Frequencies

<u>Frequency (kHz)</u>	<u>Reason for Selection</u>
14.79	minimum speed, lowest frequency
18.78	maximum speed, low frequency
26.17	possible zero dispersion frequency
41.32	maximum speed
56.25	possibly near the zero dispersion frequency
63.79	maximum speed
71.13	minimum speed
89.90	minimum speed at higher frequency
112.52	minimum speed at higher frequency
123.72	minimum speed at higher frequency
136.80	minimum speed at higher frequency
146.10	minimum speed at higher frequency

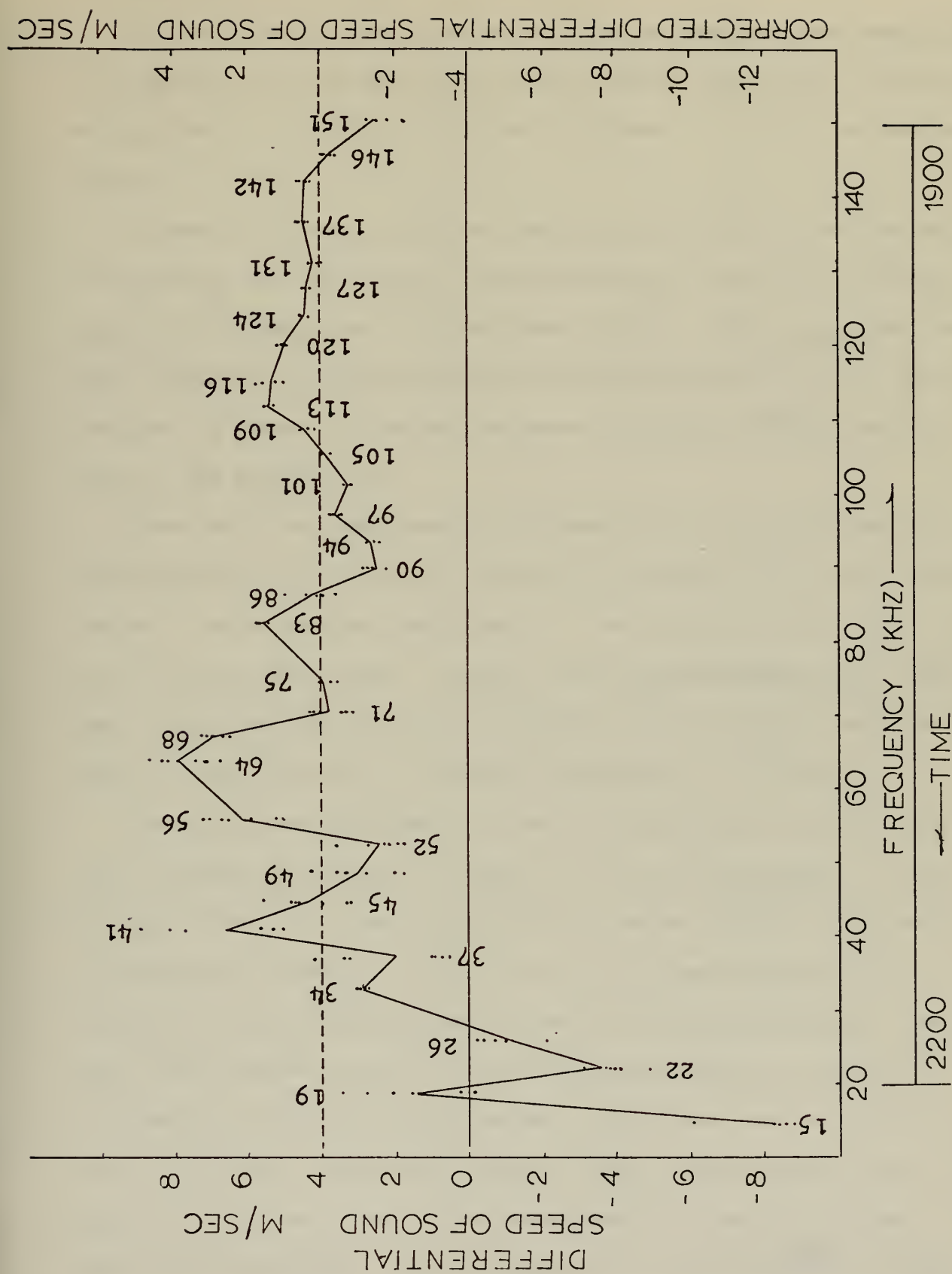


Fig. 4

A. DIFFERENTIAL SPEED OF SOUND AND VARIANCE OF SOUND SPEED AS A FUNCTION OF FREQUENCY

The variation of the speed of sound with frequency was determined by subtracting the values calculated by Leroy's equation (a function of temperature, salinity, depth and latitude) from the experimental values.

At each frequency a pre-run electrical calibration was conducted to determine the phase error correction due to differential phase shifts in the amplifier and band-pass filters. This correction was then algebraically subtracted from the phase measured during the experiment to obtain the corrected phase difference between the signals at the hydrophones.

There were two other sources of possible corrections that were investigated. The first was motion of the medium, such as an onshore current. In a previous experiment, it was determined that there was no dc flow at this point. However, any correction would have been small and would affect only the absolute values and not the relative values. This correction would be independent of frequency.

The second was measurement error in determining the exact distance between the acoustic centers of the two hydrophones. A measurement error of 2.2 mm would yield a 4 m/sec change in the speed of sound at a frequency of 136.80 kHz. This measurement error would affect only the absolute values of the speed of sound. However, the relative values of the differential speed of sound are of interest, not the absolute values. Therefore this correction is not relevant. The dashed line on Figure 4 illustrates the effect on a 2.2 mm error in the measurement of the distance between the hydrophones. It is believed that this probably is close to the correct absolute value as the speed of sound correction

would be small at high frequency. In theory, the bubble effect becomes negligible as the frequency increases (section VII). As the frequency increases, the speed of sound calculated by the phase method asymptotically approaches the values predicted by the Wilson and Leroy equations. This is also the reason the Ramsey velocimeter values agree with the predicted values. The Ramsey Velocimeter operates in the megahertz range, well above any bubble effects.

The speed of sound values were calculated, and the differential sound speed determined, by subtracting the Leroy's equation values from the phase calculated values.

The values obtained from Leroy's equation were in agreement within ± 0.1 m/sec of those obtained from Wilson's equation. The Ramsey velocimeter values were within ± 1 m/sec of both the Leroy and Wilson values. The calculated values from the four methods are included as Table I.

The values are plotted in Figure 4. What are of interest are identifiable bubble concentrations of various size bubbles. The graph is similar to the one presented by Rautmann, based on measurements at the same location in October 21, 1971. Troughs and peaks of speed, presumably bounding a relative zero differential speed and loosely corresponding to the regional identification BCD defined in Figure 5, appear to be present at frequency bands roughly 15-19 kHz, 22-40 kHz, 50-65 kHz, 70-80 kHz, 100-120 kHz. This tentative description will be confronted with other statistical evidence, in sections VIII A and B.

The twelve selected frequencies of Table II. will now be considered in detail:

The frequency 14790 Hz shows a corrected differential sound speed of -12 m/sec. This suggests that this frequency is below the resonant frequency of a large concentration of bubbles. Theory predicts a maximum standard deviation in this frequency range (Region A) caused by bubbles resonant at any higher frequency. The large standard deviation calculated was 1.57 m/sec therefore again suggesting that this frequency is in the range $f < f_0$.

The frequency 18777 Hz shows a corrected differential speed of -2.4 m/sec. If the (-) sign is correct, this would suggest region A of the bulk of bubble population but in region C of a large concentration of resonant bubbles at an f_0 less than 18.9 kHz. If this is true, a batch of large bubbles (radius greater than 200 microns has been identified, which could only have come from the bottom, or which perhaps represent biological entities. The large standard deviation of 0.92 m/sec may show that this fluctuation in f_0 is indeed taking place.

At 26170 Hz, the corrected differential sound speed is -5.7 m/sec. This may imply region B of a large population of bubbles. The standard deviation is large at 0.84 m/sec.

At 41320 Hz the corrected differential sound speed is +2.6 m/sec. The standard deviation is 0.58 m/sec. This value of the standard deviation implies this frequency is above the resonant frequency of a major bubble concentration.

The 56245 Hz record shows strong evidence of a slowly changing speed of sound, such as for an internal wave. The internal wave inferred from phase information reached a phase trough approximately 40 seconds into the 4 minute record. This resulted in

measured instantaneous phase angles on the order of ± 13 degrees, at the beginning of the record, to $+ 25$ degrees at the passage of the peak of the wave. During this period, the values of the instantaneous sound speed measured by our phase difference technique decreased 1.7 m/sec while the Ramsey Velocimeter showed no appreciable change. That this is not clearly reflected in Table I is due to the 31 second intervals, chosen in the attempt to eliminate these effects, over which the means and statistics were computed. More will be said about this apparent discrepancy later. The results here seem to indicate evidence of a resonant bubble population. The corrected differential sound speed is $+ 2$ m/sec and the standard deviation is large at 0.55 m/sec. This large value for the standard deviation may mean this frequency is in or near an f_0 . As in the 18777 Hz record a small fluctuation in f_0 would cause this large σ_c .

The 63790 Hz record has the maximum corrected differential sound speed value of $+ 3.8$ m/sec. The standard deviation is also large, 0.55 m/sec. This may mean that a frequency close to the resonant frequency of a large bubble population.

At 71130 Hz the record shows the largest local value in the standard deviation of the speed, 0.71 m/sec, (Figure 6). If the variance is due to change of number of bubbles it would represent a peak in the standard deviation at $f_0\sqrt{1+\delta}$ or $f_0\sqrt{1-\delta}$. However, if near a concentration of resonant bubbles, whose frequency is changing in Region C, the fluctuations of the surface wave and upper ocean particle velocity may also cause a large variance. It remains then to investigate the correlation functions to interpret

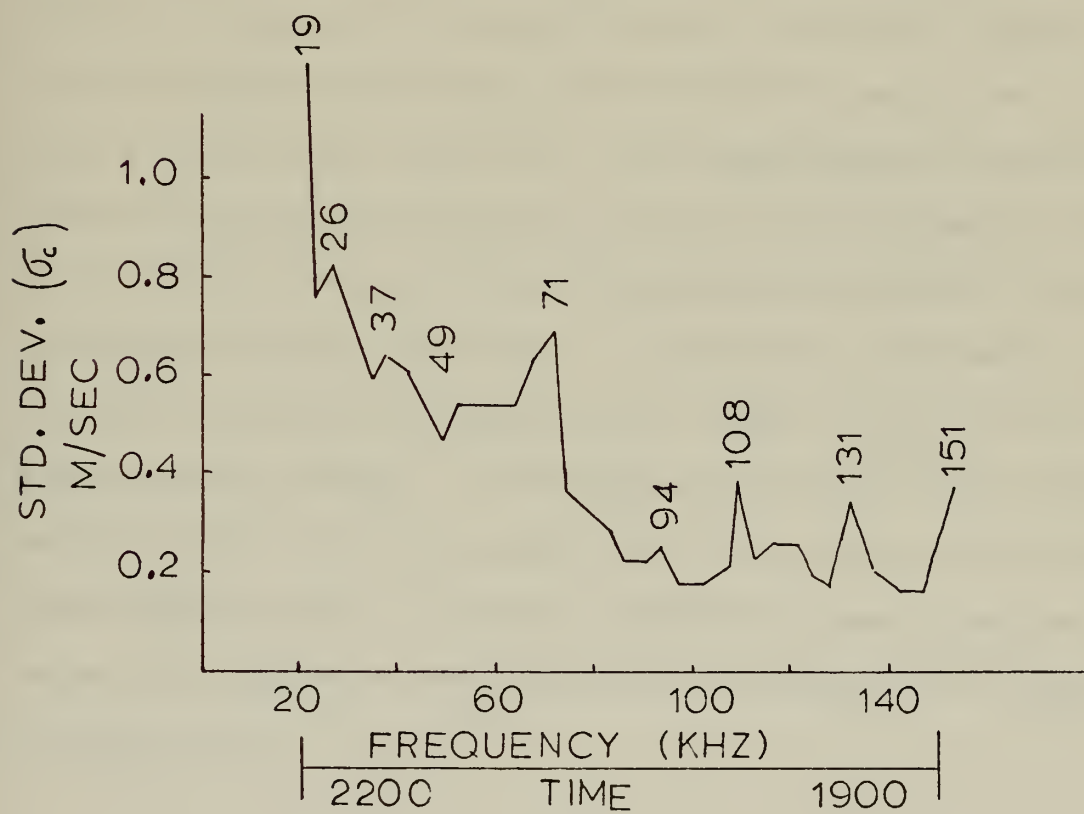
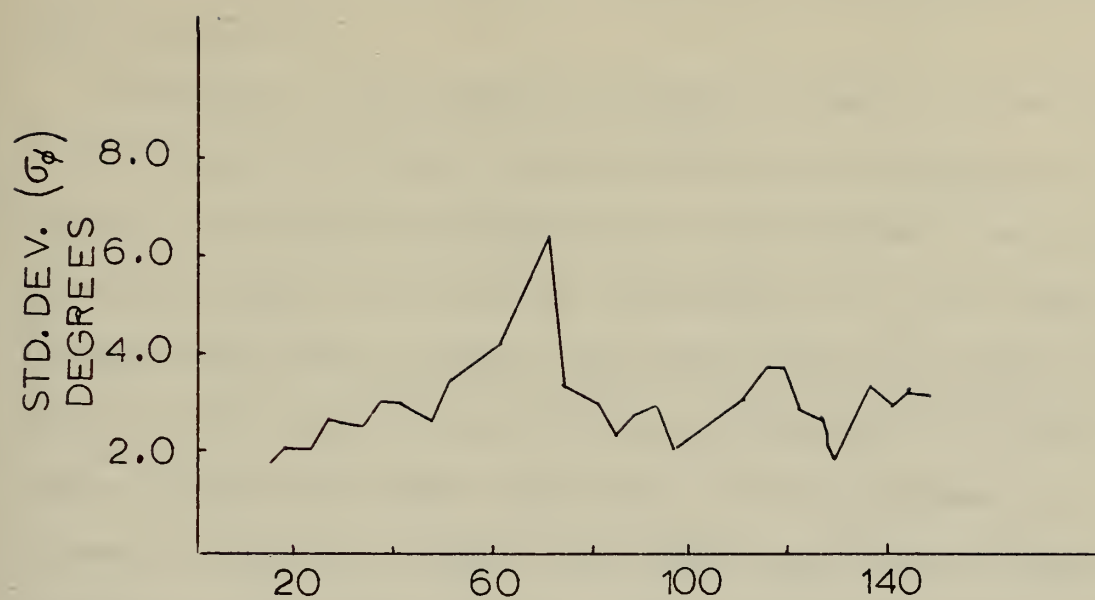


Fig. 6

this record. In any event, since $\delta \approx 0.1$, the peak standard deviation at a frequency is within 5% of the resonance of a large bubble population.

At 89900 Hz, the corrected differential speed of sound is down to -1.4 m/sec and a small standard deviation of 0.28 m/sec. This suggests a resonance above 89.9 kHz. The remaining records at 112519 Hz, 123720 Hz, 136800 Hz, and 146100 Hz all have small standard deviations and small corrected differential sound speed values. This would indicate that these frequencies are above the region of any major bubble populations. As the frequency increases, in theory, the sound speed should approach the empirically predicted or velocimeter values. That the speeds are now reasonably constant in the frequency region 130-150 kHz suggests that the sound speed is approaching this asymptote, perhaps with a small error in the 4 m/sec correction. This suggestion, in the case of the sound speed, is supported by the now slowly increasing value of the variance of the phase as the frequency increases from approximately 100 kHz to 150 kHz. An increase proportional to f^2 is predicted by Chernov (equation 141, page 75, Ref. 5), for a medium without bubbles. At frequencies above 100 kHz, it appears that movement of the sea surface has little effect on the sound phase except insofar as the wave induced well correlated particle velocities underwater move temperature inhomogeneities through the sound path.

B. OTHER STATISTICAL ANALYSES

1. Probability Density Functions

Computer program 2 was used to compute the instantaneous values of the speed of sound and to form histograms for each of the 30.72 second intervals. This allowed interpretation of the speed of sound distribution functions. The predominant pattern of the envelopes followed a Gaussian distribution for the lower of the frequencies. This was expected because in the measurements many weak fluctuations in temperature and salinity would cause small random fluctuation.

In studying the distributions of the selected frequencies, a change is observed at frequencies where the probability of resonant bubble populations were noted. At 14790 Hz the distribution is well defined and sharply Gaussian. At 18777 Hz, 26170 Hz, and 41130 Hz, the shape is still that of a Gaussian distribution but now flatter with wider skirts.

At 56145 Hz, the frequency where clear effects of bubbles were noted, the PDF begins to change the shape of its envelope. The envelope now shows two peaks in the distribution of velocities. Because of the presence of the internal wave it is difficult to determine whether this is predominantly due to the wave effects or the proximity of the resonant bubble population.

The envelope at 63790 Hz also shows this double peaked behavior. This may again be due to the sound frequency being in the proximity of the resonance frequency of a major population of bubbles. The passage of these bubbles back and forth through the acoustic path and their size modulation due to the changes in the

hydrostatic pressure as the wave passes over are suggested as the cause of the non-Gaussian PDF. The PDF's at 71130 Hz also display this same behavior.

The PDF behavior above these frequencies is not clear. At 89900 Hz a double peaked envelope appears in 4 of the 7 segments analyzed. At 112519 Hz the distribution again appears Gaussian. In the remaining 3 records studied, the envelope was not consistent, one segment of a record being Gaussian and the next double peaked. It is less likely that bubbles are important here, which suggests that the velocity distributions at higher sound frequencies are the result of influence by internal waves. Because of the relatively diffuse nature of the data from the 84 PDF graphs, they have not been reproduced here.

2. Correlation Analysis

The temporal autocorrelation function is the normalized temporal autocovariance function, normalized by dividing the autocovariance function by the variance, its maximum value at $\tau = 0$. The temporal autocorrelation function is then:

$$R(\tau) = \frac{\langle x(t)x(t+\tau) \rangle}{\sigma_x^2}.$$

The plots of the autocorrelation functions of the phase and wave height are included as Figures 7 - 18.

Similiarly the temporal crosscorrelation function is the normalized temporal crosscovariance function, normalized by dividing the crosscovariance function by the square root of the product of the maximum values of the two signals. The temporal crosscorrelation function is then:

$$R_c(\tau) = \frac{\langle x(t)y(t+\tau) \rangle}{[\sigma_x^2 \sigma_y^2]^{\frac{1}{2}}}$$

The plots of the crosscorrelation function of the phase with the wave height are included as Figures 19 - 30.

At 14790 Hz (Figure 7) the phase and wave height remain correlated only for approximately the first 3 seconds. The cross-correlation (Figure 19) of the phase with the wave height has a peak to trough value of 0.45, and is good over only a time of approximately 25 seconds. The periodicity of the crosscorrelation, approximately 16 seconds, corresponds to a surface swell and therefore a particle motion through the sound field. The cross-correlation does not peak at $\tau = 0$, which suggests that there is a time lag between those two effects. This time lag could identify transport of bubbles into and out of the sound path and represent the time difference between peak wave height at the wave height probe 6 ft away and the maximum particle velocity of the sound path.

At 18777 Hz (Figure 8) the phase and wave height remain relatively in step. The crosscorrelation (Figure 20) is good for approximately 16 seconds and has a peak to trough value of 0.4. This again suggests a resonant bubble population as implied in the previous discussion of this frequency in Section VIII A.

The 26170 Hz (Figure 9) correlation functions show a phase periodicity on the order of 12 seconds, while the surface wave height periodicity was again 16 seconds. The crosscorrelation (Figure 21) function is not a maximum at $\tau = 0$ but has a high peak to trough value of approximately 0.6.

The 41320 Hz (Figure 10) correlation functions of the phase and wave height are uncorrelated indicating that this

frequency was not at a resonant frequency of a bubble population. The crosscorrelation (Figure 22) has a peak to trough value of only 0.16. There is evidence of good crosscorrelation with an internal wave of periodicity perhaps 200 seconds.

At 56245 Hz (Figure 11) the correlation functions are in step for a time lag up to approximately 28 seconds. Note the peak of crosscorrelation at zero time lag. The crosscorrelation (Figure 23) function has a peak to trough value of 0.6 at the swell average periodicity and also shows the effect of an internal wave. This is strong evidence of a resonant bubble population superimposed on internal wave effects. It was observed previously that the Ramsey Velocimeter showed no evidence of an internal wave at this time. In fact, the phase measurement is so close to the surface, and in the mixed layer, that large temperature changes are not expected. The contradiction can be resolved if it is speculated that bubbles of resonant frequency 56245 Hz were generated in step with the internal wave activity in the thermocline.

The 63790 Hz (Figure 12) record shows a region of bubble concentration is near. The peaks of the phase correlation are mostly in step with the wave height; only the magnitude here differs. However, the phase correlation is not as narrow banded as the wave height and shows some evidence of an internal wave. The wave height displays the same narrow band and magnitude as the previous records. The peak to trough crosscorrelation (Figure 24) value occurs at zero time lag and has now increased to 0.8, the second largest value of the experiment. The double peak in the phase record near 30 seconds shows up here as in the 41320 Hz

functions, and is apparently a component of the sea surface height spectrum. This is verified by observation of the spectrum (Figure 37).

At 71130 Hz (Figure 13) it is found that the temporal correlations of the phase and wave height are of equal narrow band and have the same values at the same lag times. The cross-correlation function (Figure 25) has a peak to trough value of 1 and is in step at $\tau = 0$. This is the strongest evidence that the sound phase is changing in step with the ocean hydrostatic pressure. If the analysis is correct, this means that the phase is increasing and decreasing as the wave height increases and decreases. That is to say, this frequency is at the resonant frequency of a major population of bubbles and the speed is moving up and down the steep portion of the slope of the dispersion curve (Region C) for these prominent bubbles at this frequency.

The correlation functions at 89900 Hz (Figure 14) show that the phase at this frequency is poorly correlated with the wave height. The crosscorrelation function (Figure 26) shows almost no correlation with wave height. There is some evidence of long period correlation with an internal wave. This means that the sound phase is almost undisturbed by the surface wave or the orbital particle motion. This implies this frequency is not near any major resonant bubble population frequencies. Note also the sound phase and surface wave height are no longer in step $\tau = 0$.

The wave height temporal correlation function at 112519 Hz (Figure 15) is particularly simple and that of a narrow band swell. This is a good example of a simple damped cosine auto-correlation function. The phase correlation is poor but shows small peaks

at 7, 12, 19, 28, 32, and possibly 40 seconds. The cross-correlation function (Figure 27) shows very weak correlation between sound phase and wave height. The peak correlation does not occur at $\tau = 0$.

At 123720 Hz (Figure 16) the phase remains correlated with itself longer than the wave height and shows some contribution due to the wave height periodicity at 16 seconds. Additional phase correlation peaks show up at 26 and again possibly 40 seconds. The crosscorrelation (Figure 28) has a relatively strong correlation for approximately 25 seconds. The peak to trough value is 0.65 but it now shows a full 180 degree phase shift between sound phase and wave height. This means that instead of phase increasing with wave height, it decreases. This is interpreted to mean Region E for all bubbles, that is, there are no significant bubbles resonant above this frequency.

In the remaining two records, 136800 Hz (Figure 17) and 146100 Hz, (Figure 18) which were studied for the higher frequency effects, the phase again remains correlated with itself longer than the wave height, that is, it is relatively uninfluenced by wave height. The crosscorrelation has a weak peak to trough value of approximately 0.3. This means again that the phase is relatively undisturbed by the surface waves or that the sound speed is undisturbed by the particle motion. The 136800 Hz phase correlation shows small peaks at 12 and 18 seconds. The 146100 Hz phase correlation shows small peaks at 10 and again at 18 seconds of lag.

The peak-to-trough range of crosscorrelation values (Figures 29, 30) at the swell frequency, constitutes an important

parameter showing the ability of the sound phase to follow the surface wave height (or orbital particle velocity). A curve of this variation with frequency is shown in Figure 31.

3. Spectral Analysis

The power auto-spectral density of the phase and wave height records gives the distribution, in the frequency domain, of average power of the fluctuations vs. frequency. The method used was to compute the autocovariance function and take an FFT and applying a Hamming window. This was done using computer program (3) and yielded plots of phase angle squared and wave height squared vs. frequency in Hz. The frequency resolution is 0.024 Hz. To improve the pictorial representation in amplitude, $10 \log_{10}$ of the ordinate values was taken so that the power spectrum is a power spectrum level¹ in dB re 1 cm².

For all records of the wave height, there is a distinct peak at 0.06 Hz due to the observed ocean swell component, and some smaller peaks up to 0.4 Hz. The peaks up to approximately 0.4 Hz could be due to a smaller wind generated wave superimposed on the larger swell component. The constancy of the spectral characteristics below 0.4 Hz, implies that over the 3 hour duration of the experiment, the ocean was not changing significantly. However, the higher frequencies (above 0.4 Hz) with relatively constant levels are apparently some form of generated noise.

¹An error appears to have slipped into the ordinate of Figures 36, 40, 41, 42. The wave height power levels can be corrected by subtracting 26 dB from these ordinates. The visually observed rms wave height of approximately 2 ft, agrees with this correction.

The phase spectral records are not as consistent as the wave height records. The surface wave component contribution at 0.06 Hz is readily identifiable in all except the 41.3 kHz record. Beyond that, any consistency is not so clear. The phase plots are in relative dB only.

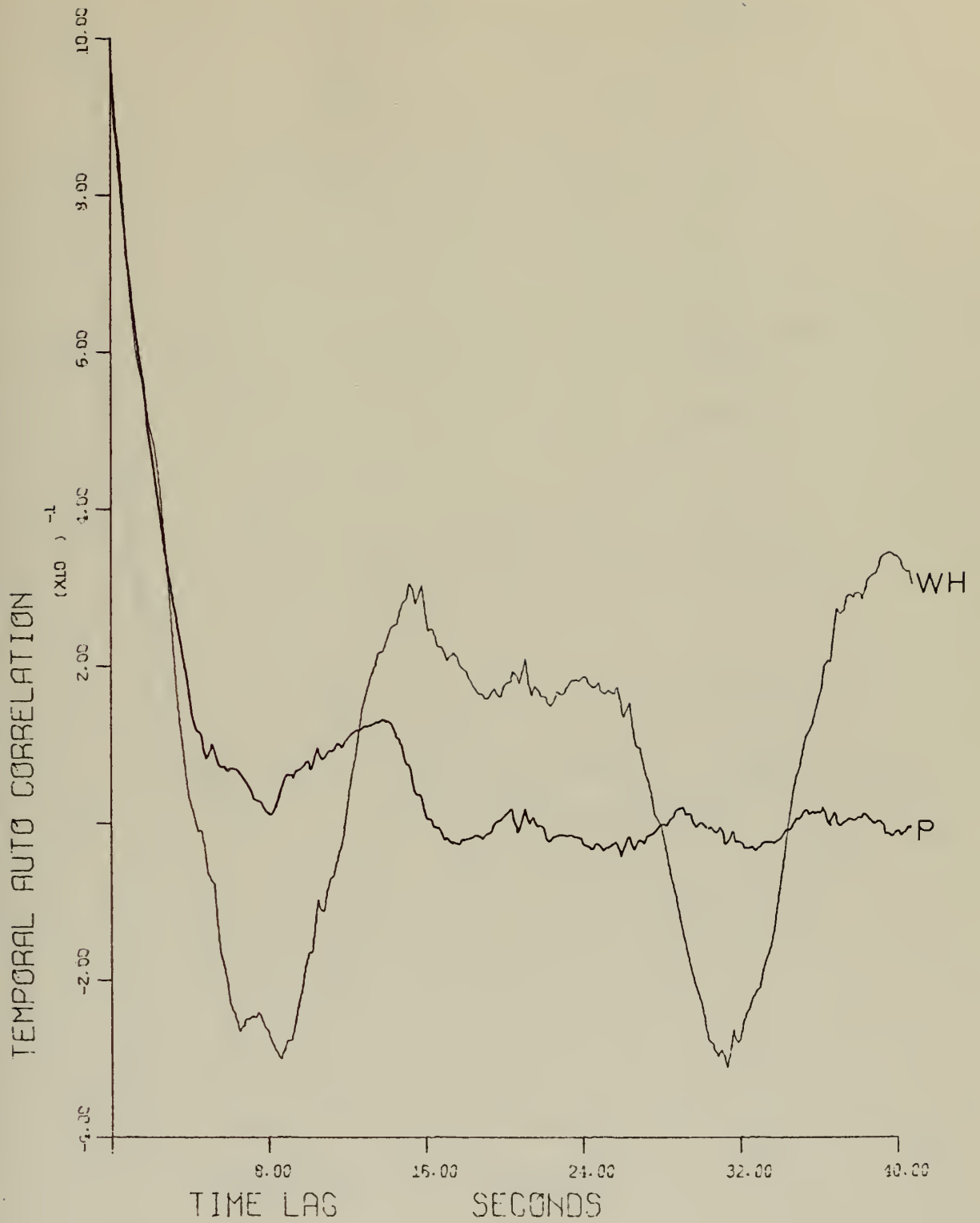
The peak at 0.4 that was observed in all the wave height spectrums was only observed in the lower three frequency phase records analyzed. The 0.4 Hz peak was again probably a surface wave component. In the vicinity of bubble population effects, this frequency could not be identified.

The coherence and cross spectral phase angle is computed (computer program 4) by taking the Fourier Transform of the cross-covariance function and finding the cross-spectral density using a Parzen lag window. This yields a real part; the co-spectrum, and an imaginary part; the quad-spectrum. The magnitude is then the square root of the sum of the squares of the co and quad-spectra. The square of the magnitude is then divided by the product of the individual spectral densities to yield the coherence function. The values so obtained range from -1 to +1. The cross spectral phase angle is found by taking the arctangent of the quotient of the quad-spectrum with the co-spectrum. The maximum values are then ± 180 degrees. Interpretation of these functions is such that for a high coherence value, a value of the relative phase lead, or lag between the two signals, can be obtained.

An overview shows, that at frequencies above and below the three frequencies studied where a strong possibility of a resonant bubble population existed, the phase and coherence

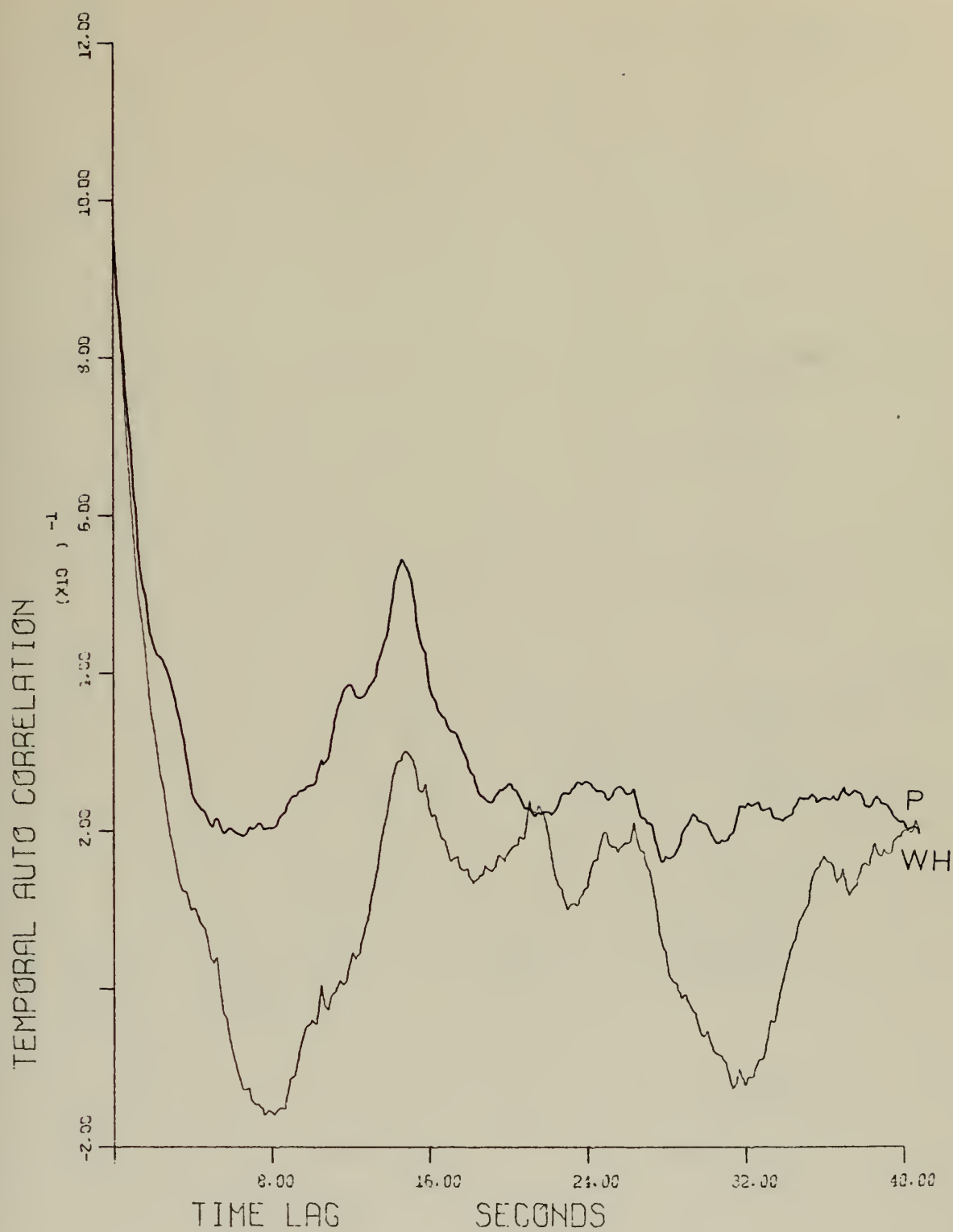
functions appeared much more confused. In all records, the signals are in phase at low frequencies. For all the maximum phase shifts and zero crossings, the coherence values are very low.

At the bubble frequencies of 56.2, 63.8, and 71.1 kHz, the coherence values are around 0.6 to 0.8 and the two signals are in phase within 30 degrees in the vicinity of the surface wave height frequency. This again underscores the affect of the sea surface wave height at these frequencies.



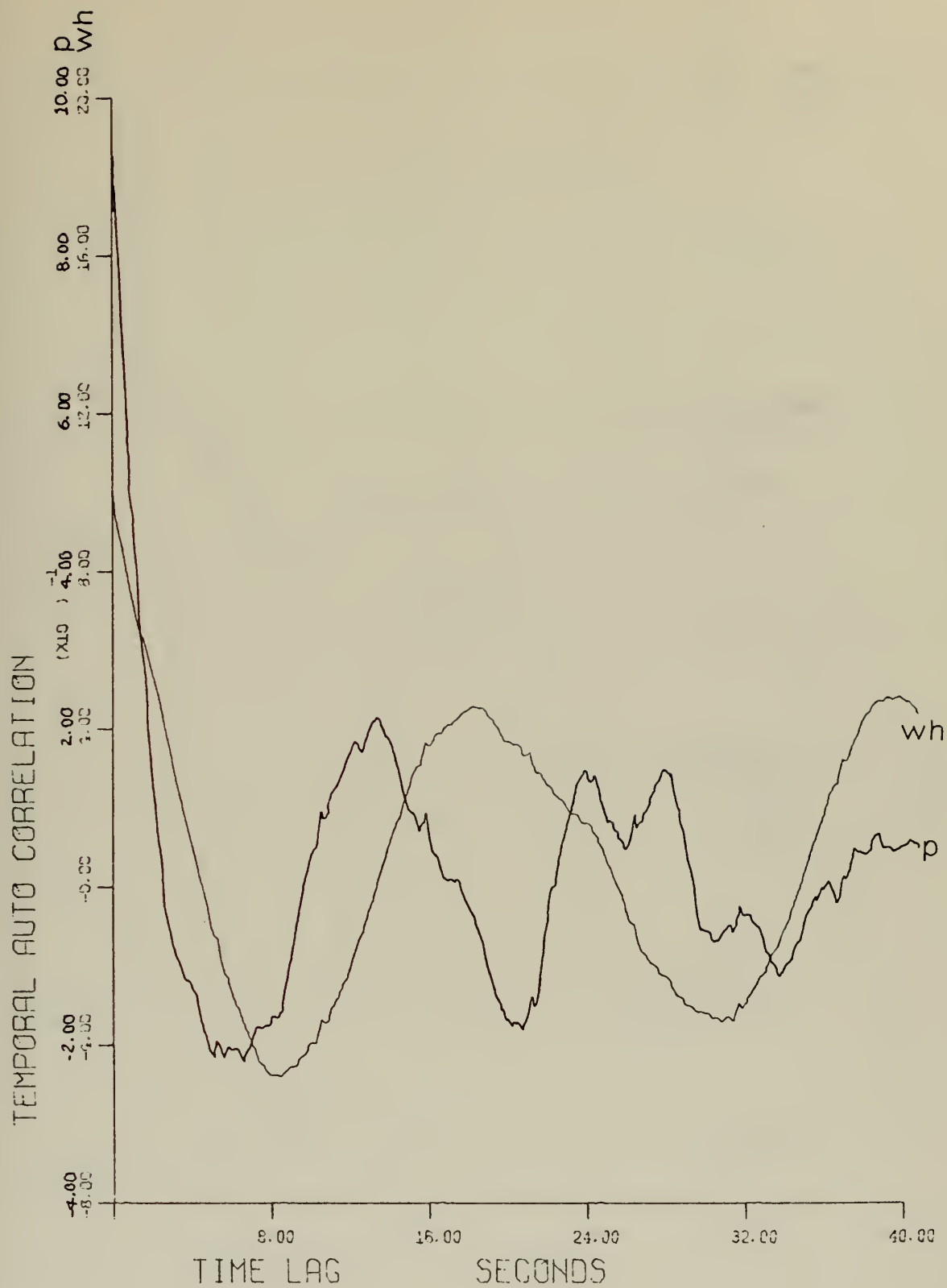
WAVE HEIGHT AND PHASE
FREQUENCY = 14790

Fig. 7



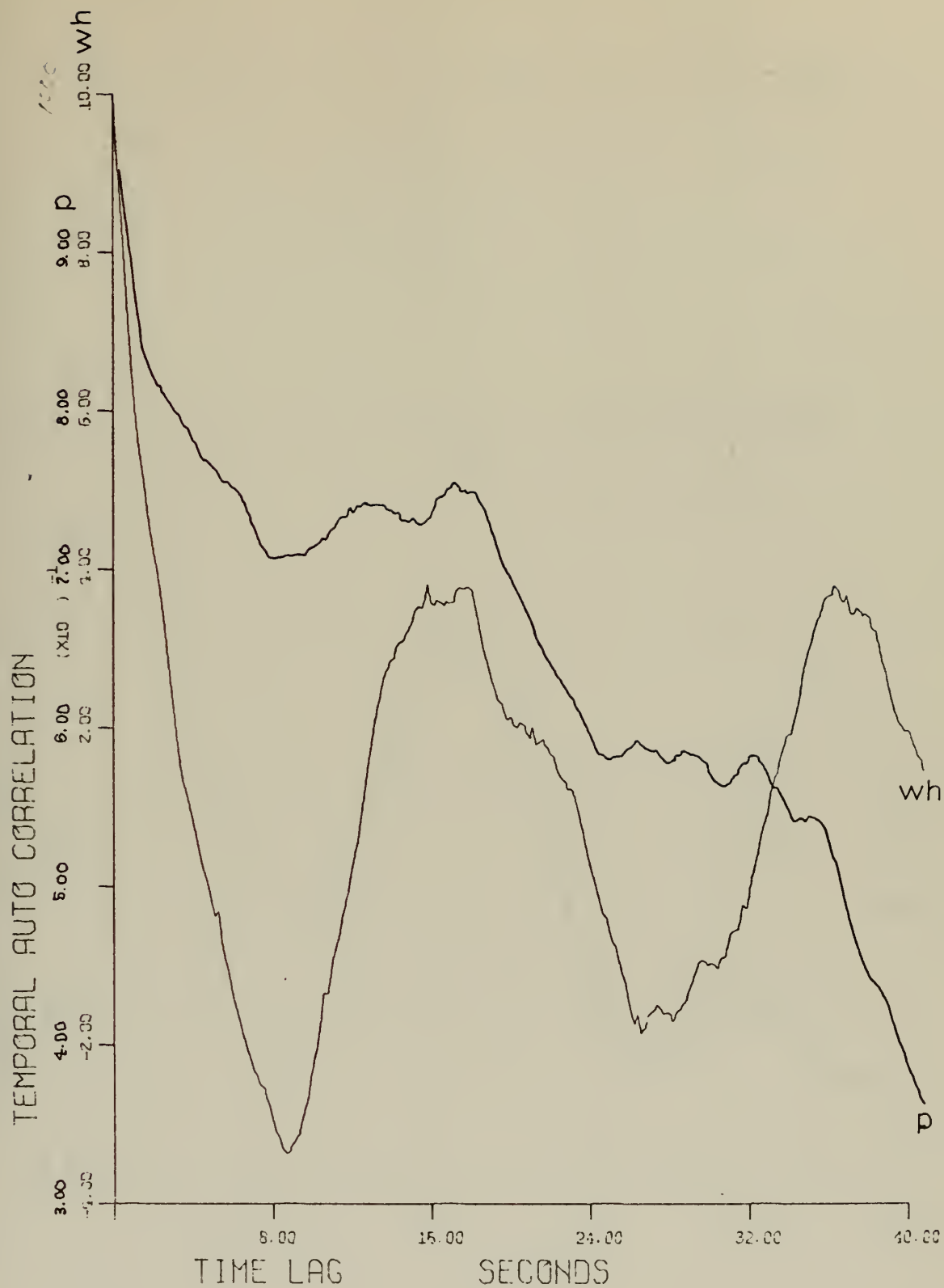
WAVE HEIGHT AND PHASE
FREQUENCY = 18777

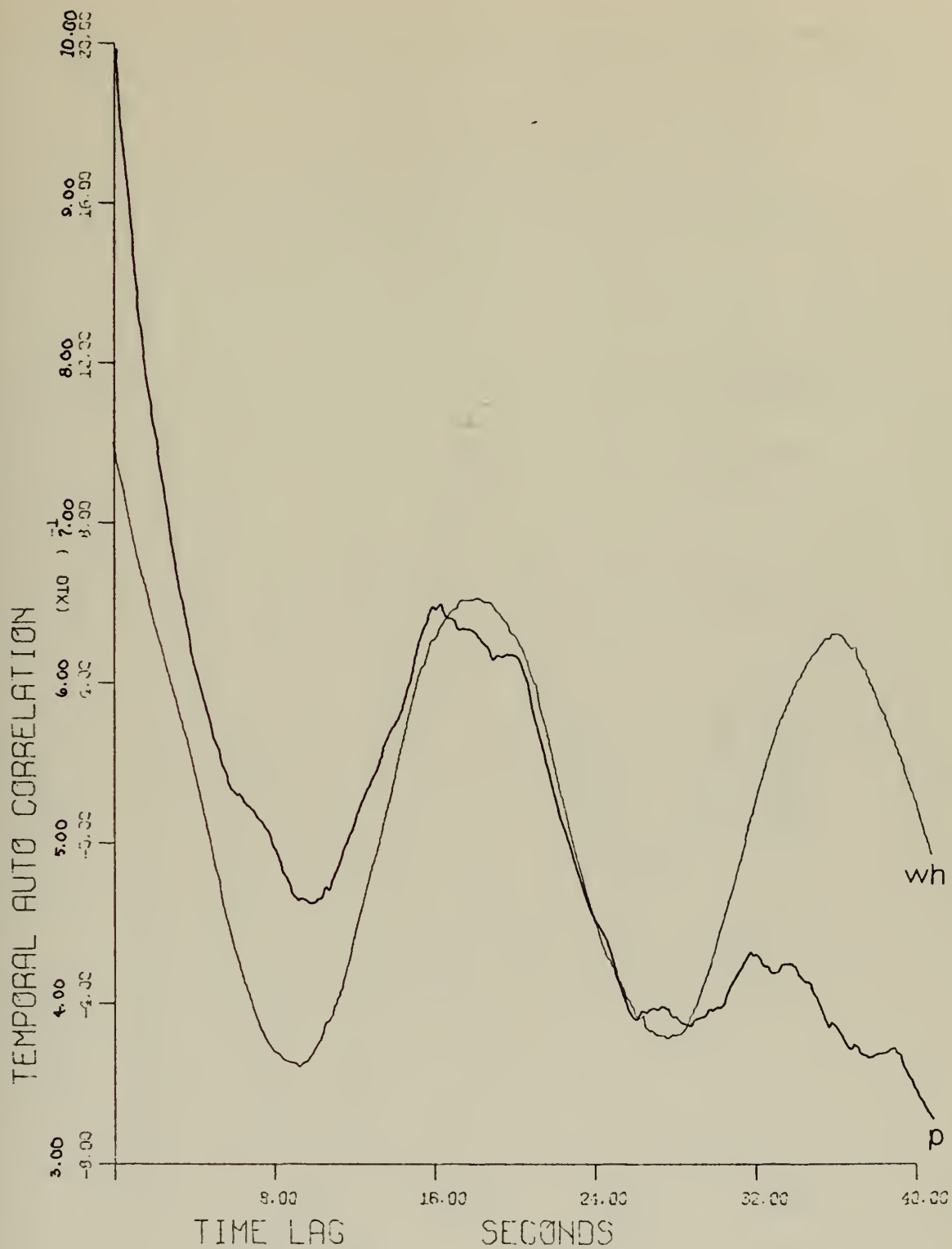
Fig. 8



WAVE HEIGHT AND PHASE
 FREQUENCY = 26170

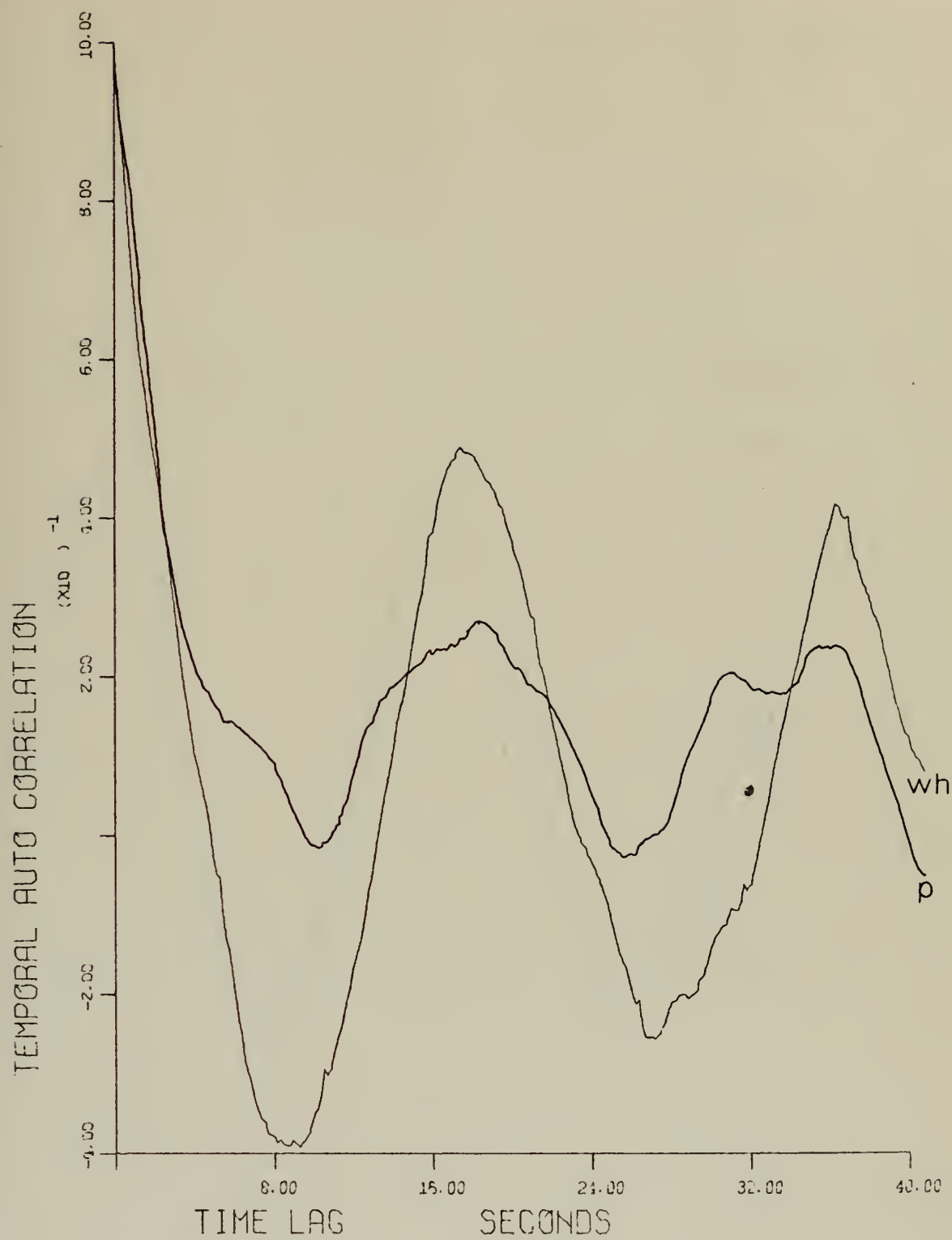
Fig. 9





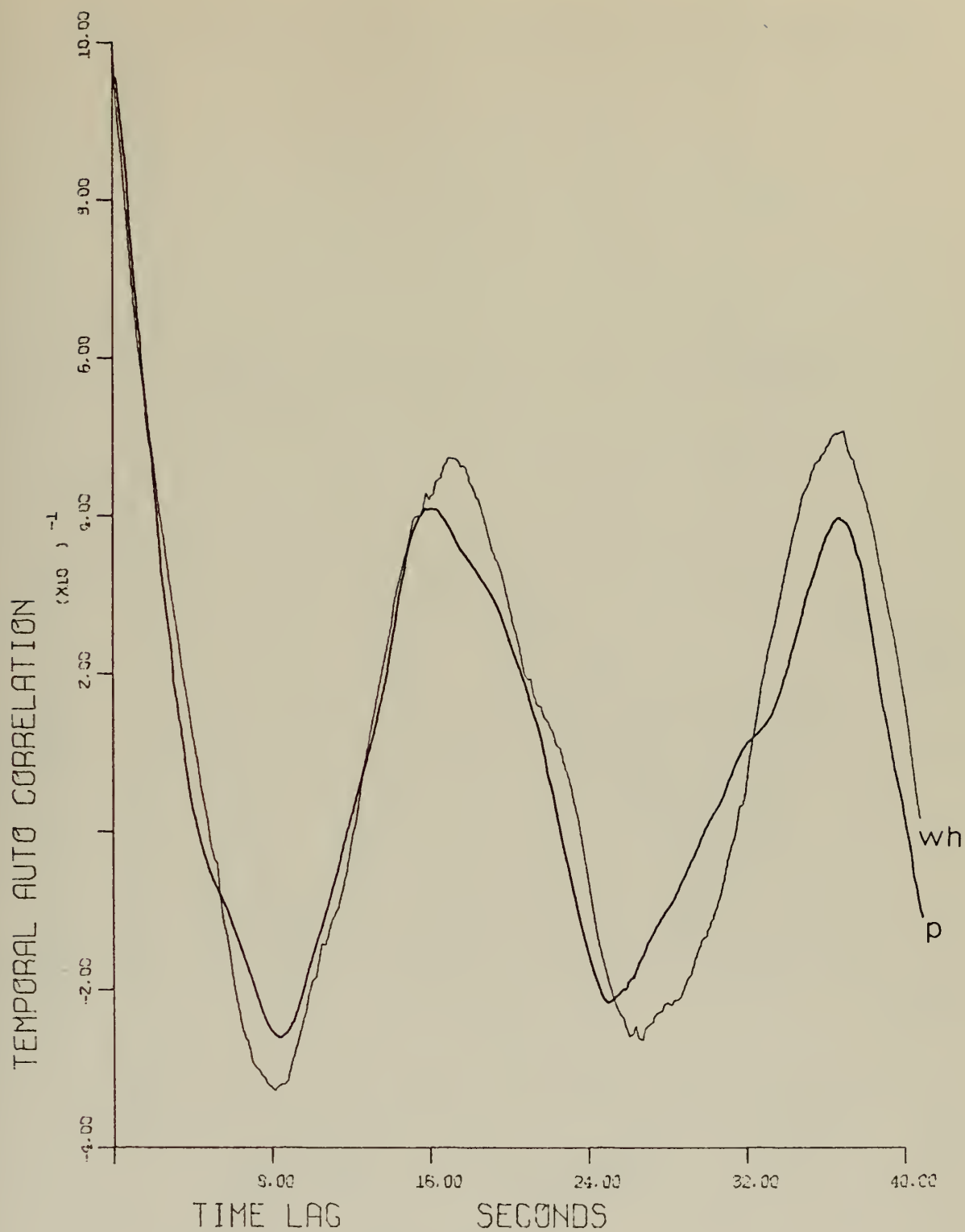
WAVE HEIGHT AND PHASE
 FREQUENCY = 56245

Fig. 11



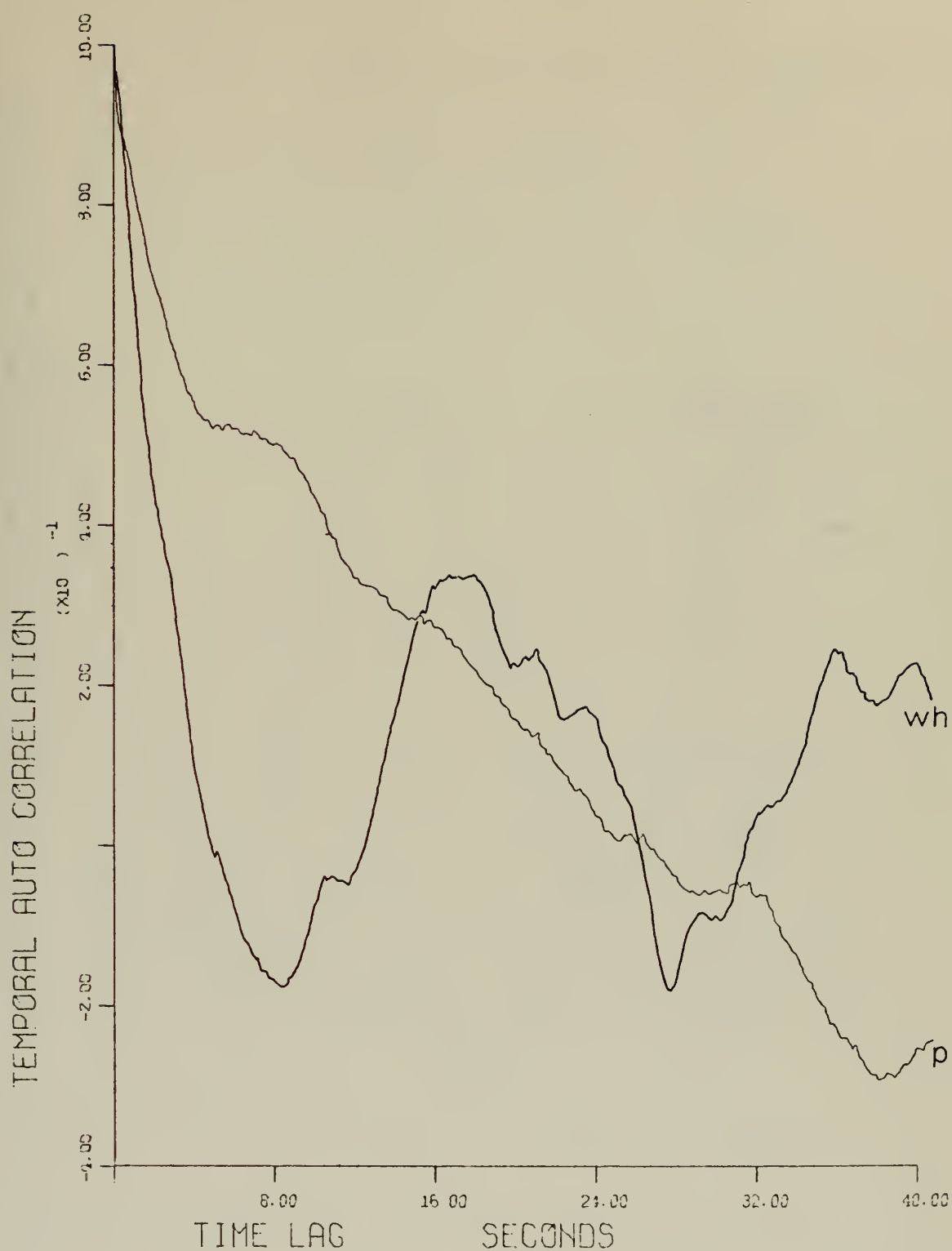
WAVE HEIGHT AND PHASE
FREQUENCY = 63790

Fig. 12



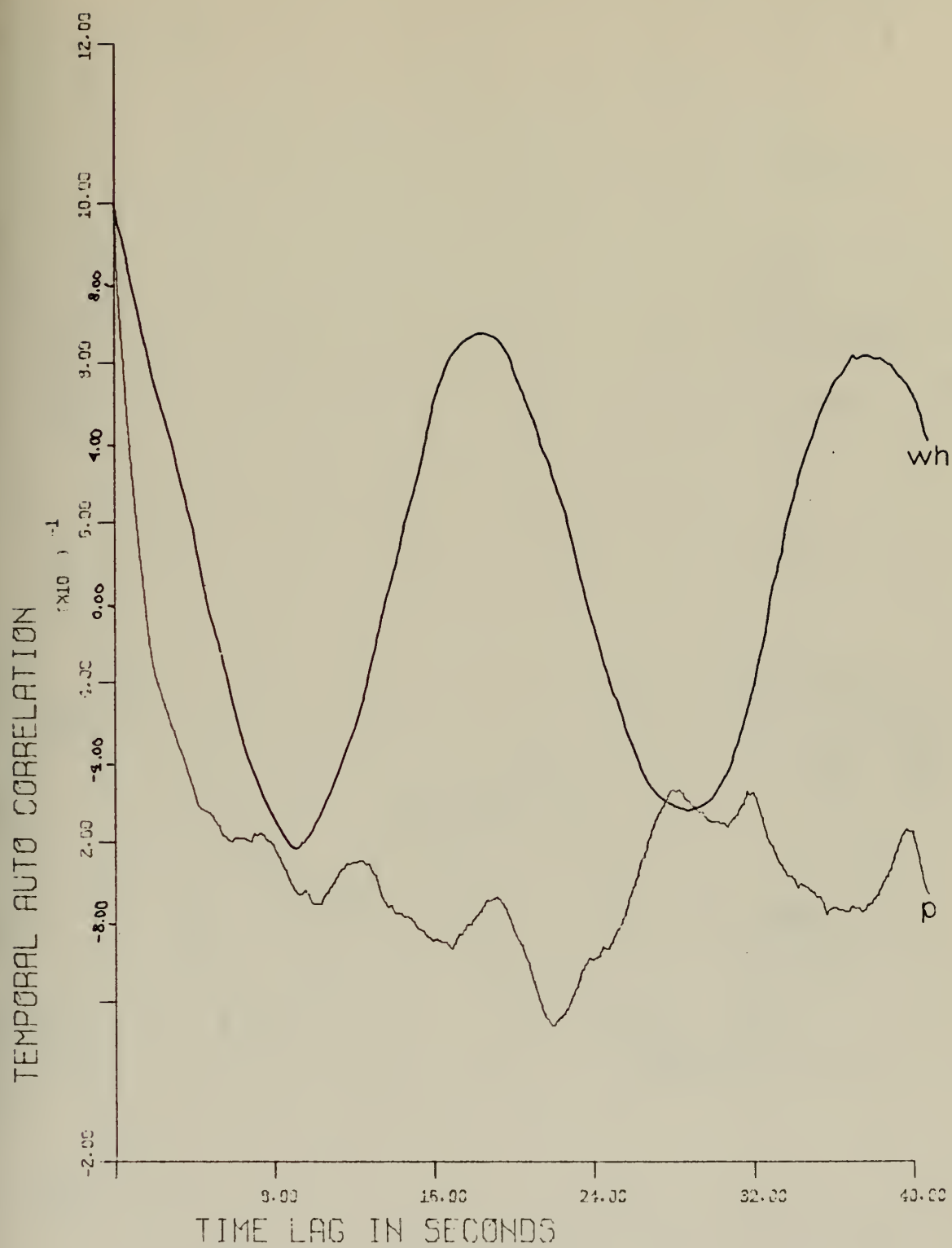
WAVE HEIGHT AND PHASE
FREQUENCY = 71130

Fig. 13



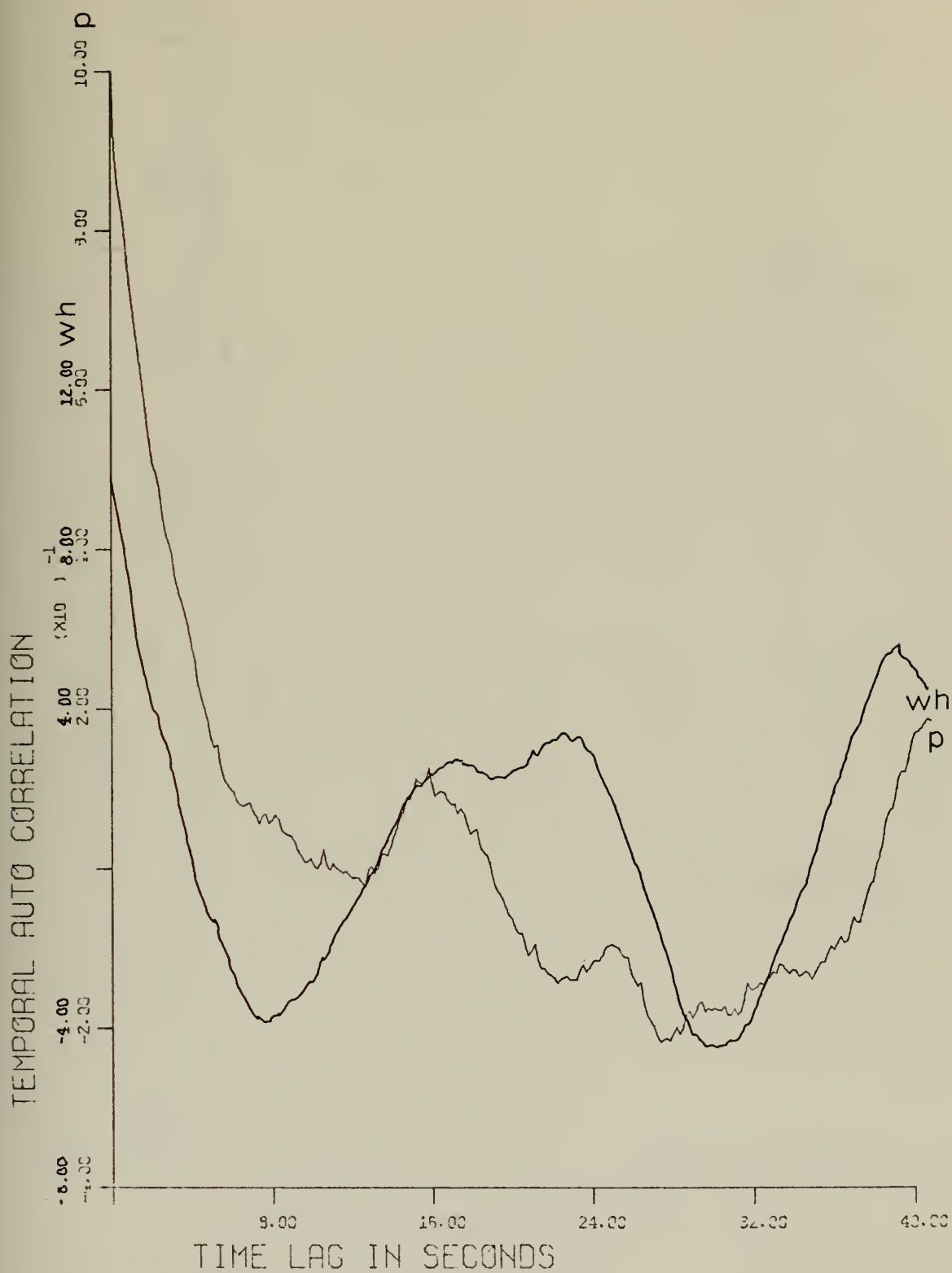
PHASE AND WAVE HEIGHT
FREQUENCY = 89900

Fig. 14



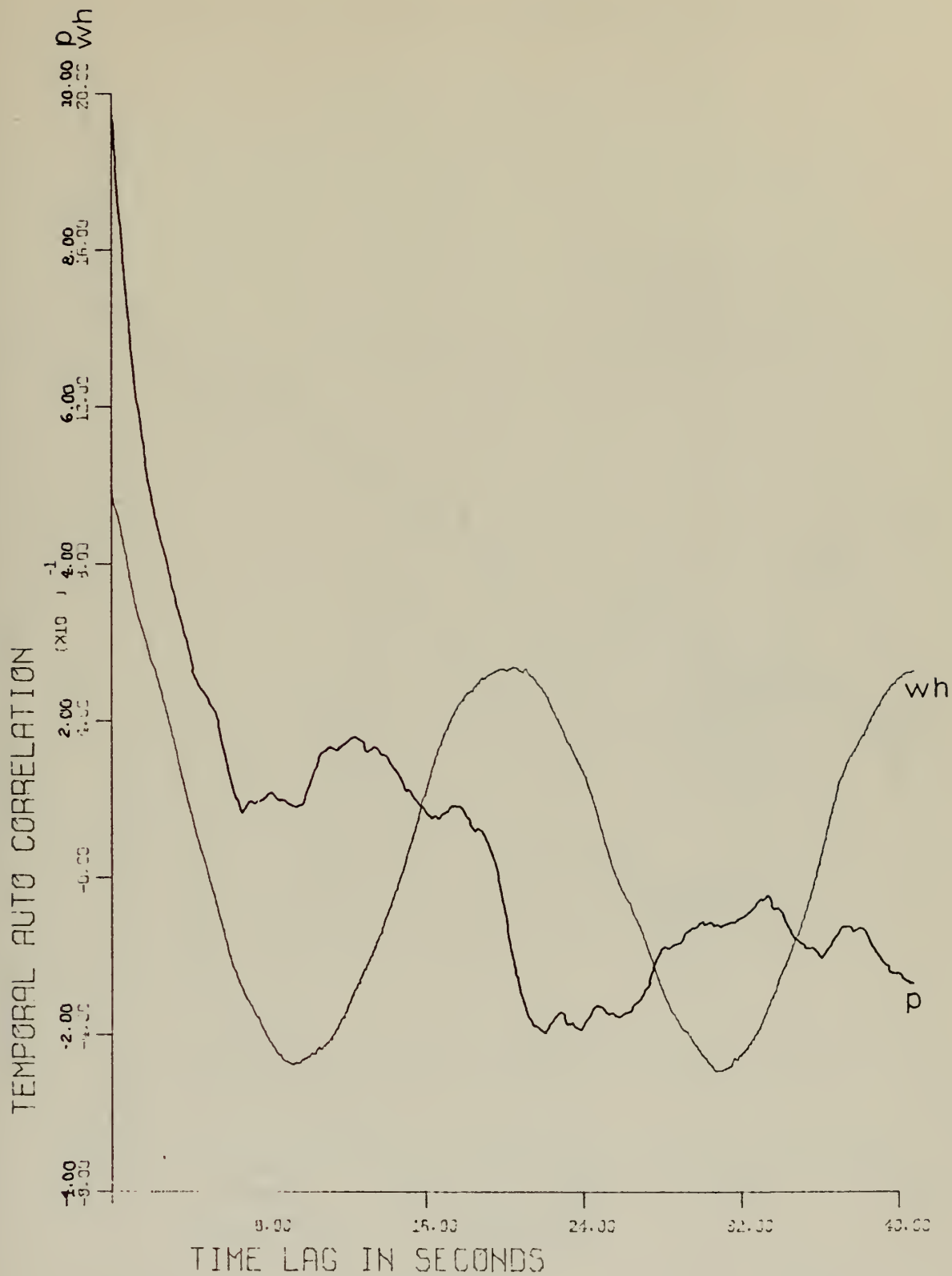
PHASE AND WAVE HEIGHT
FREQUENCY = 112519

Fig. 15



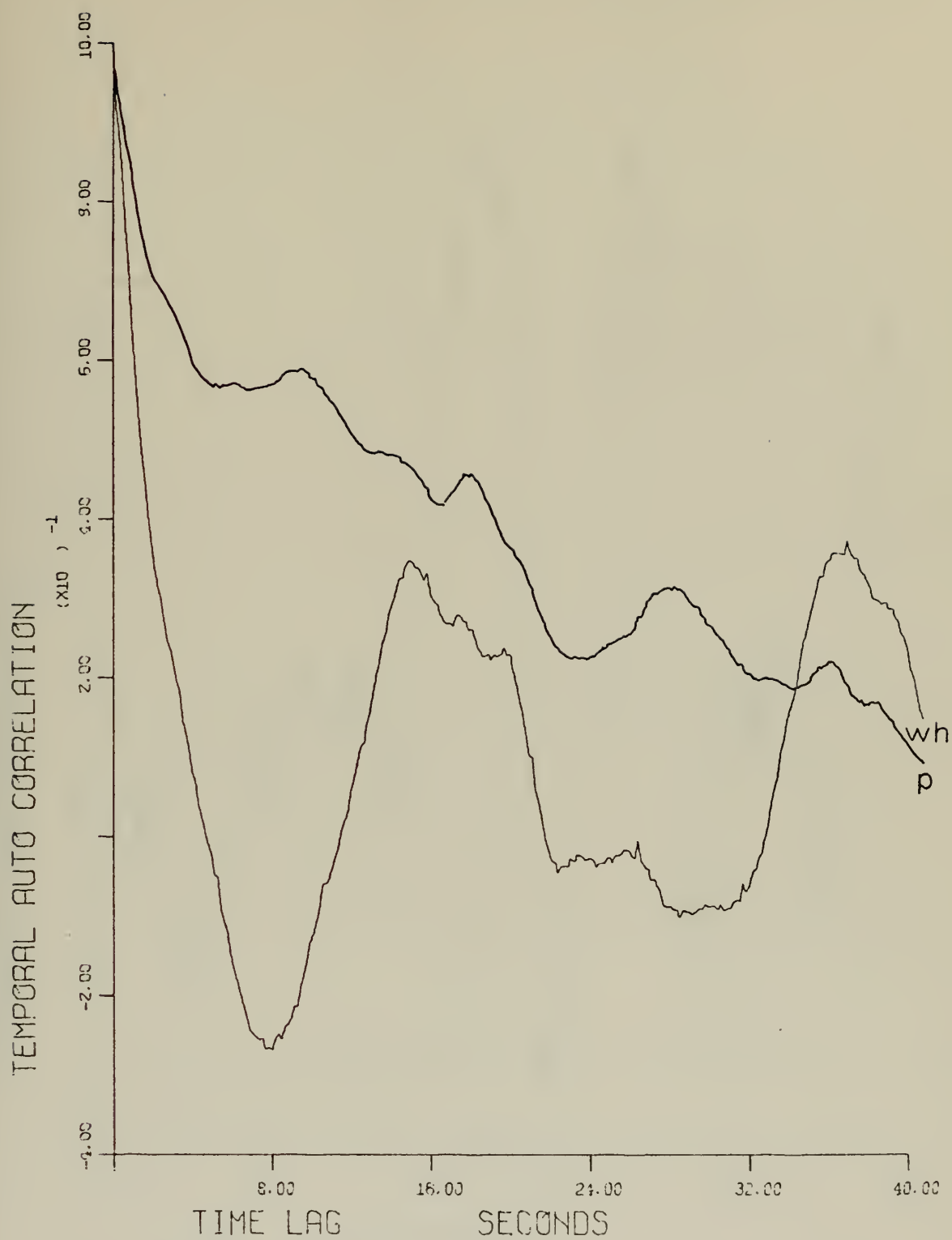
PHASE AND WAVE HEIGHT
 FREQUENCY = 123720

Fig. 16
 49



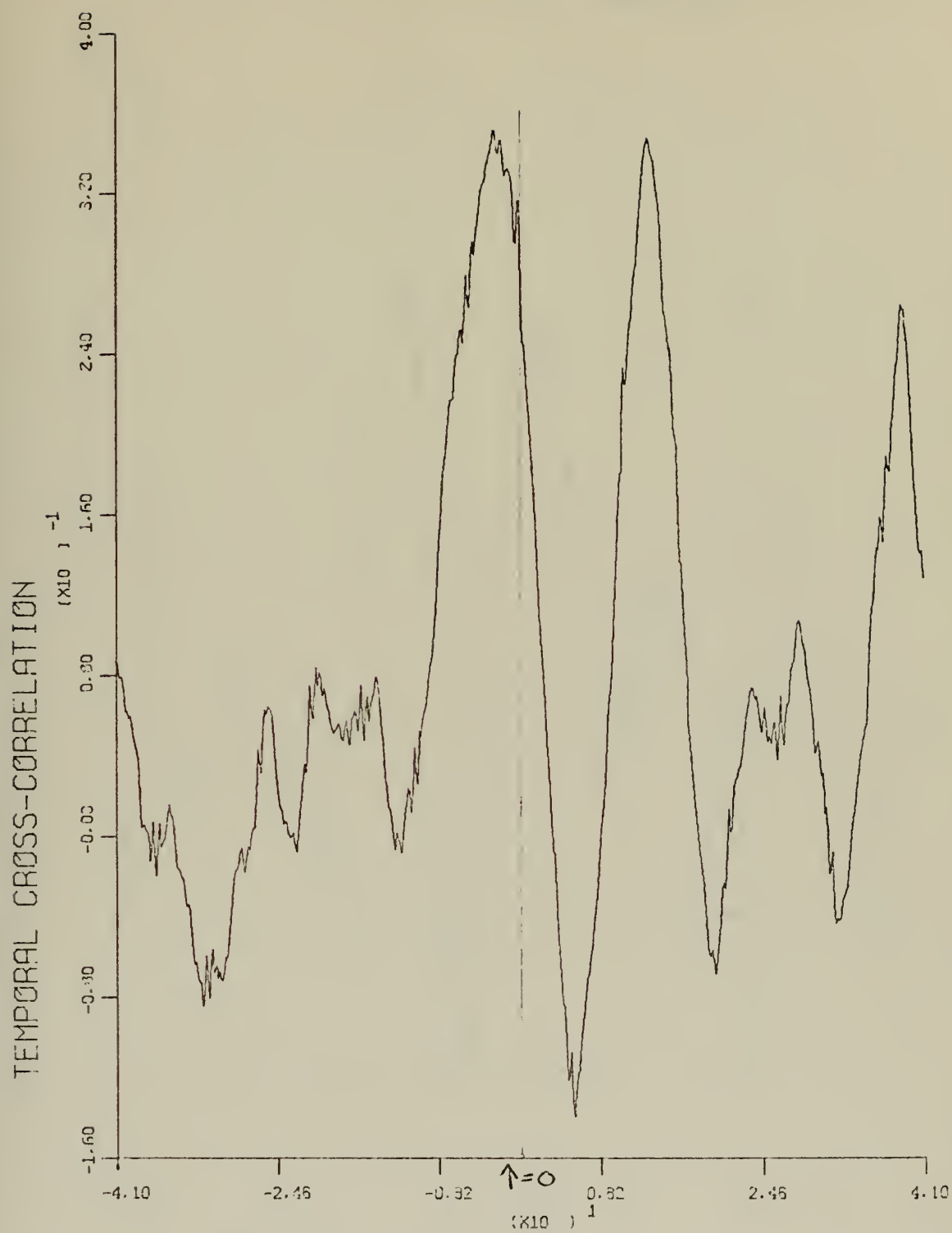
WAVE HEIGHT AND PHASE
 FREQUENCY = 136800

Fig. 17



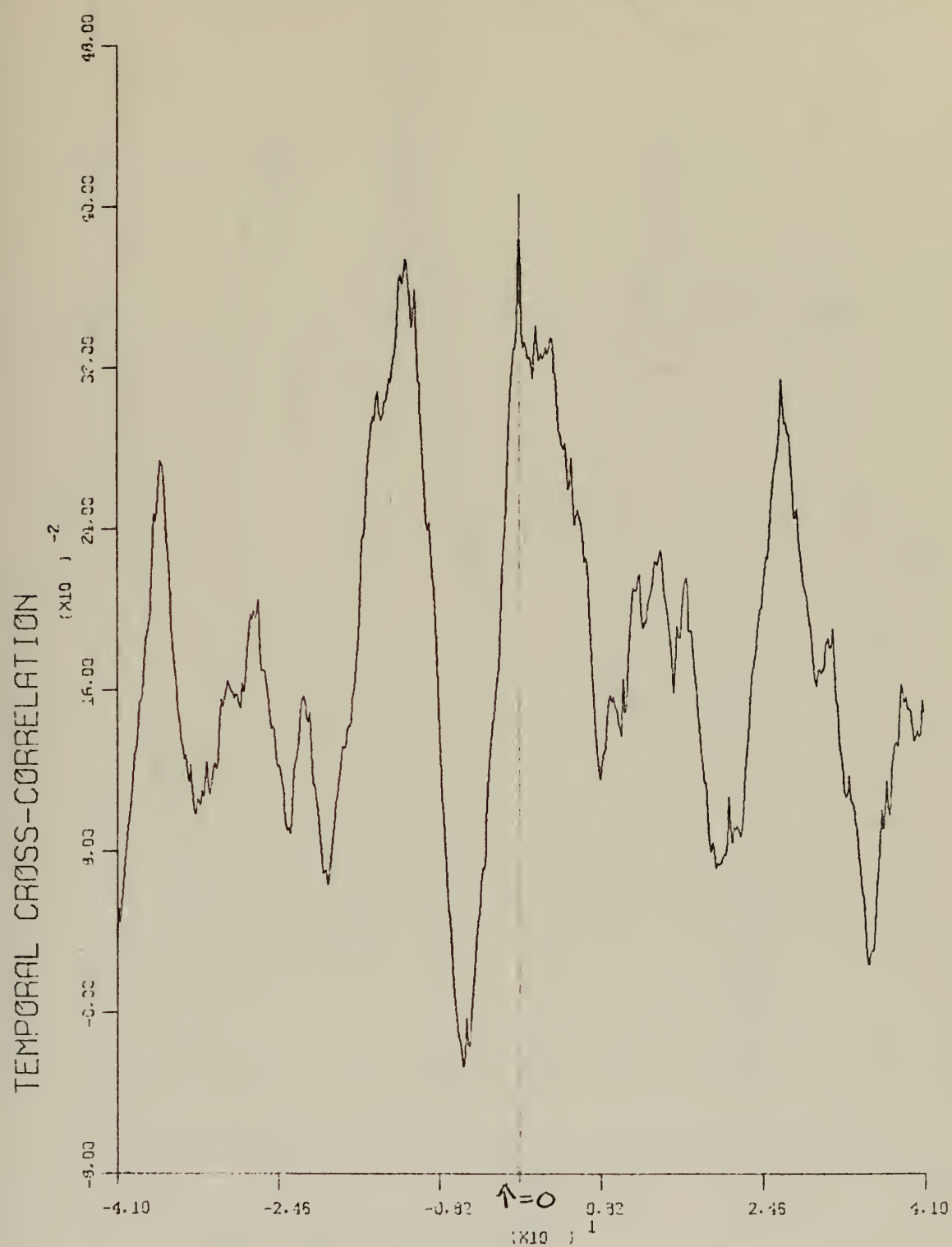
WAVE HEIGHT AND PHASE
 FREQUENCY = 146100

Fig. 18



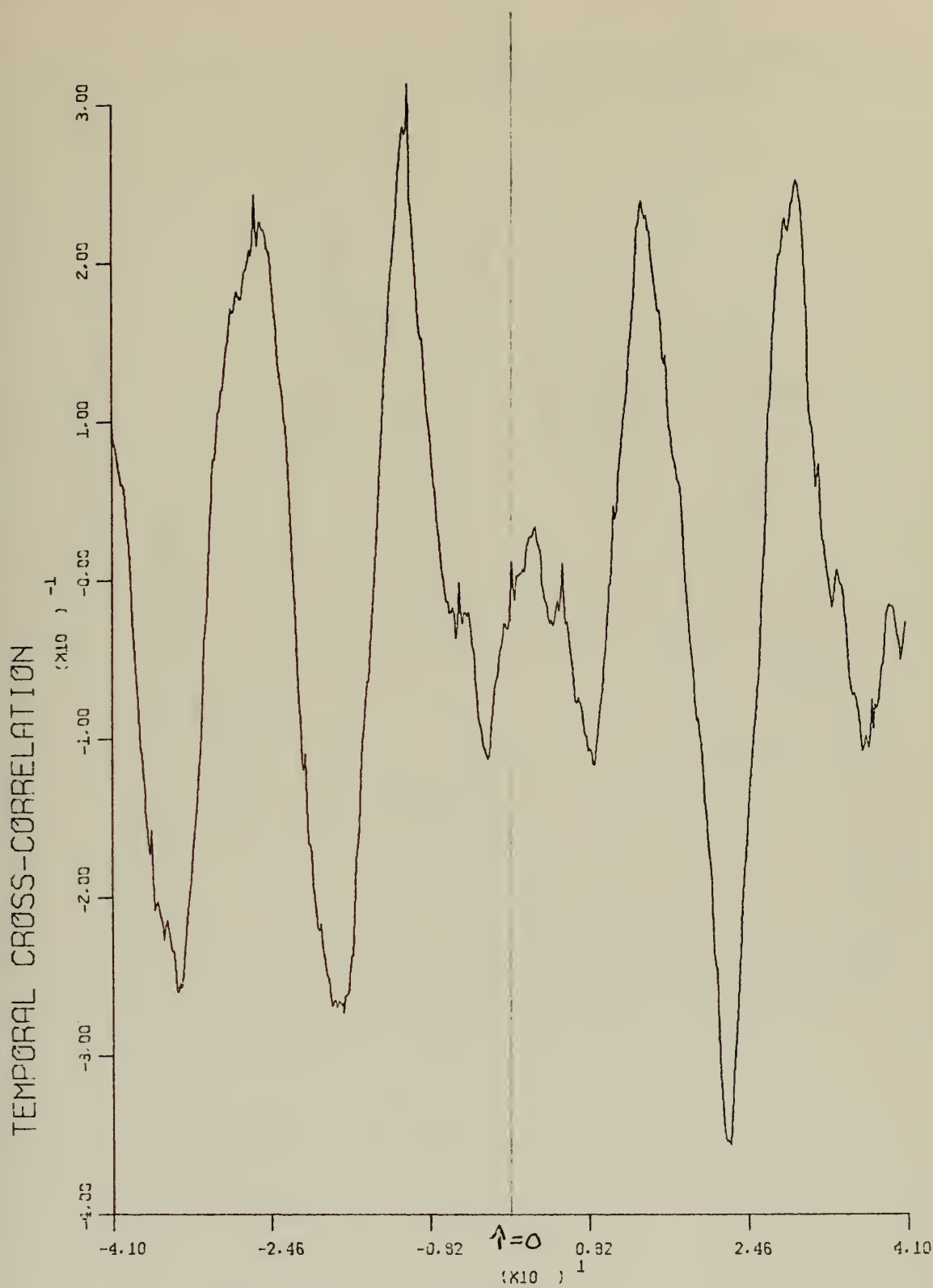
TIME LAG IN SECONDS
 PHASE WITH WAVE HEIGHT
 FREQUENCY = 14790

Fig. 19



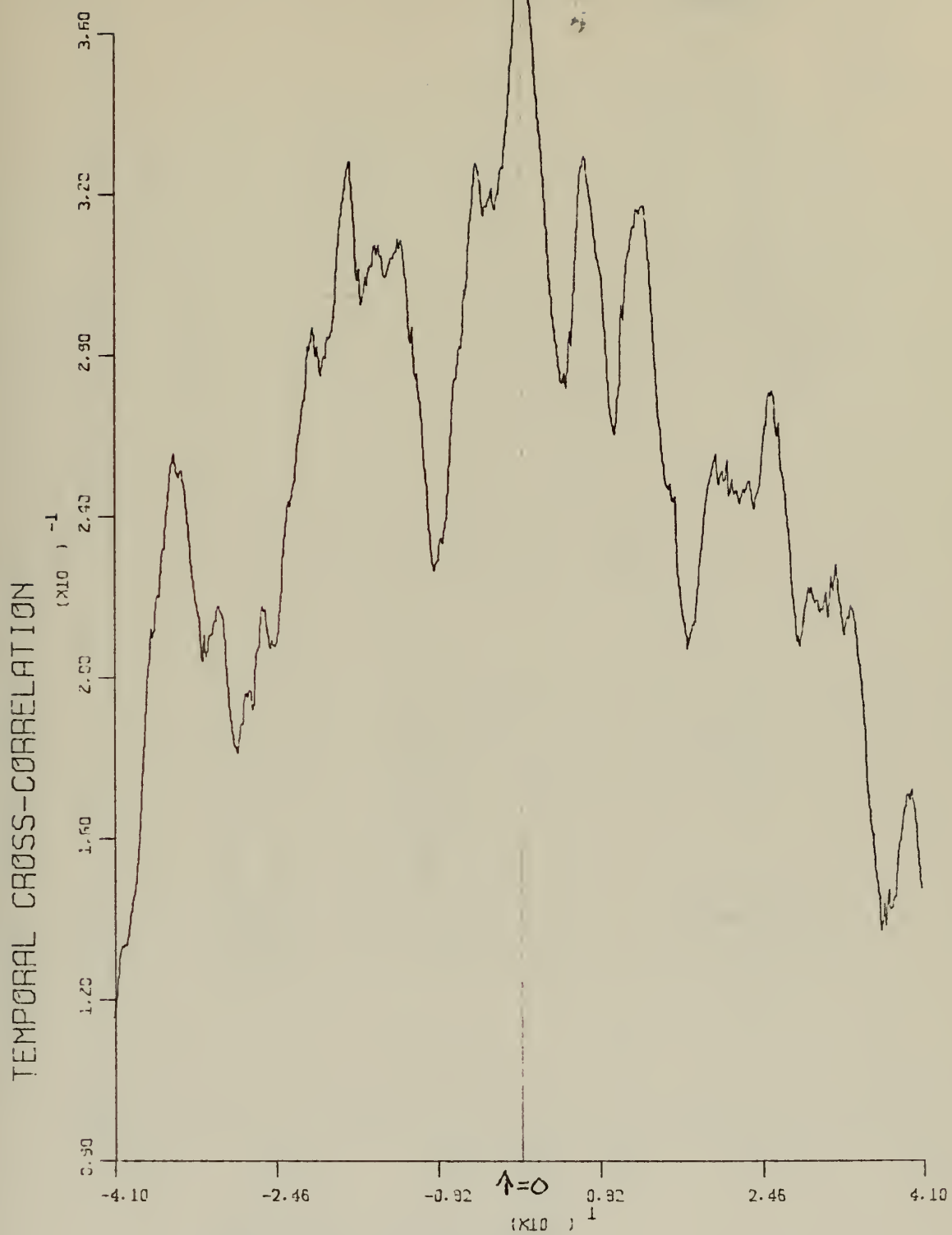
TIME LAG IN SECONDS
 PHASE WITH WAVE HEIGHT
 FREQUENCY = 18777

Fig. 20



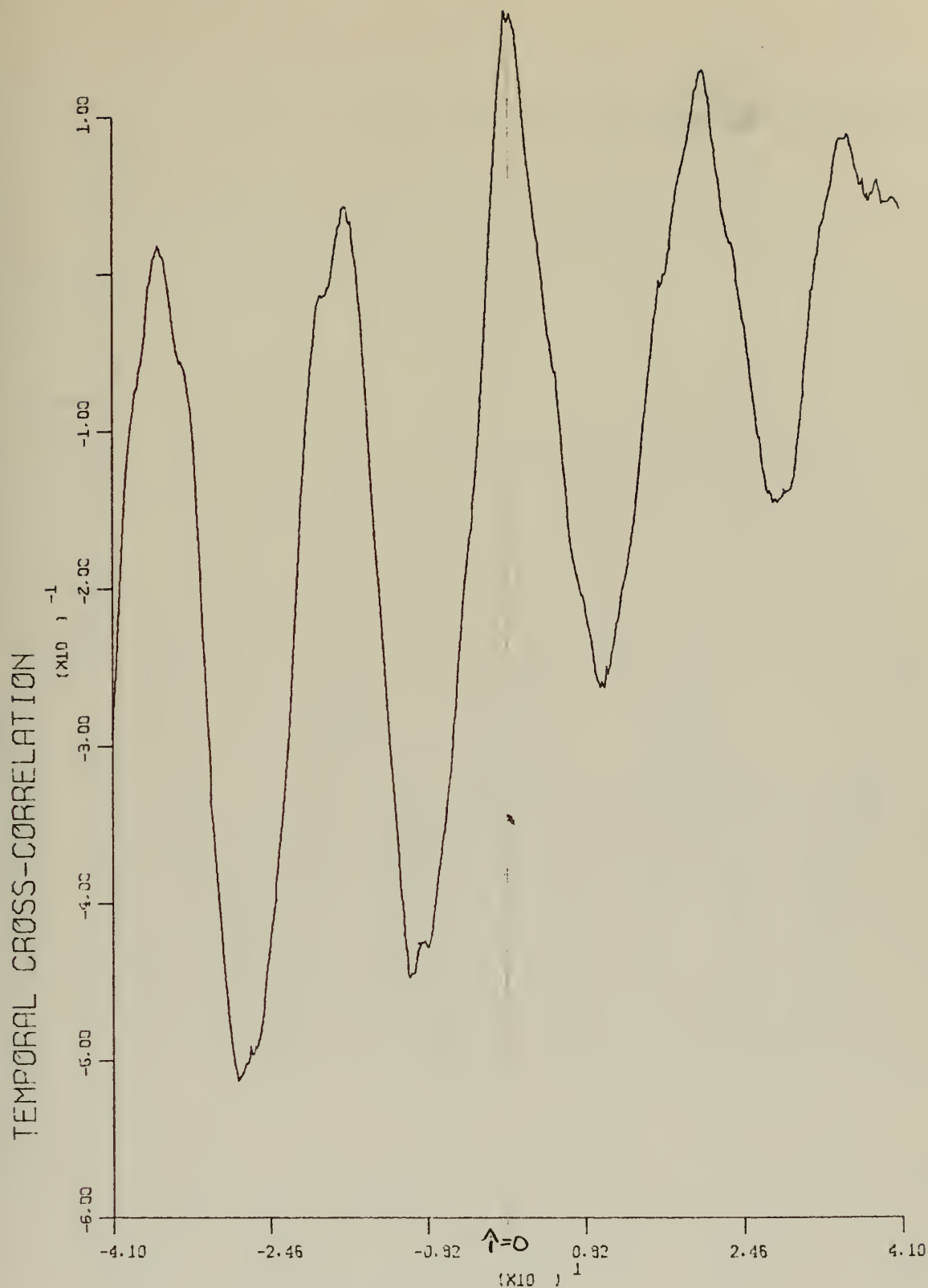
TIME LAG IN SECONDS
 PHASE WITH WAVE HEIGHT
 FREQUENCY = 26170

Fig. 21



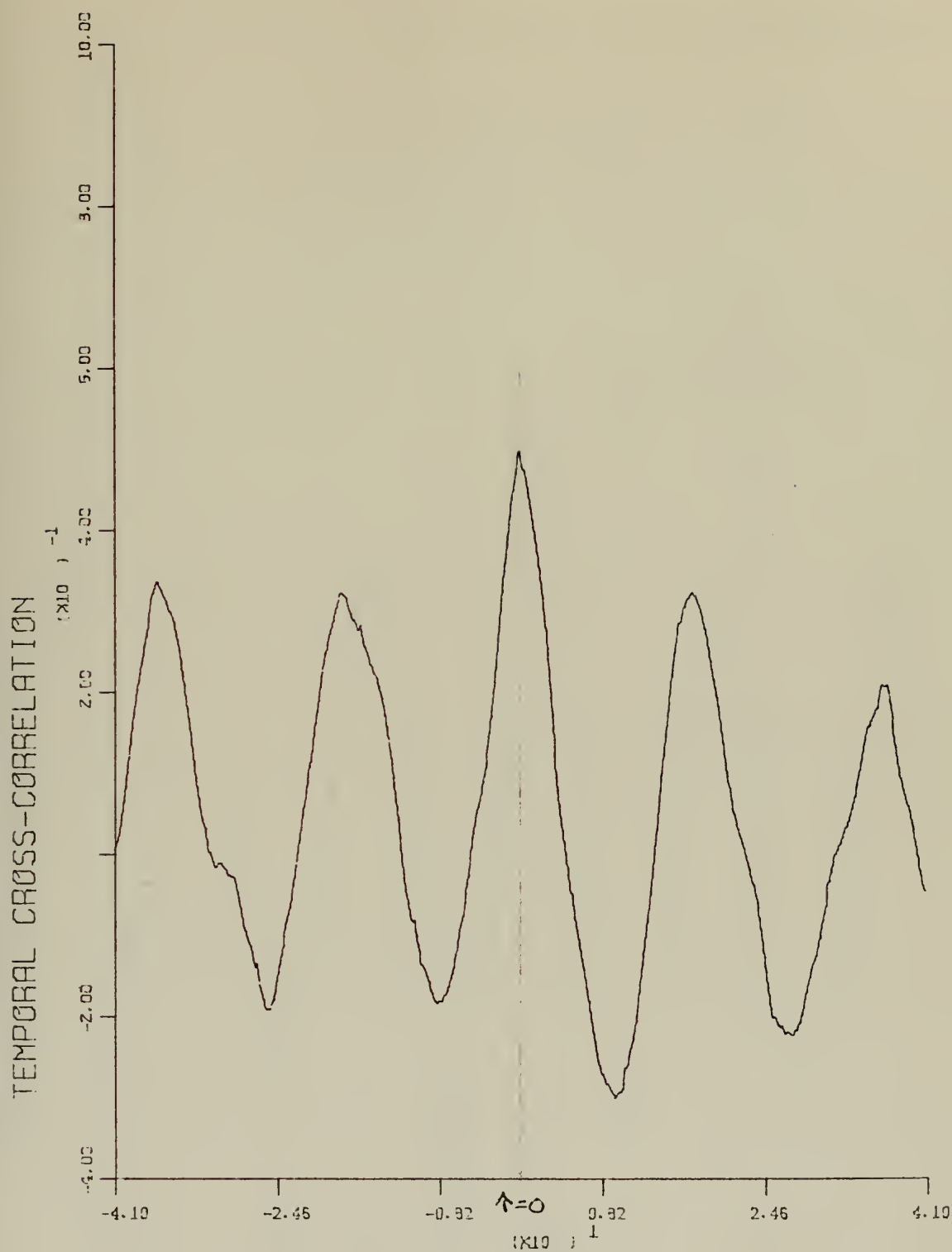
TIME LAG IN SECONDS
 PHASE WITH WAVE HEIGHT
 FREQUENCY = 41320

Fig. 22



TIME LAG IN SECONDS
 PHASE WITH WAVE HEIGHT
 FREQUENCY = 56245

Fig. 23



PHASE WITH WAVE HEIGHT
 FREQUENCY = 63790

Fig. 24

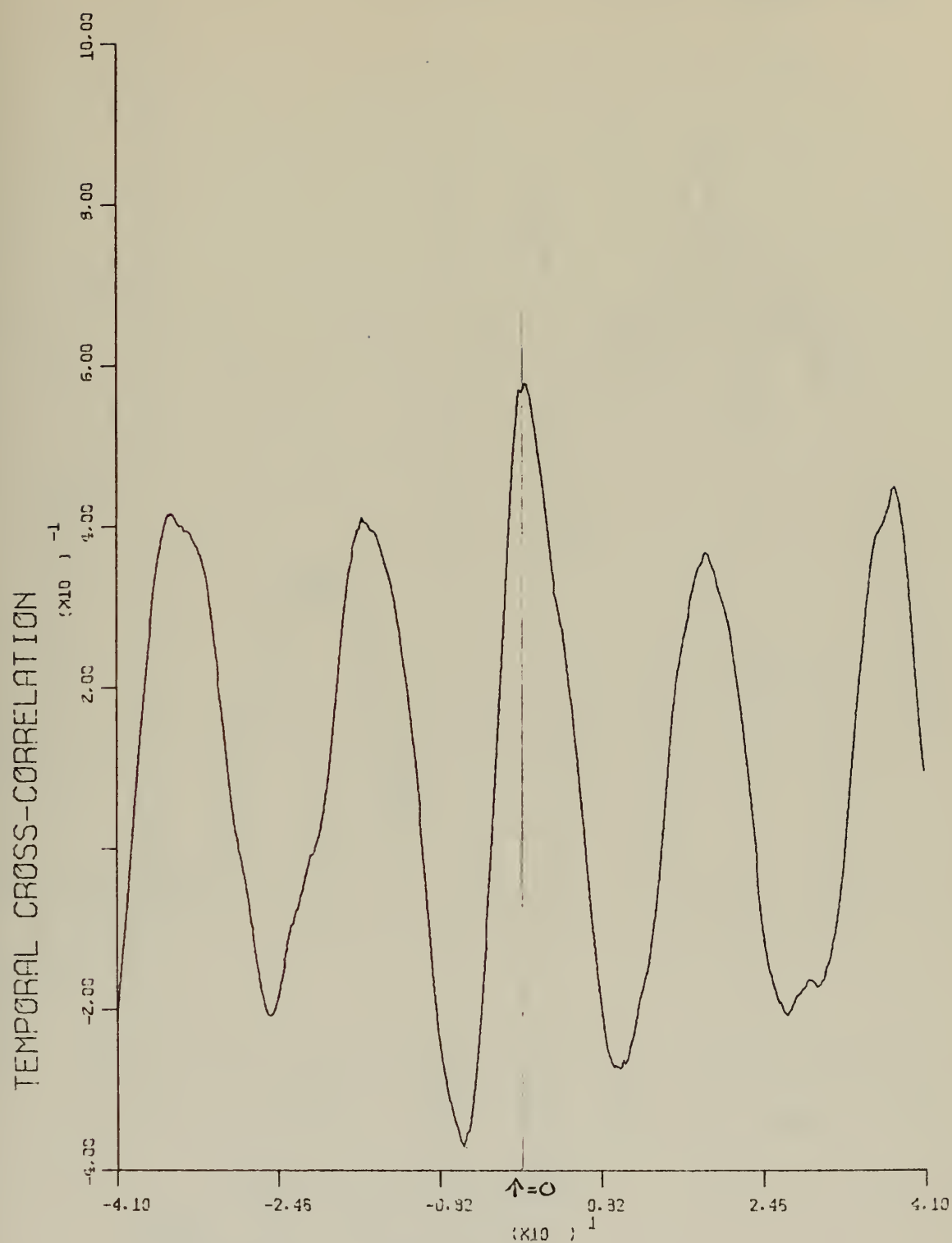
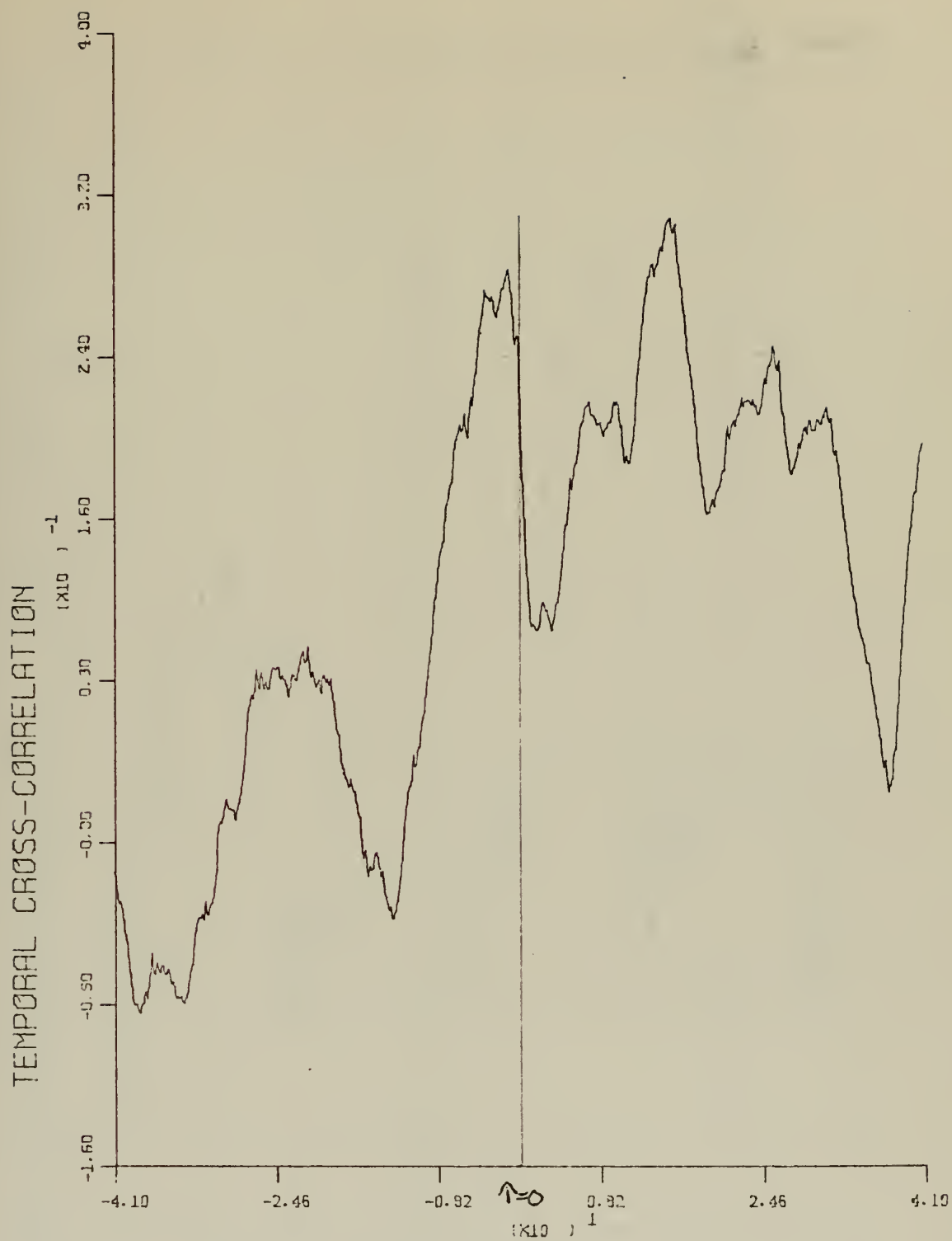
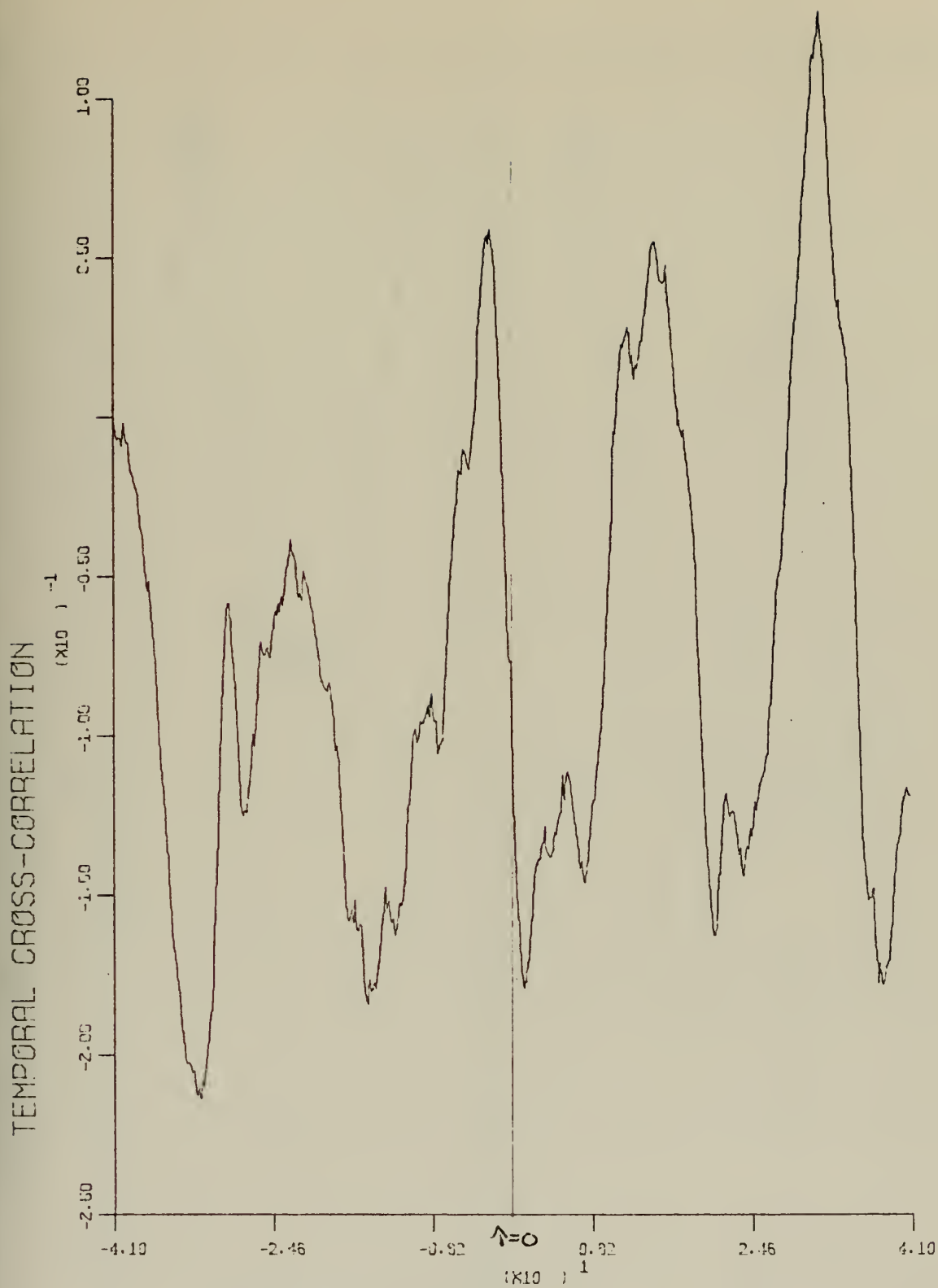


Fig. 25



TIME LAG IN SECONDS
 PHASE WITH WAVE HEIGHT
 FREQUENCY = 89900

Fig. 26



PHASE WITH WAVE HEIGHT
 FREQUENCY = 112519

Fig. 27

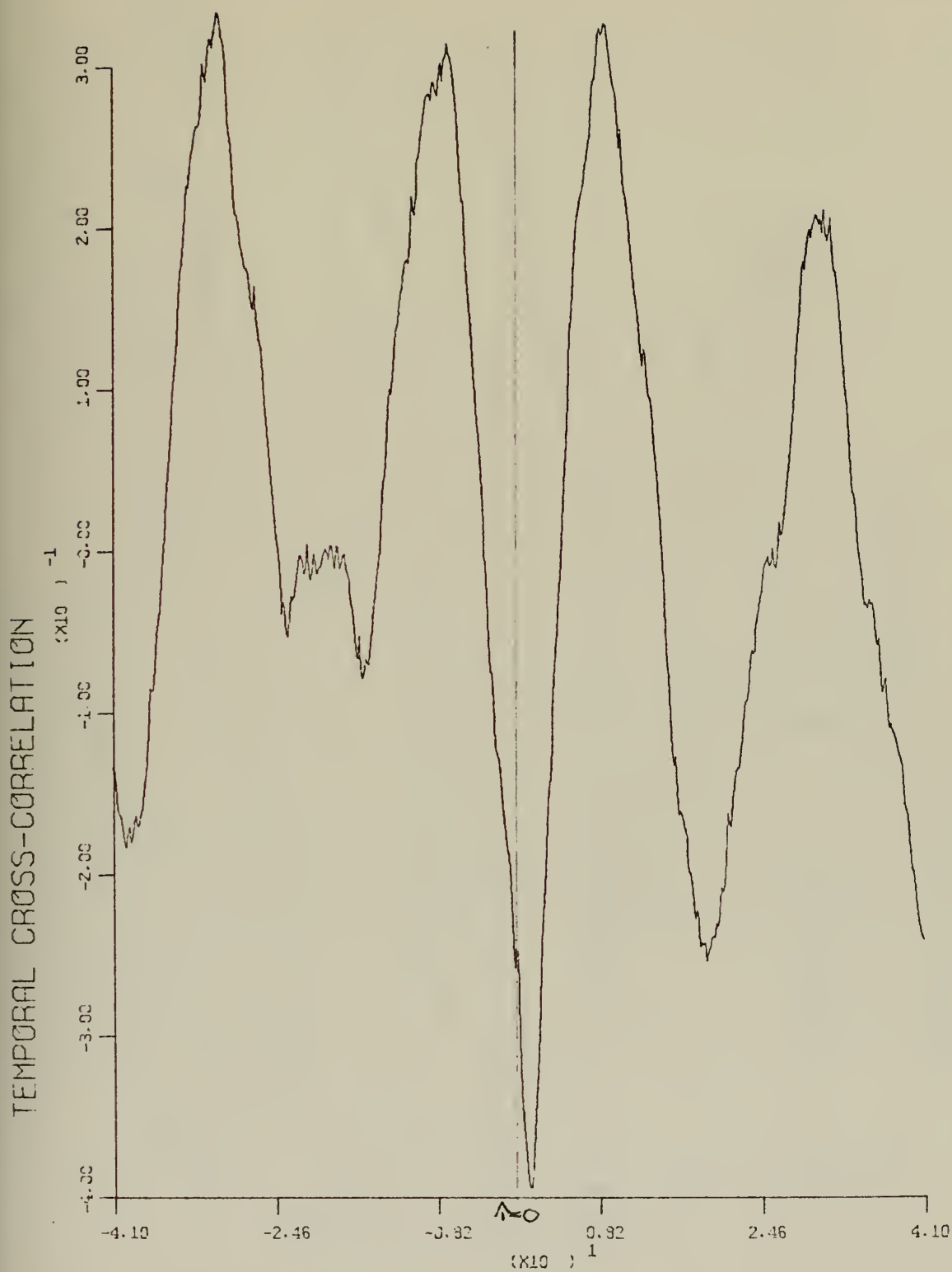
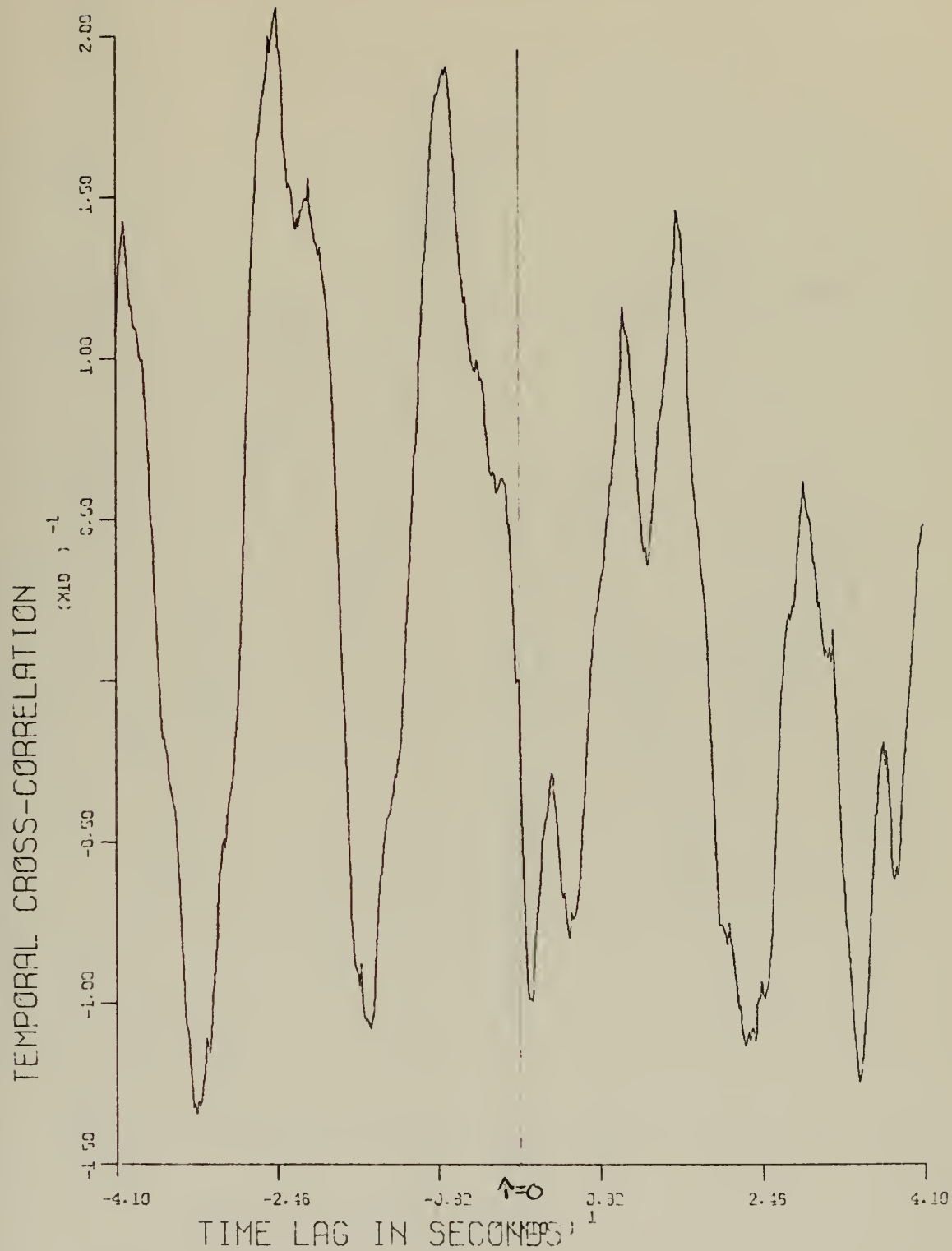
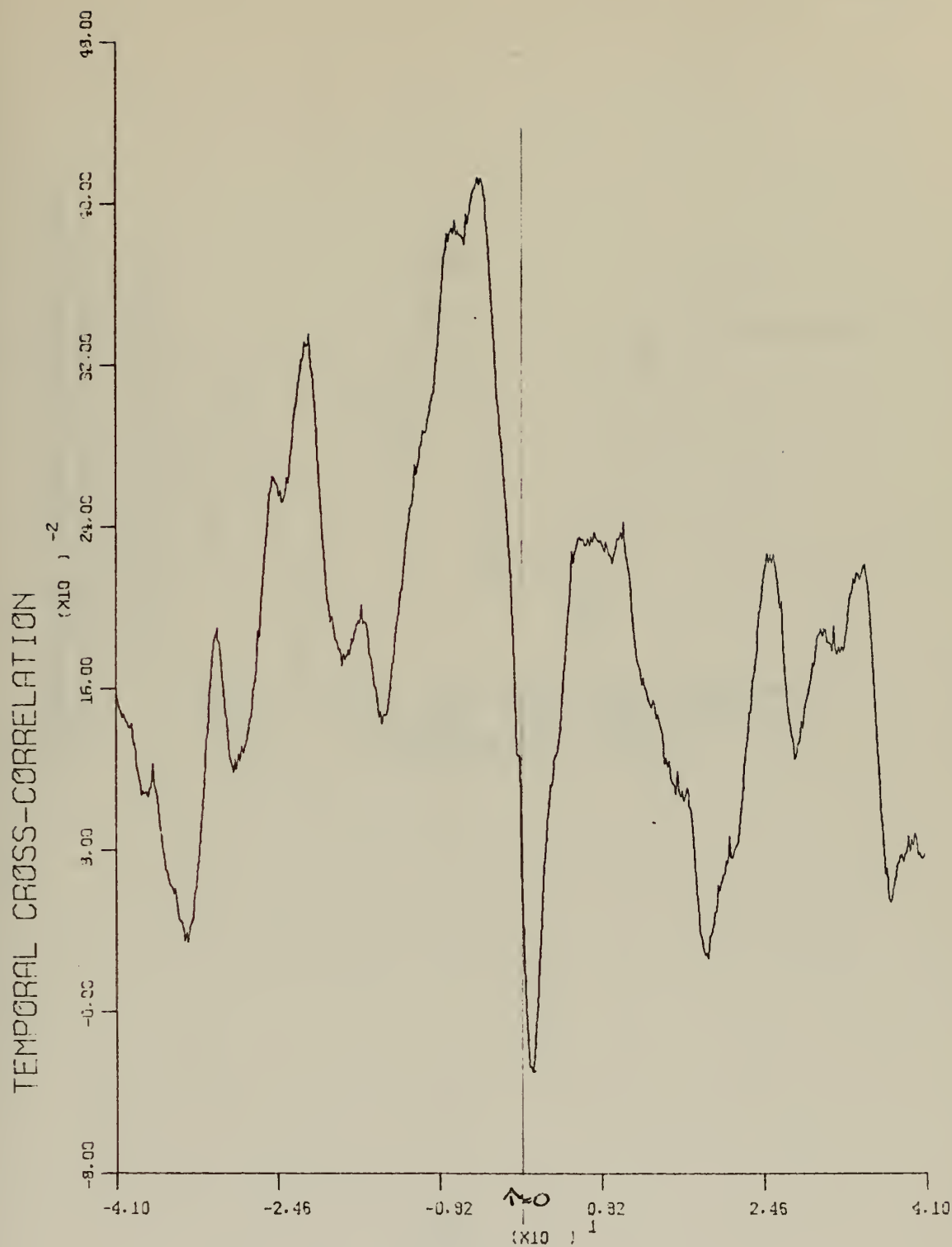


Fig. 28



PHASE WITH WAVE HEIGHT
FREQUENCY = 136800

Fig. 29



TIME LAG IN SECONDS
 PHASE WITH WAVE HEIGHT
 FREQUENCY = 146100

Fig. 30

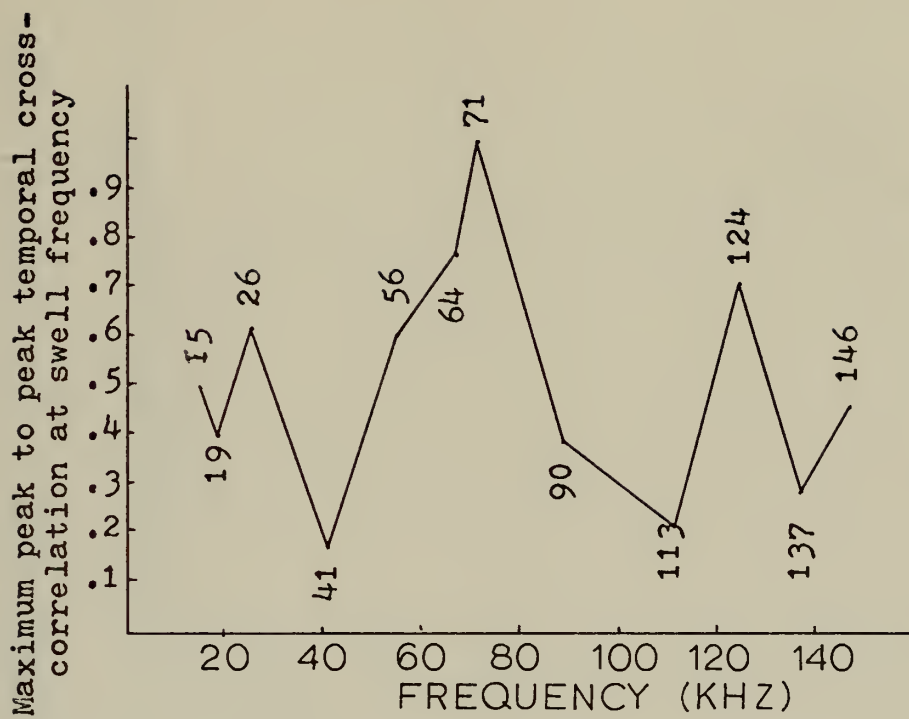
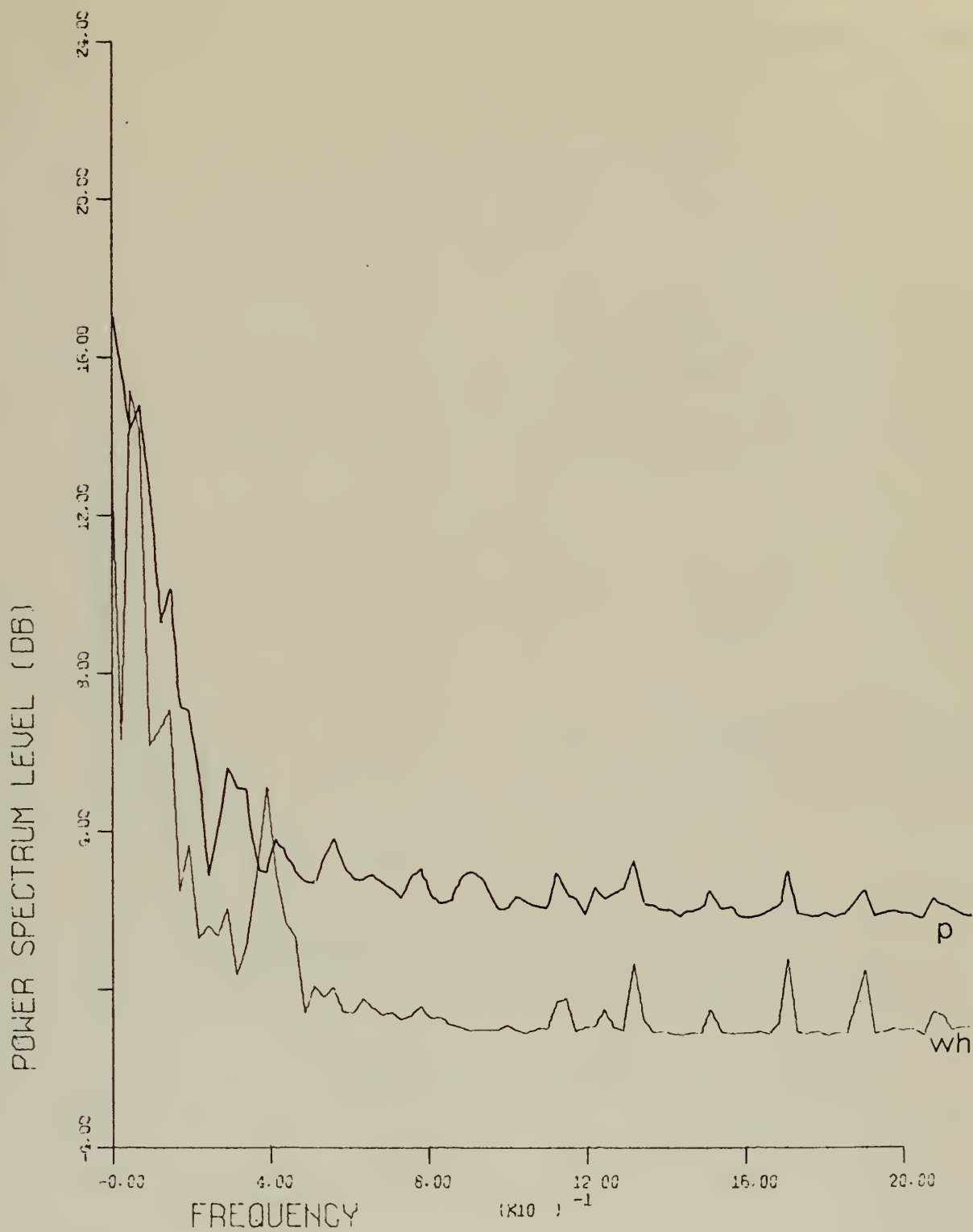
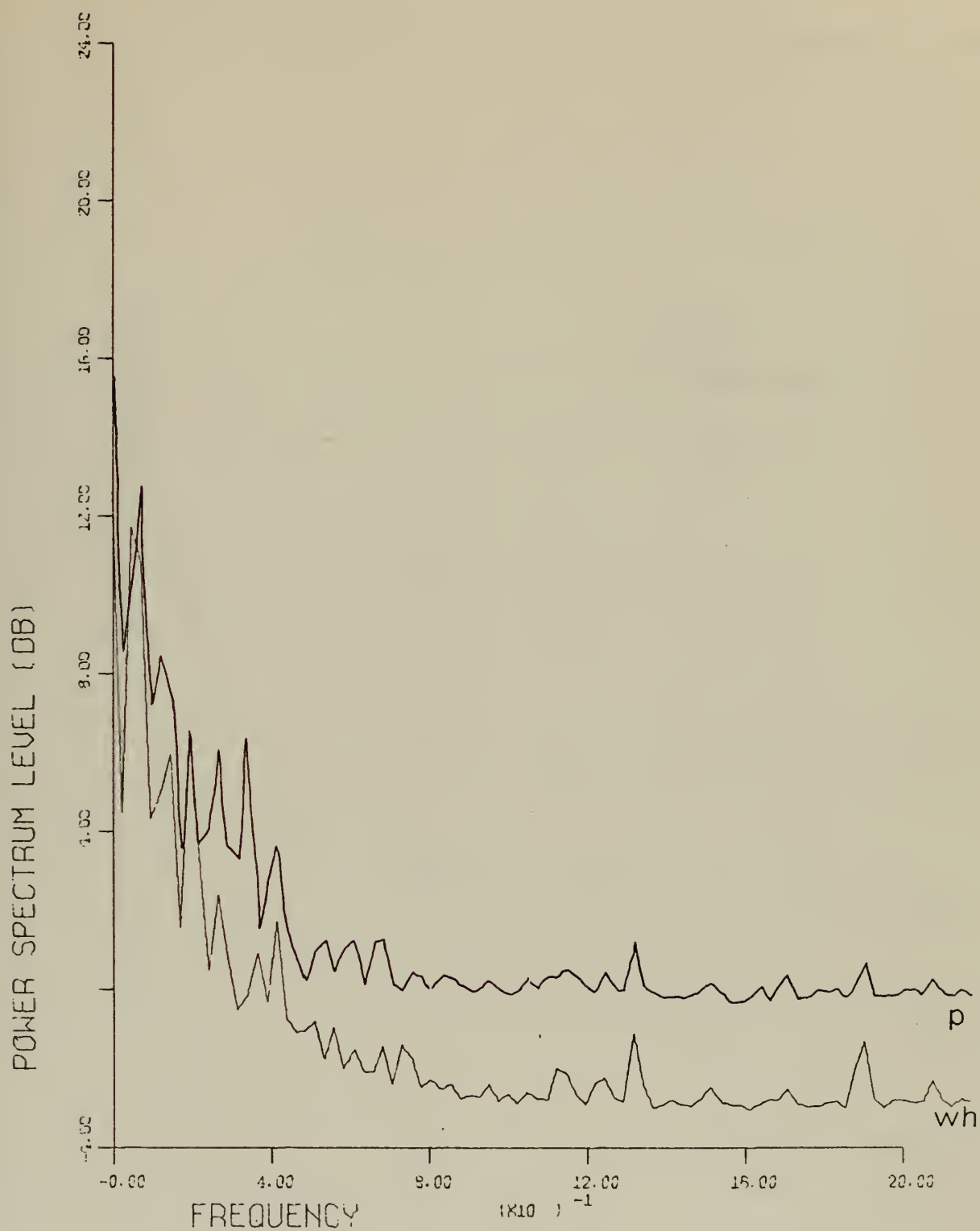


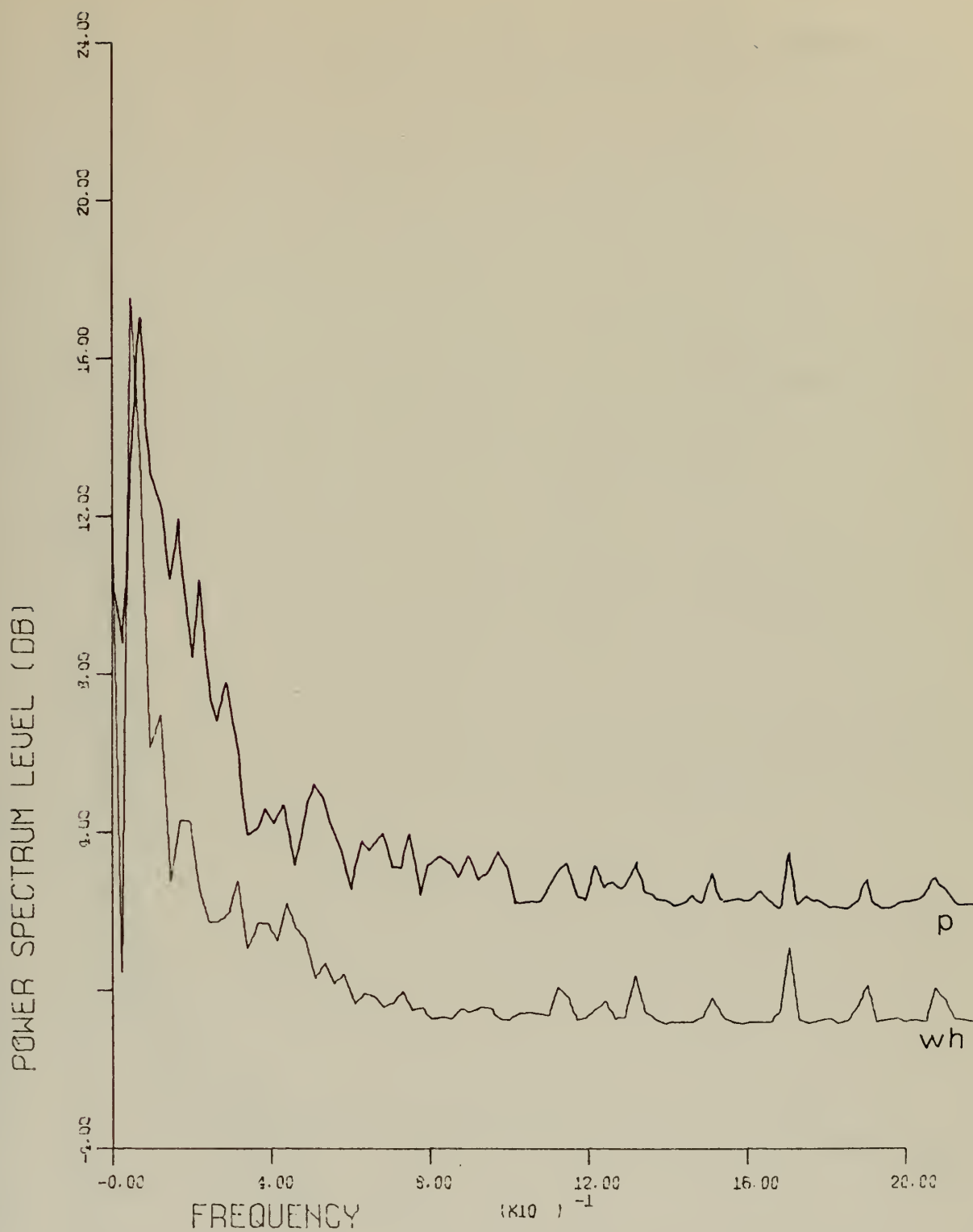
Fig. 31



HAMMING
FREQUENCY = 14790
Fig. 32

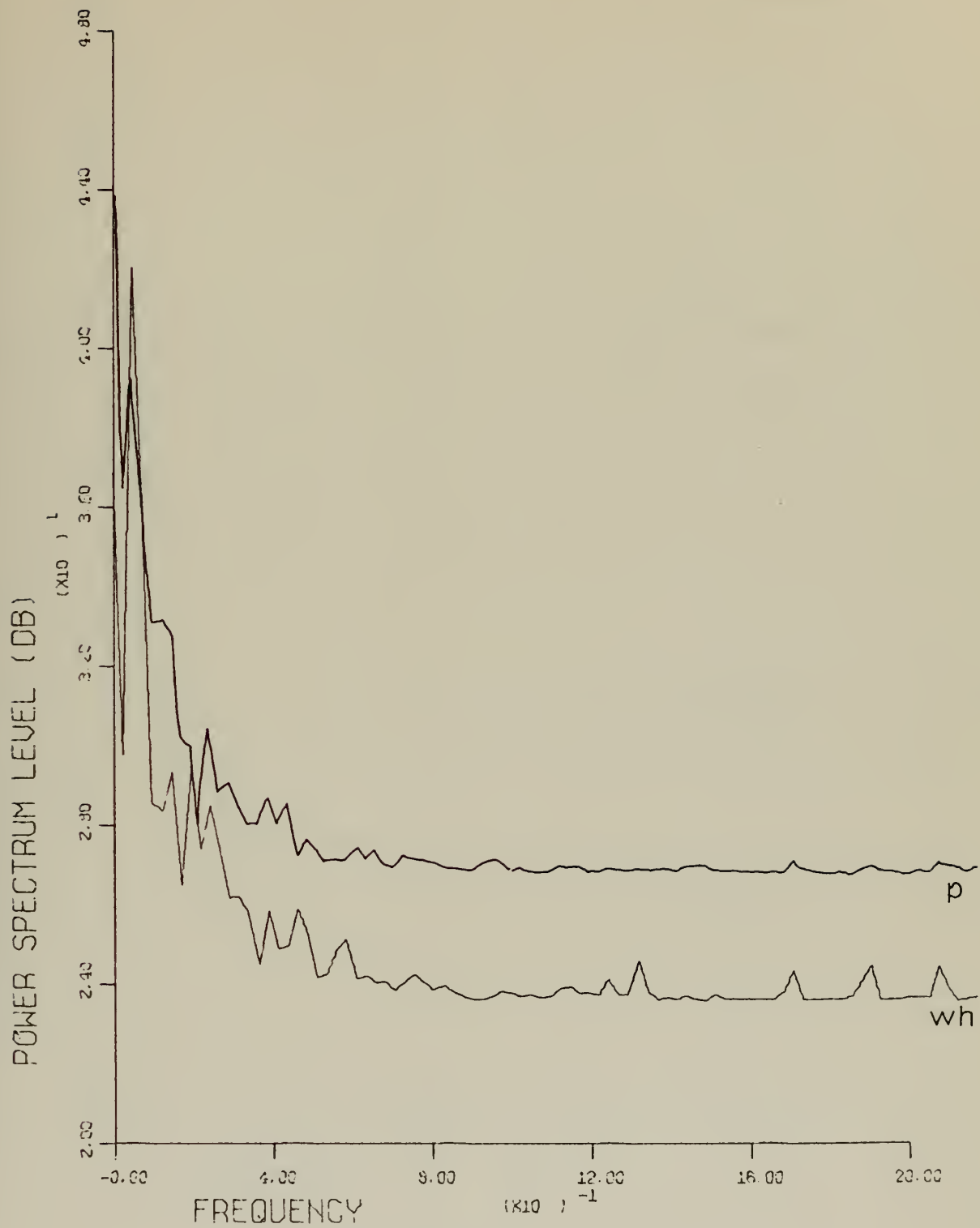


HAMMING
FREQUENCY = 18777
Fig. 33

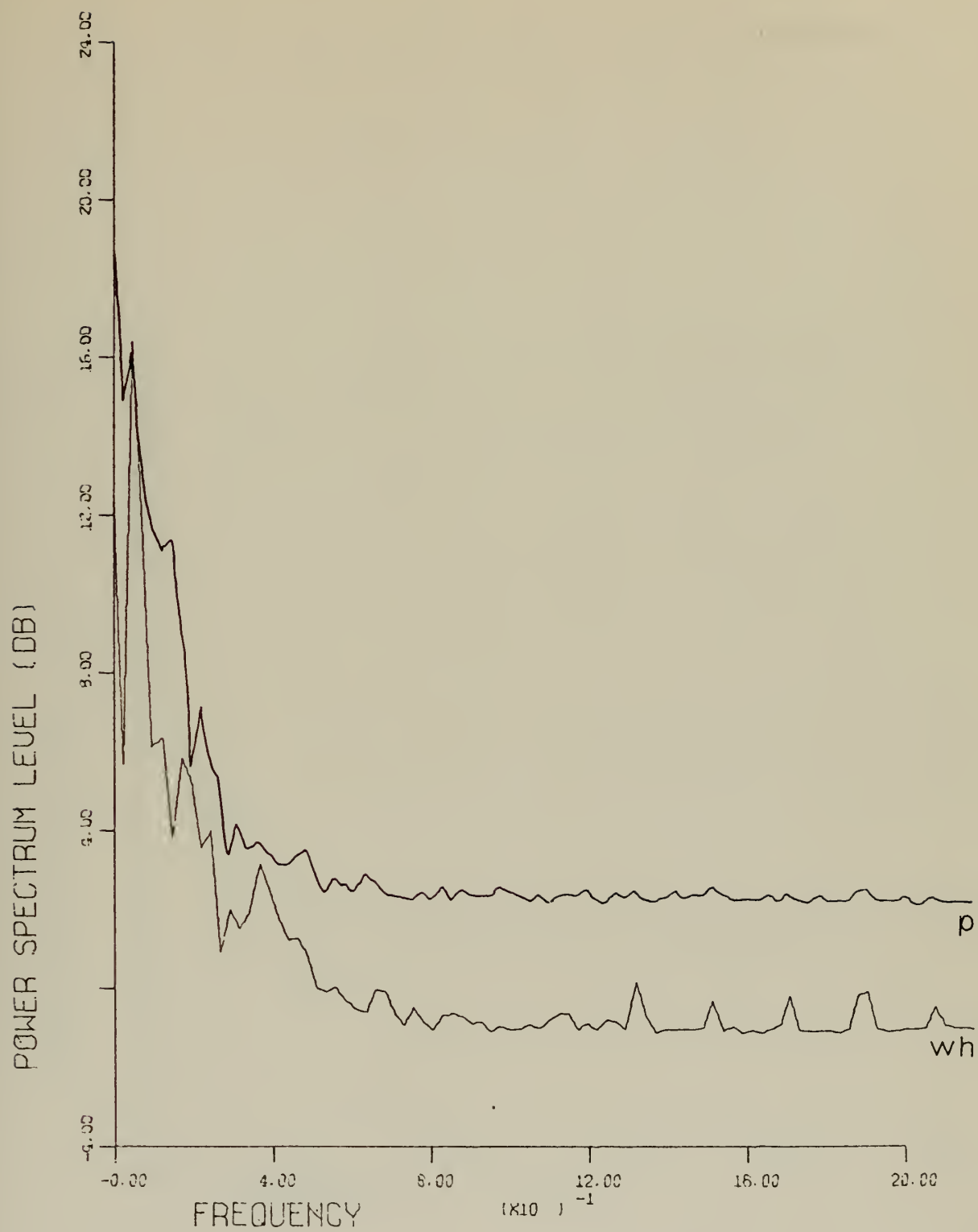


HAMMING
FREQUENCY = 26170
Fig. 34

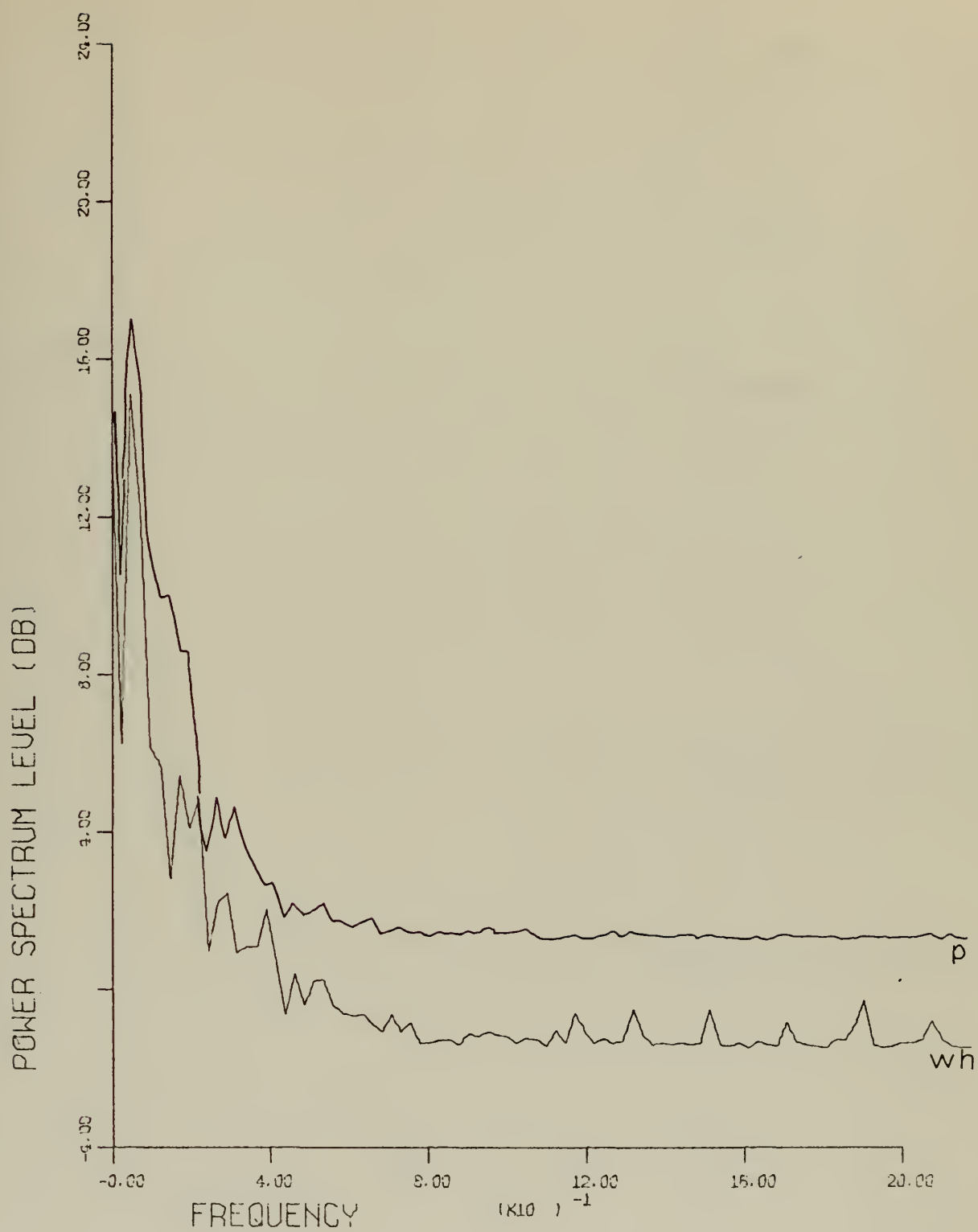




HAMMING
 FREQUENCY = 56245
 Fig. 36



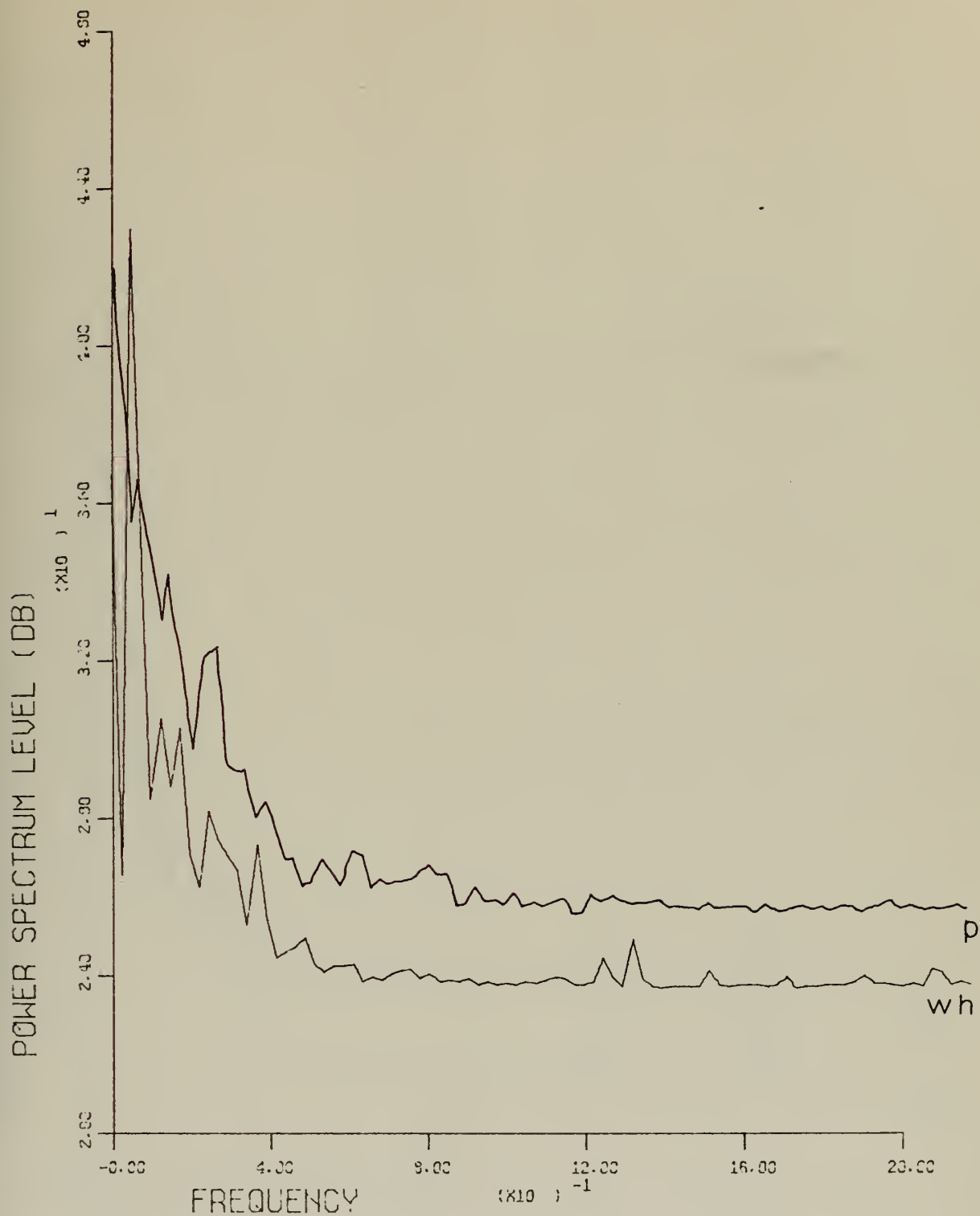
HAMMING
FREQUENCY = 63790
Fig. 37



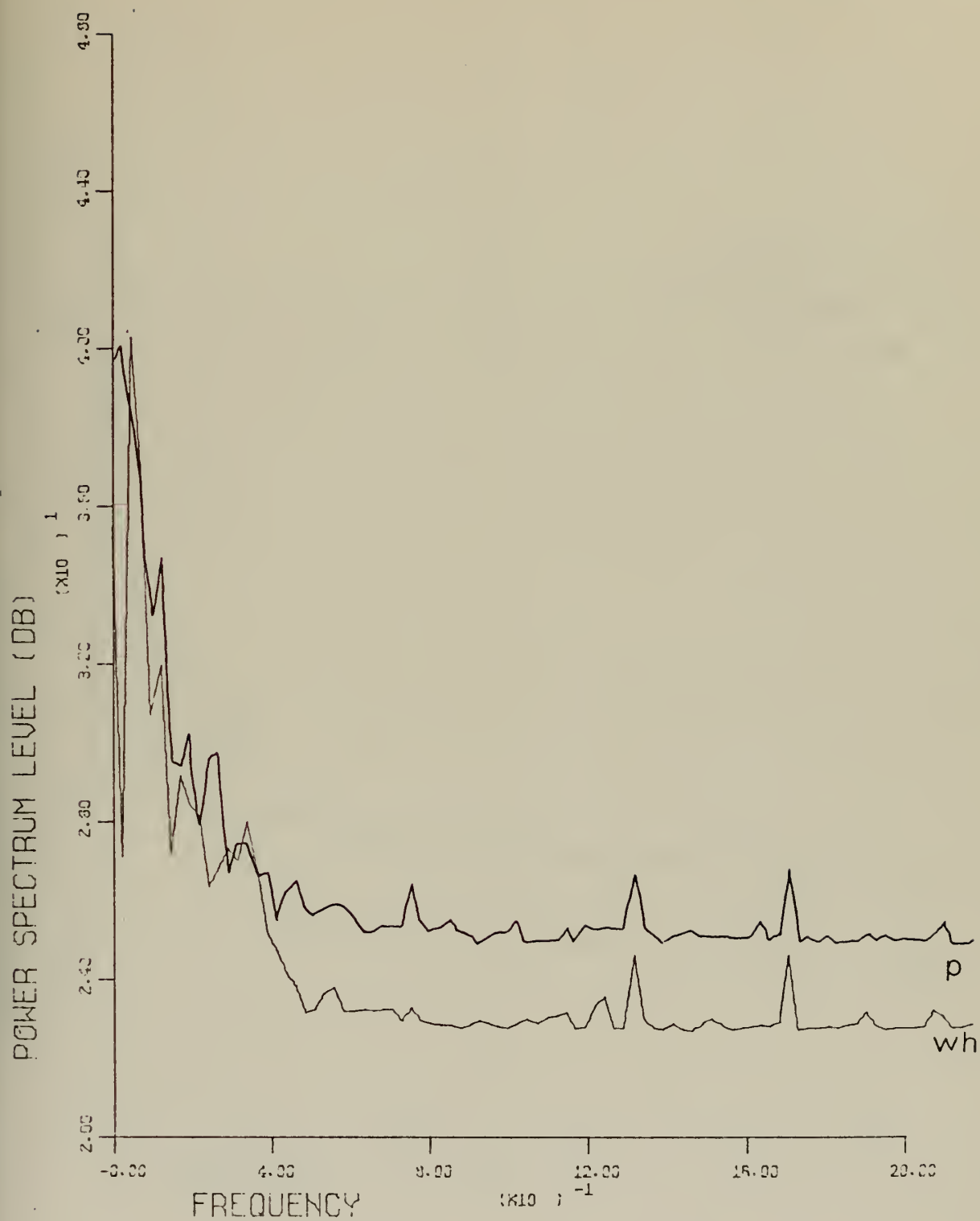
HAMMING
FREQUENCY = 71130
Fig. 38



HAMMING
FREQUENCY = 89900
Fig. 39

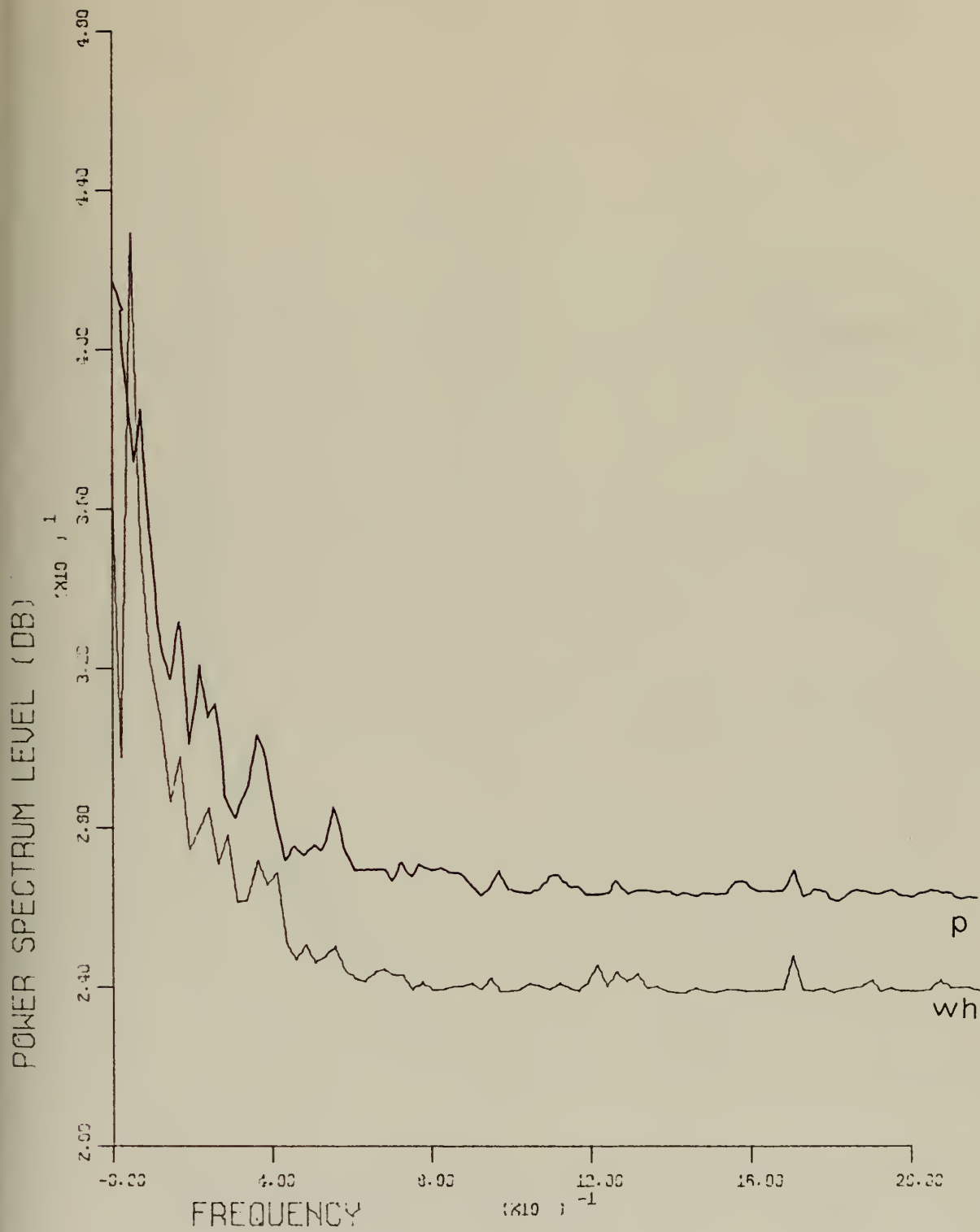


HAMMING
FREQUENCY = 112519
Fig. 40



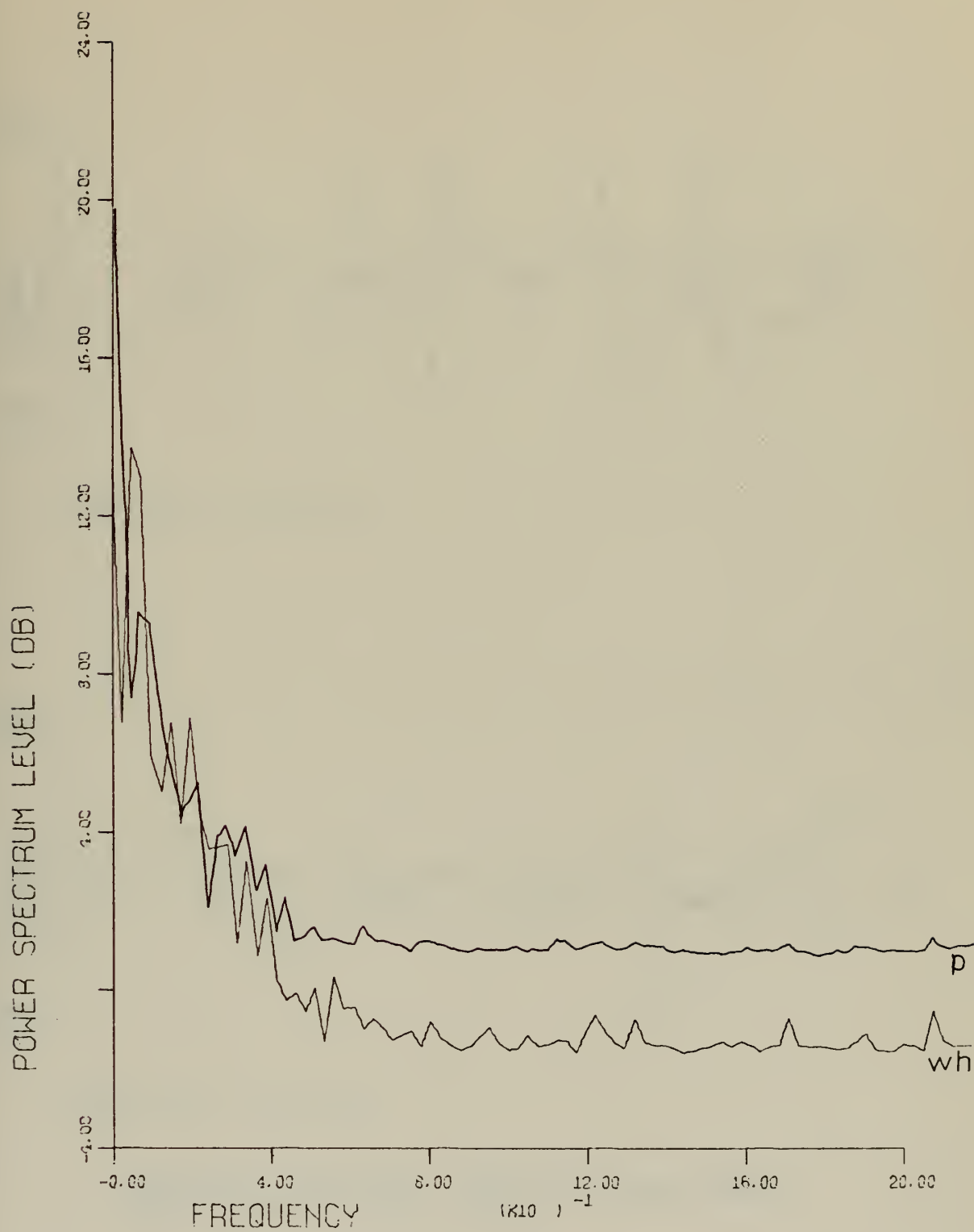
HAMMING
FREQUENCY = 123720

Fig. 41

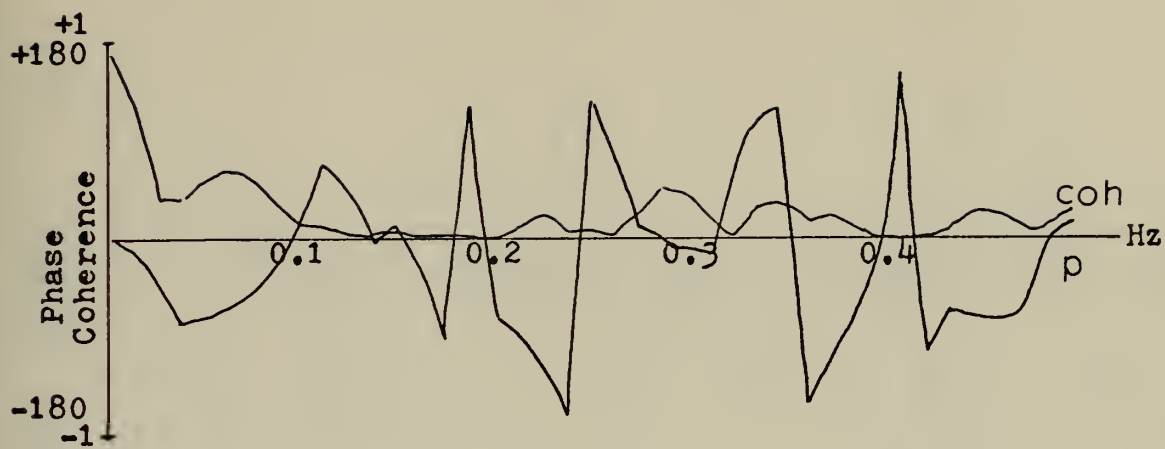


HAMMING
FREQUENCY = 136800

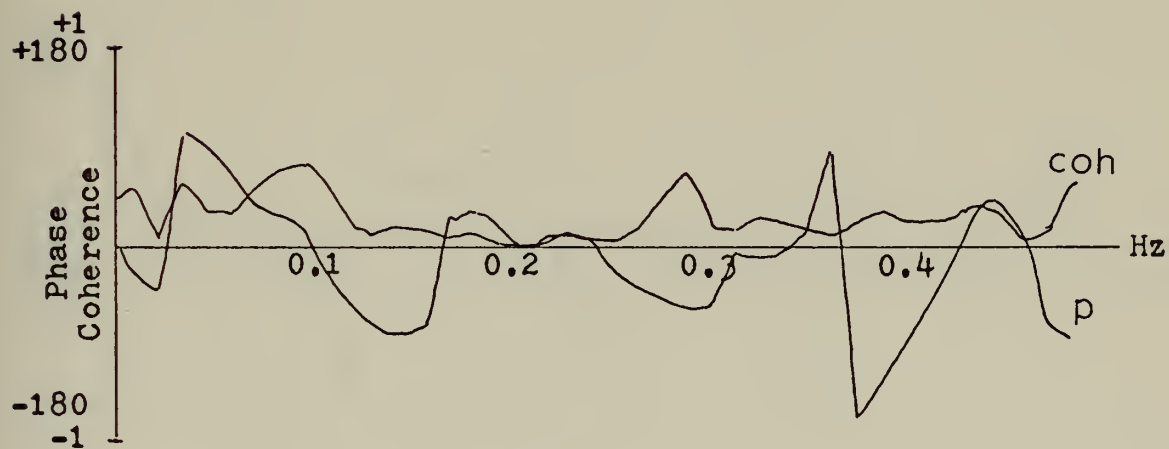
Fig. 42



HAMMING
FREQUENCY = 146100
Fig. 43



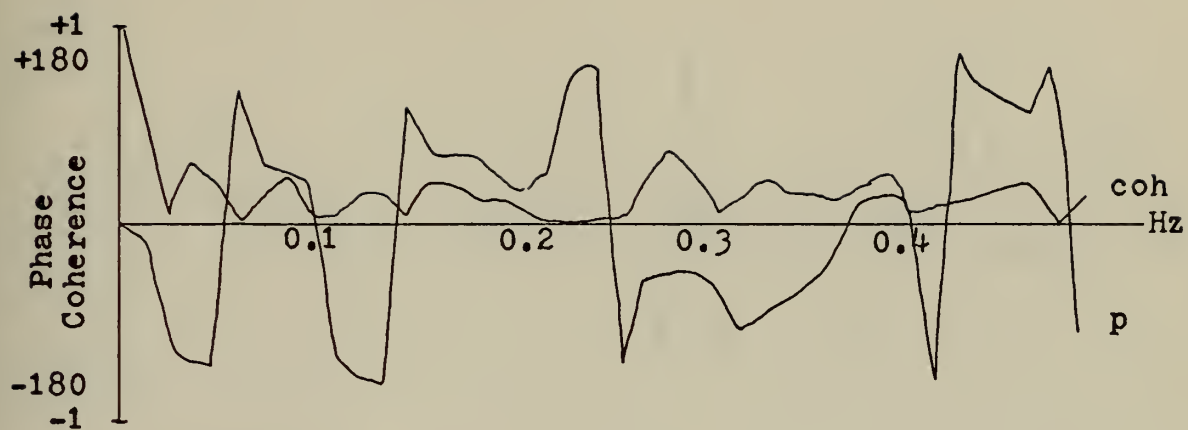
Frequency = 14790 Hz



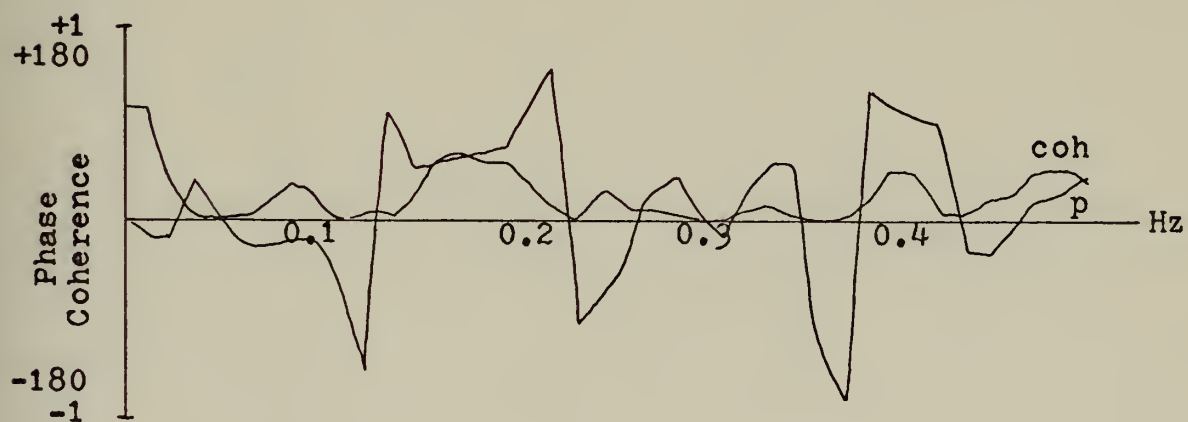
Frequency = 18777 Hz

Coherence Function: Phase and Wave Height
Cross-Spectral Phase Angle

Fig. 44



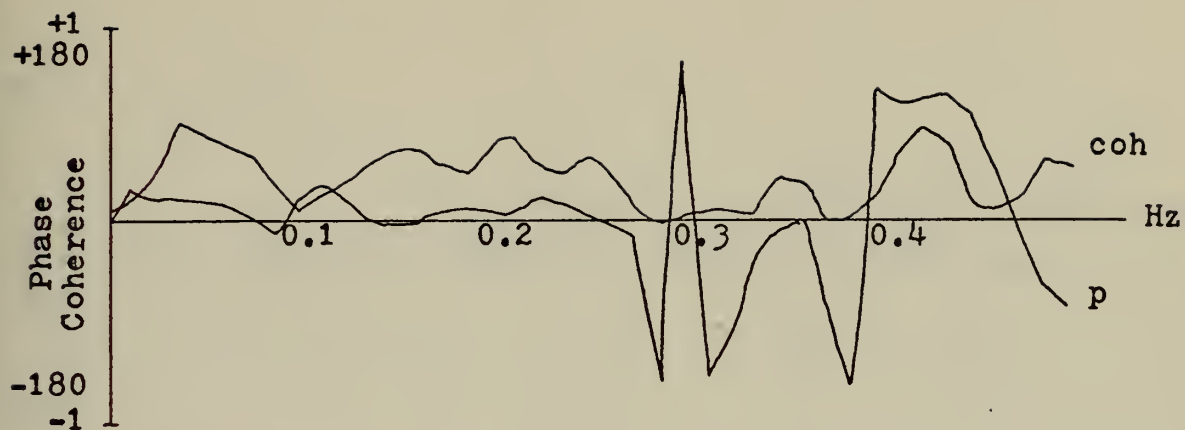
Frequency = 26170 Hz



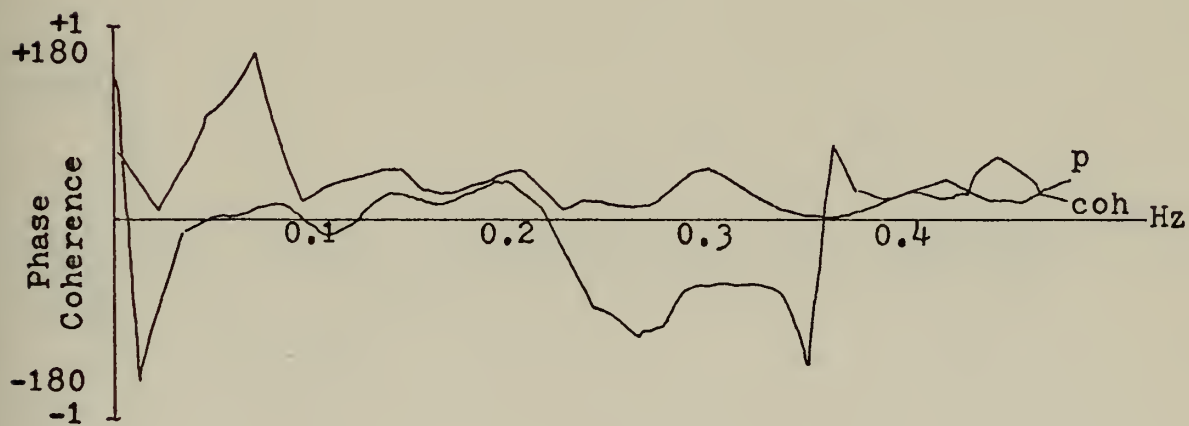
Frequency = 41320 Hz

Coherence Function: Phase and Wave Height
Cross-Spectral Phase Angle

Fig. 45



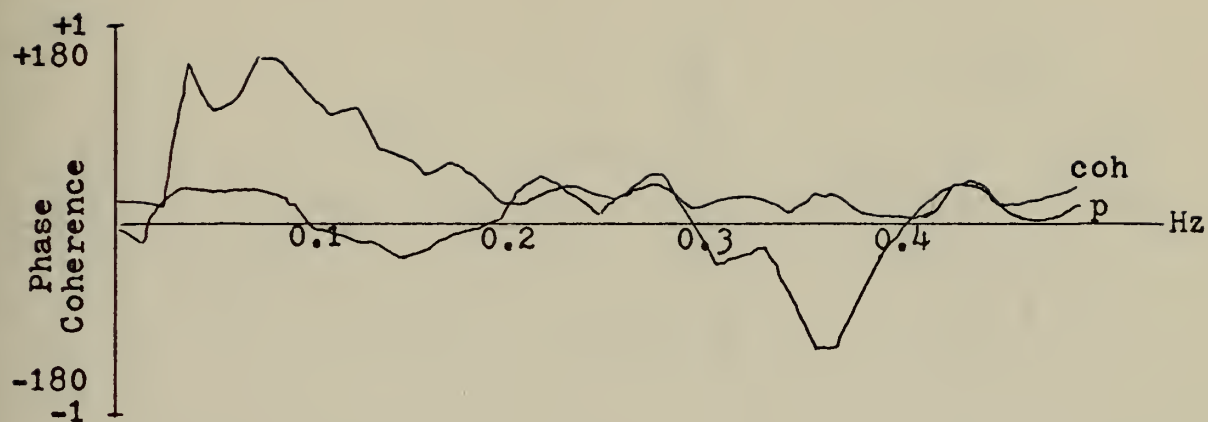
Frequency = 56245 Hz



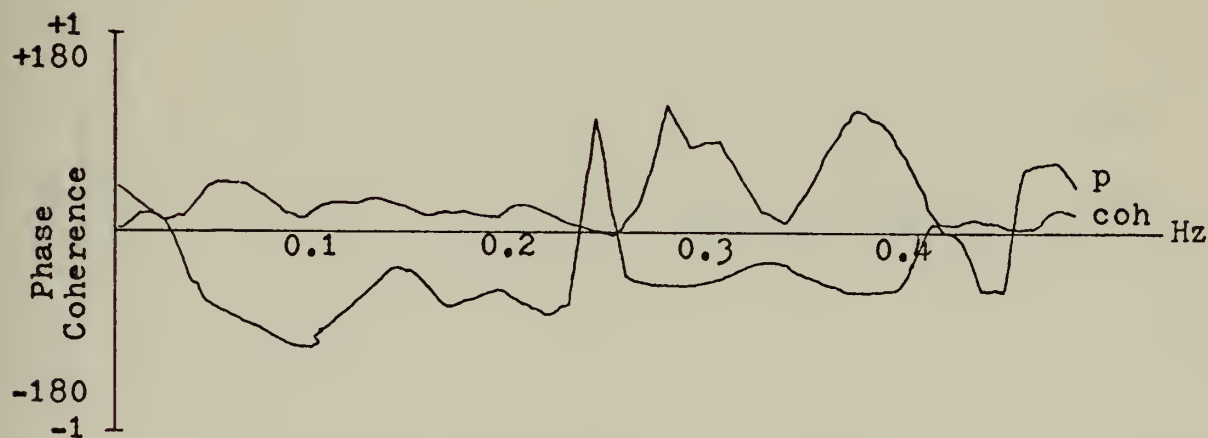
Frequency = 63790 Hz

Coherence Function: Phase and Wave Height
Cross-Spectral Phase Angle

Fig. 46



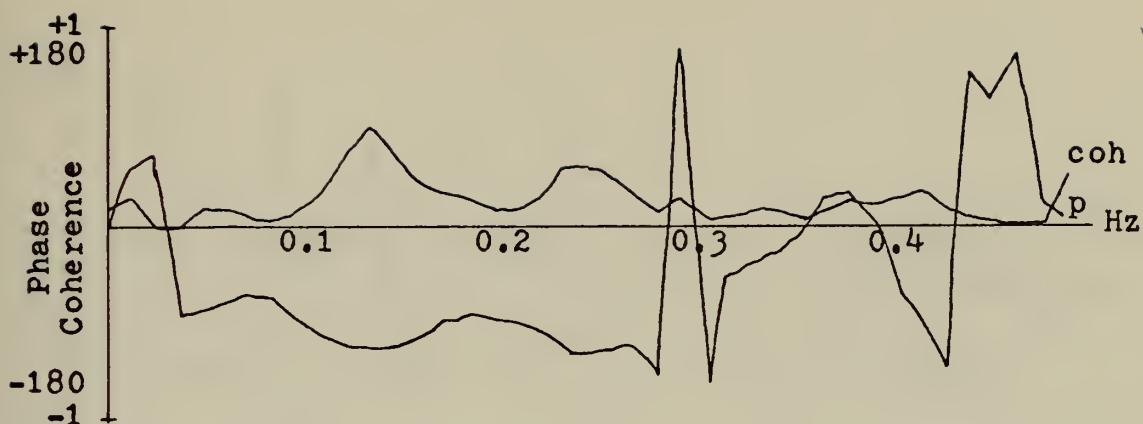
Frequency = 71130 Hz



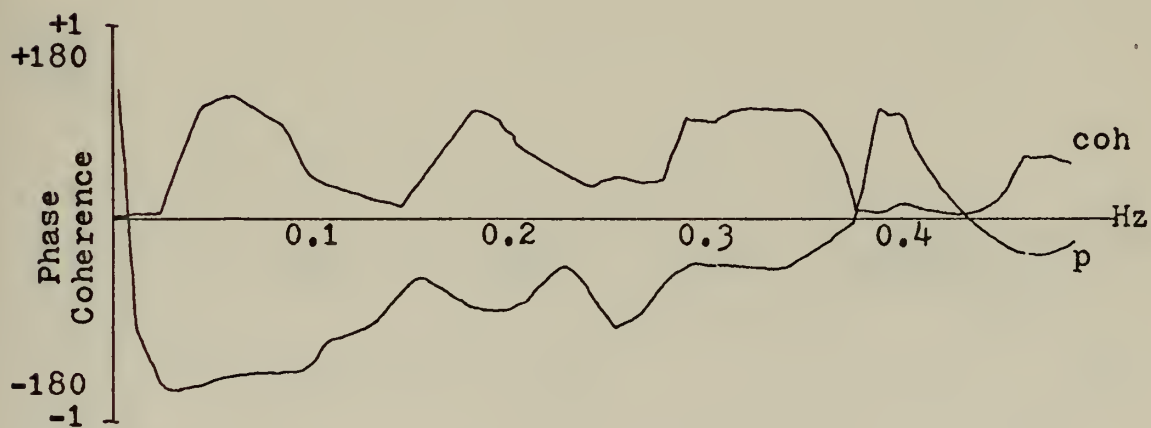
Frequency = 89900 Hz

Coherence Function: Phase and Wave Height
Cross-Spectral Phase Angle

Fig. 47



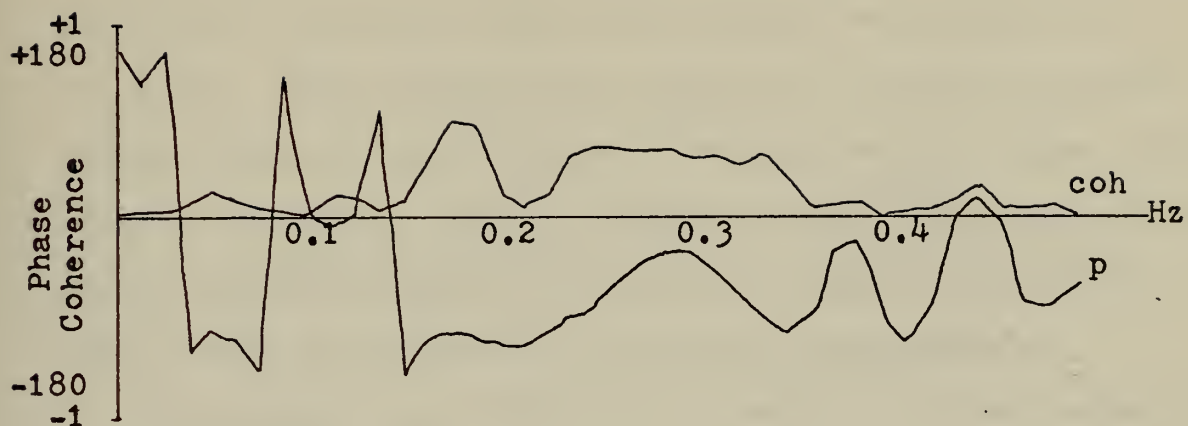
Frequency = 112519 Hz



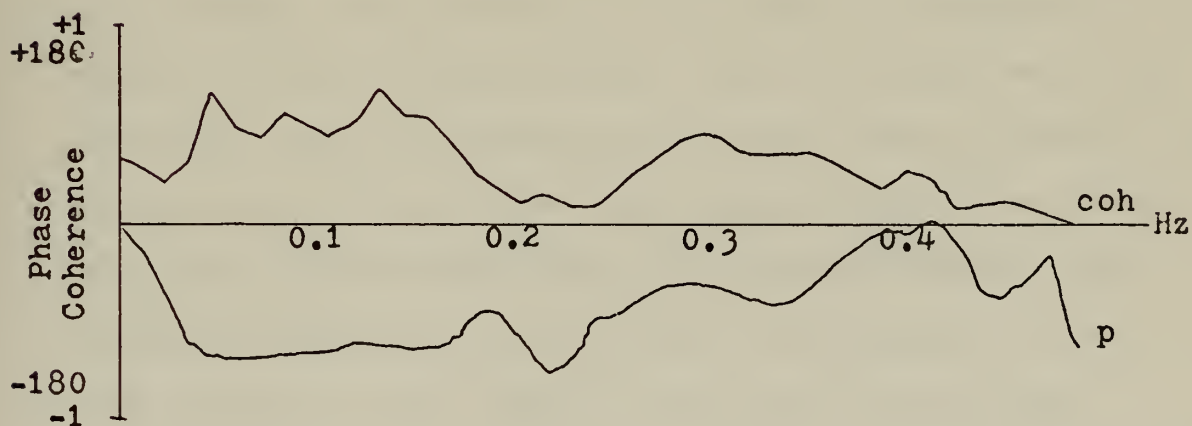
Frequency = 123720 Hz

Coherence Function: Phase and Wave Height
Cross-Spectral Phase Angle

Fig.48



Frequency = 136800 Hz



Frequency = 146100 Hz

Coherence Function: Phase and Wave Height
Cross-Spectral Phase Angle

Fig. 49

IX. SUMMARY AND CONCLUSIONS

The statistics of the instantaneous output of two hydrophones separated by one meter were studied between the frequencies of 15 to 151 kHz. The experiment was carried out from the NUC Oceanographic Research Tower off-shore at Mission Bay, San Diego. This study is of interest because bubbles and upper ocean fluctuations have significant effects on the speed of sound in addition to those caused by temperature and salinity inhomogeneities.

The experiment was conducted at a depth of 11 feet during sea state 1 conditions and a 4 ft peak to trough swell wave in the evening hours 19-2200 on 5 June 1972. The values ranged from +7.8 m/sec to -8 m/sec relative to the empirically predicted values of the Wilson and Leroy equations. The differential speed had a minimum corrected value of -2.4 m/sec at 19 kHz which suggests a batch of bubbles greater than 200 microns have been identified. Possible explanations are that these are bubbles that come from the bottom, or that they represent biological entities. There were speed of sound peaks at 41, 68 and 86 kHz. These identify a large population of bubbles, particularly in the range 56.3 to 71.1 kHz (bubble radii of 50 to 60 microns).

The statistical analysis shows that for frequencies below the peak bubble populations the distribution of the instantaneous sound speed can be approximated by a Gaussian probability density function. At frequencies in and above the bubble populations, the variations in the sound speed lose the smooth Gaussian envelope and become irregular, sometimes double peaked.

The correlation functions show the surface wave height and phase fluctuations are in step at frequencies where bubble populations appear. Above these frequencies the phase and wave height are relatively uncorrelated. There is evidence of long period correlation with internal waves.

The spectral densities of both the phase and wave height show strongest values at frequencies of 0.4 Hz and below. The strongest values in the phase modulation spectrum were for sound in the range 41 to 71 kHz and were identifiable with the surface wave spectrum.

APPENDIX A: PRESENTATION OF DATA

TABLE I. Speed of Sound in Meters per Second

Frequency (kHz)	Segment	Wilson	Leroy	Ramsey	Phase
14.97	1	1515.82	1515.79	1514.70	1509.76
	2	1515.73	1515.70	1514.53	1507.74
	3	1515.85	1515.82	1514.71	1507.82
	4	1515.84	1515.84	1514.75	1507.71
	5	1516.06	1516.02	1514.93	1507.51
	6	1515.97	1515.93	1514.86	1507.73
	7	1515.85	1515.82	1514.73	1507.29
18.78	1	1515.20	1515.17	1514.15	1518.70
	2	1515.29	1515.26	1514.25	1518.10
	3	1515.65	1515.61	1514.58	1517.70
	4	1516.03	1515.99	1514.95	1517.28
	5	1516.09	1516.05	1515.00	1516.39
	6	1516.00	1515.96	1515.00	1517.09
	7	1515.97	1515.03	1514.95	1516.85
22.42	1	1515.85	1515.82	1514.70	1512.15
	2	1515.59	1515.55	1514.56	1511.73
	3	1516.00	1515.96	1514.93	1511.15
	4	1516.06	1516.02	1514.76	1510.91
	5	1516.00	1515.06	1514.63	1511.61
	6	1516.12	1516.08	1515.03	1511.99
	7	1516.44	1516.40	1515.41	1512.53
26.17	1	1515.62	1515.58	1514.50	1515.16
	2	1516.00	1515.96	1514.96	1515.20
	3	1516.59	1516.54	1515.61	1514.80
	4	1515.82	1515.79	1514.66	1514.96
	5	1515.91	1515.87	1514.80	1515.31
	6	1515.59	1515.55	1514.08	1515.17
	7	1515.41	1515.38	1514.26	1515.13
33.70	1	1515.68	1515.64	1514.58	1518.71
	2	1515.65	1515.61	1514.58	1518.75
	3	1515.62	1515.58	1514.58	1518.38
	4	1515.71	1515.67	1514.73	1518.53
	5	1515.88	1515.84	1514.90	1518.78
	6	1515.85	1515.82	1514.86	1518.69
	7	1515.62	1515.58	1514.60	1518.66

TABLE I. (continued)

Frequency (kHz)	Segment	Wilson	Leroy	Ramsey	Phase
37.47	1	1515.08	1515.06	1514.15	1519.28
	2	1515.44	1515.41	1514.56	1518.73
	3	1516.29	1516.25	1515.31	1517.24
	4	1516.06	1516.02	1515.06	1516.50
	5	1515.59	1515.55	1514.63	1516.06
	6	1515.53	1515.50	1514.55	1516.41
	7	1515.94	1515.90	1514.98	1516.65
41.32	1	1514.52	1514.50	1513.56	1523.41
	2	1514.76	1514.74	1513.76	1522.88
	3	1515.68	1515.64	1514.60	1521.55
	4	1515.50	1515.47	1514.45	1520.85
	5	1515.38	1515.35	1514.38	1520.48
	6	1515.71	1515.67	1514.66	1520.79
	7	1515.38	1515.35	1514.38	1521.02
45.04	1	1515.56	1515.53	1514.51	1521.24
	2	1515.68	1515.64	1514.55	1520.48
	3	1515.47	1515.44	1514.41	1520.38
	4	1515.50	1515.47	1514.48	1520.27
	5	1515.85	1515.82	1514.81	1519.79
	6	1516.09	1516.05	1515.08	1519.37
	7	1516.09	1516.05	1515.06	1519.16
48.73	1	1515.20	1515.17	Invalid	1519.81
	2	1515.35	1515.32	1514.40	1519.10
	3	1515.35	1515.32	1514.31	1519.02
	4	1515.35	1515.32	1514.33	1518.91
	5	1515.29	1515.26	1514.30	1518.47
	6	1515.29	1515.26	1514.30	1518.09
	7	1515.59	1515.55	1514.60	1517.89
52.46	1	1515.44	1515.41	1514.45	1519.09
	2	1515.71	1515.67	1514.73	1518.46
	3	1515.79	1515.76	1514.78	1518.08
	4	1515.71	1515.67	1514.75	1517.64
	5	1515.79	1515.76	1514.88	1517.97
	6	1515.73	1515.70	1514.70	1517.57
	7	1515.32	1515.29	1514.36	1517.51

TABLE I. (continued)

Frequency (kHz)	Segment	Wilson	Leroy	Ramsey	Phase
56.25	1	1515.82	1515.79	1514.55	1520.98
	2	1515.59	1515.55	1514.53	1520.53
	3	1515.56	1515.53	1514.41	1520.75
	4	1515.17	1515.15	1514.16	1521.86
	5	1515.50	1515.44	1514.43	1522.07
	6	1515.08	1515.06	1514.05	1522.16
	7	1515.79	1514.76	1513.73	1521.99
63.79	1	1515.76	1515.73	1514.61	1523.16
	2	1515.08	1515.06	1513.88	1522.95
	3	1514.67	1514.65	1513.40	1523.41
	4	1515.05	1515.03	1513.86	1523.26
	5	1515.03	1515.00	1513.86	1523.30
	6	1515.44	1515.41	1514.23	1522.65
	7	1515.56	1515.53	1514.33	1522.27
67.50	1	1516.06	1516.00	1514.73	1522.46
	2	1515.65	1515.61	1514.36	1522.74
	3	1515.65	1515.61	1514.51	1522.44
	4	1515.62	1515.58	1514.31	1522.48
	5	1515.32	1515.29	1514.20	1521.93
	6	1515.44	1515.41	1514.13	1522.41
	7	1515.44	1515.41	1514.23	1522.18
71.13	1	1515.47	1515.44	1514.26	1519.81
	2	1515.76	1515.73	1514.53	1519.95
	3	1516.15	1516.11	1514.88	1519.38
	4	1515.65	1515.61	1514.25	1518.98
	5	1515.68	1515.64	1514.30	1519.51
	6	1515.91	1515.87	1514.58	1519.58
	7	1516.09	1516.05	1514.68	1519.08
74.97	1	1517.66	1517.60	1517.03	1521.76
	2	1517.69	1517.63	1517.18	1521.59
	3	1517.58	1517.51	1516.80	1521.50
	4	1517.40	1517.34	1516.90	1521.47
	5	1517.72	1517.66	1517.13	1521.58
	6	1518.01	1517.94	1517.63	1521.65
	7	1518.18	1518.11	1517.60	1521.55

TABLE I. (continued)

Frequency (kHz)	Segment	Wilson	Leroy	Ramsey	Phase
82.55	1	1518.13	1518.05	1517.48	1523.69
	2	1517.87	1517.80	1517.38	1523.49
	3	1517.90	1517.83	1517.42	1523.44
	4	1517.98	1517.91	1517.50	1523.37
	5	1518.33	1518.25	1517.62	1523.67
	6	Invalid	Invalid	1517.62	1523.50
	7	Invalid	Invalid	1517.72	1523.27
86.21	1	1518.27	1518.20	1517.42	1521.76
	2	1517.98	1517.91	1517.20	1521.87
	3	1517.87	1517.80	1517.10	1521.93
	4	1517.66	1517.60	1516.88	1621.93
	5	1516.88	1516.83	1516.97	1521.91
	6	1517.90	1517.83	1517.12	1522.10
	7	1517.98	1517.91	1517.20	1522.20
89.90	1	Invalid	Invalid	1517.53	1521.05
	2	Invalid	Invalid	1517.40	1520.70
	3	1517.87	1517.80	1517.00	1520.62
	4	1518.16	1518.08	1517.27	1520.74
	5	1518.36	1518.28	1517.58	1520.48
	6	1518.41	1518.33	1517.65	1520.54
	7	1518.44	1518.37	1517.62	1520.82
93.67	1	1518.50	1518.42	1517.77	1521.21
	2	1518.50	1518.42	1517.78	1521.17
	3	1518.53	1518.45	1517.83	1521.10
	4	1518.47	1518.39	1517.75	1520.89
	5	1518.39	1518.30	1517.78	1521.14
	6	1518.50	1518.42	1517.85	1521.19
	7	Invalid	Invalid	1517.87	1521.22
97.44	1	1518.44	1518.37	1517.73	1521.86
	2	1518.27	1518.20	1517.63	1521.87
	3	1518.39	1518.31	1517.77	1521.88
	4	1518.39	1518.31	1517.73	1521.83
	5	1518.36	1518.28	1517.68	1521.82
	6	1518.41	1518.34	1517.57	1522.09
	7	1518.27	1518.20	1517.62	1521.89

TABLE I. (continued)

Frequency (kHz)	Segment	Wilson	Leroy	Ramsey	Phase
101.18	1	1518.44	1518.37	1517.78	1521.82
	2	1518.44	1518.37	1517.78	1521.71
	3	1518.53	1518.45	1517.67	1521.76
	4	1518.59	1518.51	1517.93	1521.87
	5	1518.50	1518.42	1517.83	1521.78
	6	1518.47	1518.39	1517.85	1521.81
	7	1518.59	1518.51	1517.67	1521.71
104.94	1	1518.24	1518.17	1517.43	1522.19
	2	1518.36	1518.28	1517.57	1522.16
	3	1518.47	1518.39	1517.65	1522.18
	4	1518.41	1518.34	1517.60	1522.28
	5	1518.07	1518.00	1517.35	1522.21
	6	1518.47	1518.39	1517.22	1522.08
	7	1518.64	1518.56	1517.84	1522.39
108.72	1	1518.24	1518.17	1517.50	1522.66
	2	1518.24	1518.17	1517.50	1522.79
	3	1518.30	1518.22	1517.48	1522.71
	4	1518.50	1518.42	1517.77	1522.72
	5	1518.59	1518.51	1517.77	1523.02
	6	1518.62	1518.53	1517.80	1522.97
	7	1518.30	1518.22	1517.72	1522.85
112.52	1	1518.44	1518.37	1517.68	1523.69
	2	1518.39	1518.31	1517.62	1523.57
	3	1518.18	1518.11	1517.68	1523.62
	4	1518.07	1519.00	1517.48	1523.67
	5	1518.50	1518.42	1517.83	1523.89
	6	1518.53	1518.45	1517.77	1524.01
	7	1518.33	1518.25	1517.55	1523.79
116.26	1	1518.21	1518.14	1517.55	1523.84
	2	1518.41	1518.34	1517.63	1523.83
	3	1518.56	1518.48	1517.78	1523.75
	4	1518.59	1518.51	1517.76	1523.77
	5	1518.47	1518.39	1517.70	1523.50
	6	1518.56	1518.48	1517.72	1523.52
	7	1518.50	1518.42	1517.75	1523.52

TABLE I. (continued)

Frequency (kHz)	Segment	Wilson	Leroy	Ramsey	Phase
120.00	1	1518.50	1518.42	1517.76	1523.41
	2	1518.53	1518.45	1517.85	1523.34
	3	1518.56	1518.48	1517.80	1523.26
	4	1518.59	1518.51	1517.62	1523.74
	5	1518.21	1518.14	1517.62	1523.33
	6	1518.30	1518.22	1517.45	1523.23
	7	1518.21	1518.14	1517.45	1523.22
123.72	1	1518.41	1518.34	1517.55	1522.86
	2	1518.41	1518.34	1517.55	1523.01
	3	1518.47	1518.39	1517.58	1522.90
	4	1518.44	1518.37	1517.61	1522.81
	5	1518.47	1518.39	1517.65	1522.93
	6	1518.50	1518.42	1517.68	1522.80
	7	1518.50	1518.42	1517.65	1522.87
127.46	1	1518.44	1518.37	1517.45	1522.97
	2	1518.44	1518.37	1517.55	1522.82
	3	1518.44	1518.37	1517.57	1522.77
	4	1518.44	1518.37	1517.25	1522.80
	5	1518.44	1518.37	1517.58	1522.75
	6	1518.44	1518.37	1517.53	1522.78
	7	1518.39	1518.31	1517.50	1522.87
131.19	1	1518.36	1518.28	1517.22	1522.75
	2	1518.36	1518.28	1517.25	1522.70
	3	1518.39	1518.31	1517.27	1522.75
	4	1518.36	1518.28	1517.28	1522.67
	5	1518.44	1518.37	1517.38	1522.68
	6	1518.41	1518.34	1517.40	1522.38
	7	1518.39	1518.31	1517.40	1522.27
136.80	1	1518.13	1518.05	1516.83	1522.78
	2	1518.01	1517.94	1516.75	1522.71
	3	1518.07	1518.00	1516.87	1522.66
	4	1518.30	1518.22	1516.95	1522.65
	5	1518.27	1518.20	1517.17	1522.78
	6	1518.27	1518.20	1517.10	1522.79
	7	1518.27	1518.20	1517.15	1522.39

TABLE I. (continued)

Frequency (kHz)	Segment	Wilson	Leroy	Ramsey	Phase
142.39	1	1518.04	1517.97	1516.90	1522.46
	2	1517.72	1517.66	1516.98	1522.40
	3	1518.10	1518.03	1517.08	1522.78
	4	1518.07	1518.00	1517.17	1522.48
	5	1518.04	1517.97	1517.13	1522.28
	6	1517.98	1517.91	1517.10	1522.34
	7	1517.95	1517.88	1517.10	1522.36
146.10	1	1518.04	1518.00	1518.85	1523.08
	2	1518.13	1518.05	1519.38	1521.92
	3	1517.98	1517.91	1519.15	1521.76
	4	1518.10	1518.03	1519.22	1521.61
	5	1518.10	1518.03	1518.67	1521.63
	6	1517.90	1517.83	1518.75	1521.82
	7	1517.98	1517.91	1519.62	1521.66
151.63	1	1518.24	1518.17	1517.71	1519.80
	2	1518.27	1518.20	1517.42	1520.96
	3	1518.27	1518.20	1517.23	1520.83
	4	1518.21	1518.14	1517.13	1520.76
	5	1518.07	1518.00	Invalid	1520.76
	6	1518.30	1518.22	1517.63	1520.88
	7	1518.39	1518.31	1517.60	1520.72

COMPUTER PROGRAM 1: 7 TO 9 TRACK CONVERT, FILTER AND SCALE

```

DIMENSION IDAT(1024), DAT(1024), DAT1(512), DAT2(512),
1 DAT1C(512), DAT2C(512), XPL0T(5120), Y1PLOT(5120), Y2PLOT(5120),
2 Y3PLOT(5120), Y4PLOT(5120)
DIMENSION DAT1CB(512)
REAL*4 Y1/, PHNC, /
REAL*4 Y2/, PHCL, /
REAL*4 Y3/, WHNC, /
REAL*4 Y4/, WHCL, /
FACTOR=100.0/(2*23)
SCALE1=1.00000
SCALE2=6.096000
REWIND 2
REWIND 4
N=1
LRECL=1024
DIF=4.00000
CLIMB=.2330000
K=0
KEEP=0
J=0
11 READ(2,15,END=50,ERR=60) IDAT
15 FORMAT(8(128A4))
J=J+1
WRITE(6,70) J
70 FORMAT('0',10X,'RECORD NO.=',I4)
CALL FORM(IDAT,LRECL)
DO 22 I=1,LRECL
22 DAT(I)=IDAT(I)*FACTOR
23 DO 199 I=2,LRECL,2
M=I/2
DAT1(M)=DAT(I-1)*SCALE1
DAT2(M)=DAT(I)*SCALE2
199 WRITE(8,16) DAT1
16 WRITE(9,16) DAT2
433 FORMAT(4(128A4))
DO 400 LL=1,512
DAT2C(LL)=DAT2(LL)
WRITE(11,16) DAT2C
DO 293 JJ=1,512
IF(JJ.EQ.1) G3 TO 209
DEL1=ABS(DAT1(JJ-1)-DAT1(JJ))
IF(DEL1.GT.DIF) GO TO 200
IF(K.GT.0) GO TO 202
GO TO 212
200 IF(K.EQ.3) GO TO 201

```



```

201 GO TO 202
    JSAVE=JJ
    SSAVE=DAT1(JSAVE-1)
202 DELTA1=(SSAVE-DAT1(JJ))
    ADELTA=ABS(DELTAL)
    ACLIMB=CLIMB*(K+1)
206 IF(ADELTA.LT.ACLIMB) GO TO 203
    GO TO 217
203 IF(KEEP.GT.0) GO TO 214
    DO 207 KK=1,K
207 DAT1CB(JSAVE-1+KK)=SSAVE1-KK*DELTAL/(K+1)
    K=0
    GO TO 212
209 IF(J.EQ.1) GO TO 212
    IF(K.EQ.0) GO TO 213
    GO TO 214
213 DELS1=ABS(SSAVE2-DAT1(1))
    IF(DELS1.GT.DIF) GO TO 401
    GO TO 212
401 JSAVE=1
    DELTA1=DELS1
    GO TO 217
214 DELTA1=(SSAVE-DAT1(JJ))
    ADELTA=ABS(DELTAL)
    IF(ADELTA.LT.ACLIMB) GO TO 223
    GO TO 217
223 DO 237 KKK=1,KEEP
237 DAT1C(JSAVE-1+KKK)=SSAVE1-KKK*DELTAL/(K+1)
    WRITE(10,16) DAT1C
    WRITE(6,3000) K,JJ
3000 FORMAT(1H,'K=',14,5X,'JJ=',14)
    IF(JJ.EQ.1) GO TO 248
    KT=JJ-1
    WRITE(6,1000)
    FORMAT(1H,'CHECK')
245 DO 247 KIK=1,KT
247 DAT1CB(KIK)=SSAVE1-(KIK+KEEP)*DELTAL/(K+1)
2000 WRITE(6,2000) DAT1CB(KIK)
    KEEP=0
    WRITE(6,2001)
2001 FORMAT(1H,'CHECK2')
248 K=0
    GO TO 292
217 K=K+1
212 ICK=1
292 DAT1CB(JJ)=DAT1(JJ)
293 CONTINUE

```



```

IF(K.GT.0) GO TO 218
SAVE2=DAT1(512)
WRITE(10,16) DAT1CB
GO TO 10
218 SAVE1=DAT1(JSAVE-1)
KEEP=K
WRITE(6,3001) KEEP,SAVE1
3001 FORMAT(1H,'KEEP=',I4,5X,'SAVE1=',F9.4)
DO 219 L1=1,512
219 DAT1C(L1)=DAT1CB(L1)
GO TO 10
60 WRITE(6,61) J
61 FORMAT(10I,5X,'READ ERROR,RECORD NO.=',I3)
GO TO 10
50 WRITE(6,51) N,J
51 FORMAT(10I,5X,'END OF FILE',I2,'RECORD NO.=',I3)
IF(K.GT.0) WRITE(10,16) DAT1CB
REWIND 8
REWIND 9
101 READ(8,16,END=102) DAT1
WRITE(4,16) DAT1
GO TO 101
102 READ(9,16,END=104) DAT2
WRITE(4,16) DAT2
GO TO 102
104 END FILE 4
REWIND 10
REWIND 11
301 READ(10,16,END=302) DAT1C
WRITE(4,16) DAT1C
GO TO 301
302 READ(11,16,END=304) DAT2C
WRITE(4,16) DAT2C
GO TO 302
304 END FILE 4
DO 220 I=1,5120
220 XPLOT(I)=.02*I
REWIND 8
REWIND 9
REWIND 10
REWIND 11
18 READ(8,18) (Y1PLOT(J),J=1,5120)
FORMAT(4(128A4))
READ(10,18) (Y2PLOT(J),J=1,5120)
READ(9,18) (Y3PLOT(J),J=1,5120)
READ(11,18) (Y4PLOT(J),J=1,5120)
WRITE(6,20)
20 FORMAT(1H1,4X,'TIME',5X,'PHASE NC',5X,'PHASE CL',5X,'WAVEH NC',5X,

```



```

1 'WAVEH CL')
1 WRITE(6,19) (XPLLOT(I),Y1PLOT(I),Y2PLOT(I),Y3PLOT(I),Y4PLOT(I),I=1,
15120)
19 FORMAT(5(F9.4,5X))
DO 500 J1=1,2560
TEMP=Y1PLOT(5121-J1)
Y1PLOT(5121-J1)=Y1PLOT(J1)
Y1PLOT(J1)=TEMP
TEMP=Y2PLOT(5121-J1)
Y2PLOT(5121-J1)=Y2PLOT(J1)
Y2PLOT(J1)=TEMP
TEMP=Y3PLOT(5121-J1)
Y3PLOT(5121-J1)=Y3PLOT(J1)
Y3PLOT(J1)=TEMP
TEMP=Y4PLOT(5121-J1)
Y4PLOT(5121-J1)=Y4PLOT(J1)
Y4PLOT(J1)=TEMP
CALL SCALE(XPLLOT,5120,1,20,0,0.50,XMIN,DX)
CALL SCALE(Y1PLOT,5120,1,2,0,0.5,Y1MIN,DY1)
CALL SCALE(Y2PLOT,5120,1,2,0,0.5,Y2MIN,DY2)
CALL SCALE(Y3PLOT,5120,1,2,0,0.5,Y3MIN,DY3)
CALL SCALE(Y4PLOT,5120,1,2,0,0.5,Y4MIN,DY4)
CALL PLOTS
CALL AXIS(0,0,0,0,-3)
CALL AXIS(0,0,20.5,Y1,+4,2,0,0,0,Y1MIN,DY1)
CALL AXIS(2,25,20.5,Y2,+4,2,0,0,0,Y2MIN,DY2)
CALL AXIS(4,50,20.5,Y3,+4,2,0,0,0,Y3MIN,DY3)
CALL AXIS(6,75,20.5,Y4,+4,2,0,0,0,Y4MIN,DY4)
CALL PLOT(0,0,0,-3)
CALL LINE(Y1PLOT,XPLOT,5120,1,1)
CALL PLOT(2,25,0,0,-3)
CALL LINE(Y2PLOT,XPLOT,5120,1,1)
CALL PLOT(2,25,0,0,-3)
CALL LINE(Y3PLOT,XPLOT,5120,1,1)
CALL PLOT(2,25,0,0,-3)
CALL LINE(Y4PLOT,XPLOT,5120,1,1)
CALL SYMBOL(-7.75,22.0,0.49,'FITZGERALD J.R.',0.0,15)
CALL PLOT(-7.75,25.0,-3)
CALL PLOTE
REWIND 8
REWIND 9
REWIND 10
REWIND 11
N=N+1
IF (N.LT.11) GO TO 11
RETURN
END
//GO.FT06F001 DD SYSOUT=A,SPACE=(CYL,(50,1))

```



```

//GO. SYS PLOT DD SYSOUT=C, SPACE=(CYL,(25,2))
//GO. FTJ2F001 DD UNIT=2400-1, VOL=SER=CON7, LABEL=(48,NL,,IN),
// DISP=OLD, DCB=(DEN=1, RECFM=F, BLKSIZE=4096)
//GO. FT04F001 DD UNIT=2400, VOL=SER=PHASE1, DSNNAME=RUF SR2, LABEL=(83,SL),
// DISP=(OLD,KEEP), DCB=(DEN=2, RECFM=FB, LRECL=2048, BLKSIZE=2048)
//GO. FT04F002 DD UNIT=2400, VOL=SER=PHASE1, DSNNAME=RUF SR2, LABEL=(84,SL),
// DISP=(OLD,KEEP), DCB=(DEN=2, RECFM=FB, LRECL=2048, BLKSIZE=2048)
//GO. FT08F001 DD UNIT=SYSDA, DSNNAME=F2614.CHAN1A,
// DCB=(RECFM=FB, LRECL=2048, BLKSIZE=2048), DISP=(NEW,DELETE),
// SPACE=(CYL,(4,1))
//GO. FT09F001 DD UNIT=SYSDA, DSNNAME=F2614.CHAN2A,
// DCB=(RECFM=FB, LRECL=2048, BLKSIZE=2048), DISP=(NEW,DELETE),
// SPACE=(CYL,(4,1))
//GO. FT10F001 DD JNIT=SYSDA, DSNNAME=F2614.CHAN3A,
// DCB=(RECFM=FB, LRECL=2048, BLKSIZE=2048), DISP=(NEW,DELETE),
// SPACE=(CYL,(4,1))
//GO. FT11F001 DD JNIT=SYSDA, DSNNAME=F2614.CHAN4A,
// DCB=(RECFM=FB, LRECL=2048, BLKSIZE=2048), DISP=(NEW,DELETE),
// SPACE=(CYL,(4,1))

```


COMPUTER PROGRAM 2: COMPUTE STATISTICS FOR SEVEN SEGMENTS OF RECORD

```

DIMENSION PHI(1536),CJJ(1536)
REAL*8 DELC,CO
NN=1
77 READ (5,17) FREQ,N,X,DELTA
17 FORMAT (F9.1,I3,2F7.4)
EN=N
DO 30 L=1,7
  READ (4,16) (PHI(K),K=1,1536)
16 FORMAT (4(128A4))
DO 40 J=1,1536
  PHI(J)=PHI(J)-DELTA
  CO=0.0
  PHIAV=0.0
  DELC=0.0
  PHISQ=0.0
  DO 20 J=1,1536
    PHISQ=PHISQ+(PHI(J)*PHI(J))/1536.0
    PHIAV=PHIAV+(PHI(J))/1536.0
    CJJ(J)=(FREQ*X)/(EN+PHI(J)/360.0)/1536.0
    CJJ(J)=CJJ#1536.0
    CO=CO+CJ
20 CO=CO+CJ
DO 199 I=1,1536
  DELC=DELC+((CJJ(I)-CO)**2)/1536.0
199 CALL HIST(CJJ,1536,'SPEED OF SOUND',14,'OCCURRENCES',11)
  CSTAR=(FREQ*X)/(EN+PHIAV/360.0)
  RATIO=CSTAR/CO
  DELPHI=SQRT(PHISQ-PHIAV**2)
  DELC=DSQRT(DELC)
  W=(CO**2-CO*CSTAR)/(2*DELC)
  DELCN=DELC/CO**2
  WRITE (6,19)
19 FORMAT (1H0,5X,'CO',10X,'CSTAR',12X,'STDEV',10X,'DELCN',10X,'PHIAV',
10X,'W',10X,'FREQ',12X,'N',4X,'CSTAR/CO',3X,'SEGMENT')
  WRITE (6,18) CO,CSTAR,DELC,DELCN,PHIAV,W,FREQ,N,RATIO,L
18 FORMAT (7(E15.7),I3,2X,E15.7,I3)
  WRITE(6,99) PHISQ,DELPHI
99 FORMAT(1H0,'PHI MEAN SQUARE = ',E15.7,5X,'STAN DEV = ',E15.7)
30 CONTINUE
STOP
END

```



```

SUBROUTINE HIST (/X/,/N/,/XTITLE/,/NX/,/YTITLE/,/NY/)
  REAL*8 XMEAN,SUMSQ,STDEV
  REAL*4 XRANGE,XQ1,XQ2,XQ3,R
  REAL*4 XSUM,X(1),DIV,YMAX,DY,DY2,XLABEL(15)
  INTEGER J,K,L,M,N,Q1,Q2,Q3,M2M,M1,M12,FMAX,LINE,F(14)
  LOGICAL#1 SORTED,YT,POINTS(49,125),YTITLE(49),XTITLE(131)
  LOGICAL#1 BLANK/,/,EM/M/,CROSS/+,/,VERT/|,/,DASH/!-,/,
    * MEAN/.TRUE./,Q/.TRUE./,DOT/.,/,STAR/*,/,PLUS/+,/,CARRGE
    EQUIVALENCE (SORTED,YT),(Q1,K),(Q2,L,FMAX),(M2M,J)
    EQUIVALENCE (Q3,TEMP,DIV,YMAX)
  SORT BY BUBBLE-UP METHOD
  SORTED=.TRUE.
  DO 20 J=2,N
    L=N-J+2
    DO 10 K=2,L,X(K-1)) GO TO 10
    IF (X(K).GE.X(K-1)) GO TO 10
    SORTED=.FALSE.
    TEMP=X(K-1)
    X(K-1)=X(K)
    X(K)=TEMP
  CONTINUE
  IF (SORTED) GO TO 30
  10 CONTINUE
  20 CONTINUE
  DETERMINE 14 FREQUENCIES
  30 XRANGE = X(N) - X(1)
  R = 126./XRANGE
  DELTA X = XRANGE/14.
  K=1
  DO 50 J=1,14
    F(J)=0
    DIV=X(1)+J*DELTA X
    40 IF (X(K).GT.DIV) GOT050
    F(J)=F(J)+1
    K=K+1
    IF (K.GT.N) GO TO 55
    GO TO 40
  CONTINUE
  50 IF (K.GT.N+1 .OR. K.LT.N) WRITE(6,9000) K,N
  55 IF (K.GT.N) ERROR:- K=1,15,10X,'N =',I5)
  9000 IF (K.LE.N) F(14)=F(14)+N-K+1
  C-----THE FREQUENCIES ARE NOW LISTED IN ARRAY F.
  C-----SET SCALING
    FMAX=F(1)
    DO 60 J=2,14
      IF (F(J).GT.FMAX) FMAX=F(J)
    60 CONTINUE
    YMAX=1.1*FMAX
  C-----BLANK OUT ARRAY

```

```

HIST 10
HIST 20
HIST 30
HIST 40
HIST 50
HIST 60
HIST 70
HIST 80
HIST 90
HIST 100
HIST 110
HIST 120
HIST 130
HIST 140
HIST 150
HIST 160
HIST 170
HIST 180
HIST 190
HIST 200
HIST 210
HIST 220
HIST 230
HIST 240
HIST 250
HIST 260
HIST 270
HIST 280
HIST 290
HIST 300
HIST 310
HIST 320
HIST 330
HIST 340
HIST 350
HIST 360
HIST 370
HIST 380
HIST 390
HIST 400
HIST 410
HIST 420
HIST 430
HIST 435
HIST 440
HIST 450

```



```

DO 70 J=1,49
DO 70 K=1,125
70 POINTS(J,K)=BLANK
C-----DRAW THE BARS
DO 80 J=1,14
LINE = 50.5 - 50.*F(J)/YMAX
IF(LINE.GT.49) GO TO 80
J9M8=J*9-8
DO 80 K=LINE,49
DO 80 L=1,6
POINT(K,J9M8+L)=EM
80 CONTINUE
C-----COMPUTE QUARTILE VALUES
IF (.NOT.Q) GO TO 82
Q1 = N/4
Q2 = N/2
Q3 = N - Q1
M2M = 1 - MOD(N,2)
M1 = 1 - MOD(N,4)/2
M12 = 1 + M1
XQ1 = (M1*X(Q1) + X(Q1+1)) / M12
XQ2 = (M2M*X(Q2) + X(Q2+1)) / (1 + M2M)
XQ3 = (M1*X(Q3 + 1) + X(Q3)) / M12
C-----DRAW QUARTILE LINES
Q1 = R*(XQ1 - X(1)) + 0.5
Q2 = R*(XQ2 - X(1)) + 0.5
Q3 = R*(XQ3 - X(1)) + 0.5
IF (Q1.LE.0) Q1=1
IF (Q3.GE.126) Q3 = 125
DO 240 J=1,49
POINT(J,Q1) = DOT
POINT(J,Q2) = DOT
POINT(J,Q3) = DOT
240 CONTINUE
C-----COMPUTE MEAN AND DRAW IT IN
82 IF (.NOT.MEAN) GO TO 85
SUMSQ=0
XMEAN = 0
DO 25 J = 1,N
SUMSQ=SUMSQ+(X(J)**2)/1536.0
XMEAN = XMEAN + X(J)/1536.0
25 XMEAN = DSQRT(DABS(SUMSQ-XMEAN**2))
M = R*(XMEAN - X(1)) + 0.5
DO 81 J=1,49
81 POINTS(J,M) = STAR
C-----PRINT THE FREQUENCIES
85 WRITE(6,90)F
90 FORMAT ('1',3X,'FREQUENCIES',/2X,14I9)

```

```

HIST 460
HIST 470
HIST 480
HIST 490
HIST 500
HIST 510
HIST 520
HIST 530
HIST 540
HIST 550
HIST 560
HIST 570
HIST 580
HIST 590
HIST 600
HIST 610
HIST 620
HIST 630
HIST 640
HIST 650
HIST 660
HIST 670
HIST 680
HIST 690
HIST 700
HIST 710
HIST 720
HIST 730
HIST 740
HIST 750
HIST 760
HIST 770
HIST 780
HIST 790
HIST 800
HIST 810
HIST 820
HIST 830
HIST 840
HIST 850
HIST 860
HIST 890
HIST 900
HIST 910
HIST 920
HIST 930
HIST 940

```



```

C-----PRINT THE PICTURE
C L=NARGS(L)
  L=6
  NZ=0
  IF (L.EQ.6) NZ = NY
  WRITE (6,100) BLANK,BLANK,BLANK,CROSS,(DASH,K=1,125),CROSS
100  FORMAT(132A1)
  DO 110 J=1,49
  YT=BLANK
  IF (J.LE.NZ) YT=YTITILE(J)
  WRITE(6,100)BLANK,YT,BLANK,VERT,(POINTS(J,K),K=1,125),VERT
110  CONTINUE
115  WRITE(6,100) BLANK,YT,BLANK,(CROSS,(DASH,K=1,8),J=1,14),CROSS
  C-----COMPUTE AND PRINT VALUES ALONG X AXIS
  DO 120 J=1,15
  XLABEL(J)=X(1)+(J-1)*DELTA X
120  XLABEL(J)=X(1)+(J-1)*DELTA X
130  DO 130 J=2,10
  IF (XLABEL(J-1).EQ.0) GO TO 130
130  IF (ABS(XLABEL(J)/XLABEL(J-1)).LT.0.1) XLABEL(J)=0.0
  CONTINUE
  XSUM=AMAX1(ABS(X(1)),ABS(X(N)))
140  XSUM=AMAX1(ABS(X(1)),ABS(X(N)))
150  IF (XSUM.LT.1.) GO TO 150
160  IF (XSUM.LT.10.) GO TO 170
170  IF (XSUM.LT.100.) GO TO 190
180  IF (XSUM.GE.1000) GO TO 220
190  WRITE (6,140) XLABEL
140  FORMAT (1X,14(F5.0,4X),F5.0)
150  GO TO 210
160  WRITE (6,160) XLABEL
160  FORMAT (1X,14(F5.2,4X),F5.2)
170  GO TO 210
180  WRITE (6,180) XLABEL
180  FORMAT (1X,14(F5.1,4X),F5.1)
190  GO TO 210
190  WRITE (6,200) XLABEL
200  FORMAT (1X,14(F5.3,4X),F5.0)
210  GO TO 210
220  WRITE (6,230) X(1),X(N)
230  FORMAT(1X,14(F5.6),X(1) = ,E13.6,10X,'X(N)
*)=,E13.6)
C-----PRINT XTITILE
210  IF (L.LT.4) GO TO 270
214  K=121-NX
215  IF (K.LT.1) K=(133-NX)/2
216  WRITE (6,100) (BLANK,J=1,K),(XTITILE(J),J=1,NX)
270  IF (Q) WRITE (6,250) XQ1,XQ2,XQ3
250  FORMAT (' QUARTILE BOUNDARIES AT ',2(E13.6,','),E13.6)
917  CARRGE=BLANK
HIST 950
HIST 960

HIST 970
HIST 980
HIST 990
HIST 1000
HIST 1010
HIST 1020
HIST 1030
HIST 1040
HIST 1050
HIST 1060
HIST 1070
HIST 1080
HIST 1090
HIST 1100
HIST 1110
HIST 1120
HIST 1130
HIST 1140
HIST 1150
HIST 1160
HIST 1170
HIST 1180
HIST 1190
HIST 1200
HIST 1210
HIST 1220
HIST 1230
HIST 1240
HIST 1250
HIST 1260
HIST 1270
HIST 1280
HIST 1290
HIST 1300
HIST 1310
HIST 1320
HIST 1330
HIST 1340
HIST 1350
HIST 1360
HIST 1370
HIST 1380
HIST 1390
HIST 1400
HIST 1410

```



```

918 IF (Q) CARRGE=PLUS
919 IF (MEAN) WRITE (6,260) CARRGE,XMEAN,STDEV
260 FORMAT (A1,T75,'MEAN = ',E13.6,I0X,'ST DEV = ',E13.6)
920 MEAN=.TRUE.
921 Q=.TRUE.
930 RETURN
ENTRY NOMEAN
MEAN=.FALSE.
ENTRY NOQUAR
Q=.FALSE.
RETURN
END

```

```

HIST1420
HIST1430
HIST1440
HIST1450
HIST1460
HIST1470
HIST1480
HIST1490
HIST1500
HIST1510
HIST1520
HIST1530
HIST1540

```


COMPUTER PROGRAM 3: COMPUTE AUTO AND CROSS CORRELATION FNS AND SPECTRA

```

CALL AUTO(ANORM,BNORM)
CALL CROSS(ANORM,BNORM)
CALL SPECTR(ANORM,BNORM)
CALL PLOTTER
STOP
END

SUBROUTINE AUTO(ANORM,BNORM)
DIMENSION A(512),B(512),SUMA(40),SUMB(40),ATCOR(256),BTCOR(256),
1GAR(512),AX(2048),BX(2048)
REAL*8 AVERTA,AVERTB,SUMA,SUMB
REAL*4 MSQVLA,MSQVLB,MVSQA,MVSQB
CALL SETIME
READ(5,15) NDEC,NLAG,NSAMP,N,NREC
15 FORMAT(5I6)
REWIND 4
KD=NLAG/NSAMP
NREAD=5
17 FORMAT(4(128A4))
DO 3000 IN=1,NREAD
READ(4,17) (AX(K),K=1,2048)
J=0
DO 100 I=1,2048,8
J=J+1
A(J)=AX(I)
CONTINUE
WRITE(8,16) (A(K),K=1,256)
3000 CONTINUE
DO 4321 IM=1,3
READ(4,17) (GAR(K),K=1,512)
DO 3001 JN=1,NREAD
READ(4,17) (BX(K),K=1,2048)
J=0
DO 101 I=1,2048,8
J=J+1
B(J)=BX(I)
CONTINUE
WRITE(9,16) (3(L),L=1,256)
3001 CONTINUE
REWIND 8
REWIND 9
NLES=NDEC-1
FN=N*NDEC
DO 133 J=1,NLAG

```



```

133 ATCOR(J)=0.0
116 BTCOR(J)=0.0
CONTINUE
FORMAT(128A4)
AVERTA=0.0
AVERTB=0.0
DO 331 I=1,NDEC
  READ(8,16) (A(K),K=1,NLAG)
  READ(9,16) (B(L),L=1,NLAG)
DO 110 I=1,N
  AVERTA=AVERTA+A(I)
  AVERTB=AVERTB+B(I)
110 CONTINUE
AVERTA=AVERTA/FN
AVERTB=AVERTB/FN
REWIND 8
DO 131 I=1,NLES
  ILAG=2*NLAG
  READ(8,16) (A(K),K=1,ILAG)
  READ(9,16) (B(L),L=1,ILAG)
DO 130 J=1,NLAG
  FNJ=FN-J+1
  SUMA(II)=0.0
  SUMB(II)=0.0
DO 120 I=1,N
  IJ=I+J-1
  SUMA(II)=SUMA(II)+(A(I)-AVERTA)*(A(IJ)-AVERTA)
  SUMB(II)=SUMB(II)+(B(I)-AVERTB)*(B(IJ)-AVERTB)
120 ATCOR(J)=ATCOR(J)+SUMA(II)/FNJ
130 BTCOR(J)=BTCOR(J)+SUMB(II)/FNJ
DO 79 IJ=1,KD
  BACKSPACE 8
BACKSPACE 9
CONTINUE
79 CONTINUE
131 READ(8,16) (A(K),K=1,NLAG)
  READ(9,16) (B(L),L=1,NLAG)
DO 132 J=1,NLAG
  NJ=N-J+1
  FNJ=FN-J+1
  SUMA(NDEC)=0.0
  SUMB(NDEC)=0.0
DO 121 I=1,NJ
  IJ=I+J-1
  SUMA(NDEC)=SUMA(NDEC)+(A(I)-AVERTA)*(A(IJ)-AVERTA)
  SUMB(NDEC)=SUMB(NDEC)+(B(I)-AVERTB)*(B(IJ)-AVERTB)
121 ATCOR(J)=ATCOR(J)+SUMA(NDEC)/FNJ

```



```

132 BTCOR(J)=BTCOR(J)+SUMB(NDEC)/FNJ
   WRITE(11,16) ATCOR
   WRITE(12,16) BTCOR
   ANORM=ATCOR(1)
   BNORM=BTCOR(1)
DO 38 MN=1,NLAG
   ATCOR(MN)=ATCOR(MN)/ANORM
   BTCOR(MN)=BTCOR(MN)/BNORM
38 CONTINUE
   MVSQA=AVERTA*AVERTA
   MVSQB=AVERTB*AVERTB
   VARA=ANORM
   STDA=SQRT(ANORM)
   MSQVLA=ANORM+AVERTA**2
   VARB=BNORM
   STDB=SQRT(BNORM)
   MSQVLB=BNORM+AVERTB**2
   WRITE(6,22)
22 FORMAT(1H1,20X,'CORRELATION FUNCTION')
26 FORMAT(1H0,'FIRST CHANNEL',8X,'SECOND CHANNEL')
5 DO 5 I=1,NLAG
23 WRITE(6,23) ATCOR(I),BTCOR(I)
   FORMAT(1H,2(E11.4,10X))
   WRITE(6,26)
   WRITE(6,24)
24 FORMAT(1H0,40X,'MEAN')
   WRITE(6,23) AVERTA,AVERTB
33 FORMAT(1H0,40X,'MEAN VALUE SQUARED')
   WRITE(6,23) MVSQA,MVSQB
   WRITE(6,27)
27 FORMAT(1H0,40X,'VARIANCE')
   WRITE(6,23) ANORM,BNORM
   WRITE(6,29)
29 FORMAT(1H0,40X,'STANDARD DEVIATION')
   WRITE(6,23) STDA,STDB
28 FORMAT(1H0,40X,'MEAN SQUARE VALUE')
   WRITE(6,23) MSQVLA,MSQVLB
   WRITE(11,16) ATCOR
   WRITE(12,16) BTCOR
3003 CONTINUE
   CALL GETIME(IET)
   X=IET*.000026
   WRITE(6,99) X
99 FORMAT(1H0,'REAL TIME CLOCK READS',2X,E16.6,3X,'SECONDS')
   RETURN

```



```

END

SUBROUTINE CROSS(ANORM,BNORM)
DIMENSION SUMAB(40),SUMBA(40),ABTCOR(256),BATCOR(256),A(512),B(512)
1) REAL*8 AVERTA,AVERTB,SUMAB,SUMBA
ABNORM=ANORM*BNORM
READ(5,15) NDEC,NLAG,NSAMP,N,NREC
CALL SETIME
15 FORMAT(5I6)
16 FORMAT(128A4)
KD=NLAG/NSAMP
FN=N*NDEC
NLES=NDEC-1
DO 500 J=1,NLAG
ABTCOR(J)=0.0
BATCOR(J)=0.0
2001 IF(NJ) 2001,2000,2001
29 WRITE(6,29)
FORMAT(1H1,20X,'CROSS CORRELATION FUNCTIONS')
1001 WRITE(6,1001)
FORMAT(1H0,'FIRST CHANNEL WITH SECOND CHANNEL',5X,'SECOND CHANNEL
WITH FIRST CHANNEL')
1 REWIND 8
REWIND 9
AVERTA=3.0
AVERTB=0.0
DO 331 I=1,NDEC
READ(8,16) (A(K),K=1,NLAG)
READ(9,16) (B(K),K=1,NLAG)
DO 110 I=1,N
AVERTA=AVERTA+A(I)
AVERTB=AVERTB+B(I)
110 CONTINUE
331 AVERTA=AVERTA/FN
AVERTB=AVERTB/FN
REWIND 8
REWIND 9
ILAG=NLAG*2
DO 231 I=1,NLES
READ(8,16) (A(K),K=1,ILAG)
READ(9,16) (B(L),L=1,ILAG)
DO 230 J=1,NLAG
FNJ=FN-J+1
SUMBA(IJ)=0.0
SUMAB(IJ)=3.0
DO 220 I=1,N

```



```

220 IJ=I+J-1
    SUMAB(II)=SUMAB(II)+(A(I)-AVERTA)*(B(IJ)-AVERTB)
    SUMBA(II)=SUMBA(II)+(B(I)-AVERTB)*(A(IJ)-AVERTA)
230 ABTCOR(J)=ABTCOR(J)+SUMAB(II)/FNJ
    BATCOR(J)=BATCOR(J)+SUMBA(II)/FNJ
    DO 79 IJ=1,KD
    BACKSPACE 8
    BACKSPACE 9
79 CONTINUE
231 READ(8,16) (A(K),K=1,NLAG)
    READ(9,16) (B(L),L=1,NLAG)
    DO 232 J=1,NLAG
    NJ=N-J+1
    FNJ=FN-J+1
    SUMAB(NDEC)=0.0
    SUMBA(NDEC)=0.0
    DO 221 I=1,NJ
    IJ=I+J-1
    SUMAB(NDEC)=SUMAB(NDEC)+(A(I)-AVERTA)*(B(IJ)-AVERTB)
221 SUMBA(NDEC)=SUMBA(NDEC)+(B(I)-AVERTB)*(A(IJ)-AVERTA)
    ABTCOR(J)=ABTCOR(J)+SUMAB(NDEC)/FNJ
232 BATCOR(J)=BATCOR(J)+SUMBA(NDEC)/FNJ
    DO 234 J=1,NLAG
    WRITE(6,1002) ABTCOR(J),BATCOR(J)
234 CONTINUE
    WRITE(14,16) ABTCOR
    WRITE(14,16) BATCOR
1002 FORMAT(1H,2(E11.4,27X))
2000 CONTINUE
    CALL GETTIME(IET)
    X=IET*.000026
    WRITE(6,99) X
99 FORMAT(1H0,'REAL TIME CLOCK READS',2X,E16.6,3X,'SECONDS')
    RETURN
    END

SUBROUTINE SPECTR(ANORM,BNORM)
DIMENSION SPECB(256),SPECB(256),HAMMA(256),HAMMB(256),PARZAB(512),
1RHAMMA(256),RHAMMB(256),M(3),INV(256),S(256),PARZR(1025),PARZI(102
25),PHASE(256),COH(256),ATCOR(256),BTCOR(256),
3SRECA(256),SRECB(256),ABTCOR(256),BATCOR(256),
4TAU(512),FREQ(1025),SCOR(256),DCOR(256)
    READ(5,15) NDEC,NLAG,NSAMP,N,NREC
    FORMAT(5I6)
15 COMPLEX*8 SPECB,HAMMA,HAMMB,PARZAB
    IF(NO.EQ.-1) GO TO 29

```



```

REWIND 11
REWIND 12
READ(11,16) ATCOR
READ(12,16) BTCOR
FORMAT(128A4)
16 DO 1 I=1,NLAG
   SPECB(I)=CMPLX(ATCOR(I),0.0)
   SPECB(I)=CMPLX(BTCOR(I),0.0)
1 M(1)=8
M(2)=0
M(3)=0
WRITE(6,24)
24 FORMAT(1H1,50X,'SPECTRA - AUTO')
WRITE(6,25)
25 FORMAT(1H0,10X,'FIRST CHANNEL',10X,'SECOND CHANNEL')
CALL SETIME
CALL HARM(SPECA,M,INV,S,+1,IFERR)
CALL GETIME(IET)
X=IET*.000026
99 WRITE(6,99) X
FORMAT(1H0,'REAL TIME CLOCK READS',2X,E16.6,3X,'SECONDS')
CALL SETIME
CALL HARM(SPECB,M,INV,S,+1,IFERR)
DO 700 I=1,NLAG
  SRECA(I)=REAL(SPECA(I))
  SRECB(I)=REAL(SPECB(I))
  FORMAT(1H,2(11X,E11.4))
26 WRITE(6,26) SRECA(I),SRECB(I)
700 WRITE(6,24)
WRITE(6,51)
51 FORMAT(1H0,5X,'HAMMING')
WRITE(6,25)
DO 2 I=1,NLAG
  HAMMA(I)=(+.540000+.460000*COS(3.1416*(FLOAT(I-1))/(FLOAT(NLAG-1))
1) )*CMPLX(ATCOR(I),0.0)
  HAMMB(I)=(+.540000+.460000*COS(3.1416*(FLOAT(I-1))/(FLOAT(NLAG-1))
1) )*CMPLX(BTCOR(I),0.0)
  CALL HARM(HAMMA,M,INV,S,+1,IFERR)
  CALL HARM(HAMMB,M,INV,S,+1,IFERR)
DO 710 I=1,NLAG
  RHAMMA(I)=REAL(HAMMA(I))
  RHAMMB(I)=REAL(HAMMB(I))
710 WRITE(6,26) RHAMMA(I),RHAMMB(I)
READ(11,16) ATCOR
READ(12,16) BTCOR
WRITE(11,16) RHAMMA
WRITE(12,16) RHAMMB
29 WRITE(6,27)

```



```

27 FORMAT(1H1,50X,'SPECTRA - CROSS')
WRITE(6,28)
28 FORMAT(1H0,'FIRST CHANNEL WITH SECOND CHANNEL')
WRITE(6,31)
31 FORMAT(1H0,5X,'CO-SPECTRA',5X,'QUAD-SPECTRA',5X,'PHASE',10X,
1,COHERENCE')
REWIND 14
REWIND 15
READ(14,16) ABTCOR
READ(14,16) BATCOR
DO 900 J=1,256
COR1(J)=BATCOR(257-J)
900 COR(J)=BATCOR(257-J)
DO 901 I=257,512
COR1(I)=ABTCOR(I-256)
901 COR(I)=ABTCOR(I-256)
MLAG=NLAG/2
MLAG1=MLAG+1
DO 87 K=1,MLAG
MM=K-1
R=MM
RM=R/NLAG
MA=NLAG+MM
MB=NLAG-MM
UM=1.0-6.0*RM*RM*(1.0-RM)
COR(MA)=COR(MA)*UM
COR(MB)=COR(MB)*UM
87 CONTINUE
DO 88 KK=MLAG1,NLAG
MM=KK-1
R=MM
RM=R/NLAG
RM1=(1.0-RM)
MA=NLAG+MM
MB=NLAG-MM
UM=2.0*RM1*RM1*RM1
COR(MA)=COR(MA)*UM
COR(MB)=COR(MB)*UM
88 CONTINUE
FHZ=3.125
DFHZ=1.00/(DT*NLAG*2.00)
NREQ=FHZ/DFHZ+0.1
DF=DFHZ*6.28318
DT=0.1600
MT=2*NLAG-1
DO 46 JJ=1,MT
TAU(JJ)=JJ-NLAG
46 TAU(JJ)=TAU(JJ)*DT

```



```

DO 47 MM=1,NFREQ
  XN=MM
  FREQ(MM)=(XN-1.0)*DF
  DO 30 JK=1,NLAG
    MM=JK-1
    MA=NLAG+MM
    MB=NLAG-MM
    SCOR(JK)=COR(MA)+COR(MB)
    DCOR(JK)=COR(MA)-COR(MB)
  DO 40 N=1,NFREQ
    SUM1=0.5*(SCOR(1)+SCOR(NLAG)*COS(FREQ(N)*TAU(NLAG)))
    SUM2=0.5*(DCOR(1)+DCOR(NLAG)*SIN(FREQ(N)*TAU(NLAG)))
    C1=COS(FREQ(N)*DT)
    S1=SIN(FREQ(N)*DT)
    CC=1.0
    SC=0.0
    NLAGI=NLAG-1
  DO 36 KJ=2,NLAGI
    CT=CC*C1-SC*S1
    CC=CT
    SC=ST
  SUM1=SUM1+SCOR(KJ)*CC
  SUM2=SUM2+DCOR(KJ)*SC
  PARZR(N)=SUM1/NLAG
  PARZI(N)=SUM2/NLAG
  DO 703 II=1,NLAG
    IF(PARZR(II).EQ.0.0) GO TO 999
    GO TO 6000
  IF (PARZI(II)) 1000,2000,3000
  999 PHASE(II)=-90.0
  1000 GO TO 4000
  2000 PHASE(II)=0.0
  GO TO 4000
  3000 PHASE(II)=+90.0
  GO TO 4000
  6000 PHASE(II)=ATAN(PARZI(II)/PARZR(II))*180.000/3.1416
  4033 COH(II)=((PARZR(II)**2)+(PARZI(II)**2))/((RHAMMA(II))*(RHAMMB(II)))
  II=II+1
  32 FORMAT(1H,4(5X,E11.4))
  733 WRITE(6,32) PARZR(II),PARZI(II),PHASE(II),COH(II)
  38 FORMAT(1H,11X,E11.4)
  ABNORM=ANORM*BNORM
  DO 438 JK=1,512
    COR1(JK)=COR1(JK)/SQRT(ABNORM)
  438 WRITE(6,38) COR1
  WRITE(15,16) COR1
  WRITE(14,16) COH

```



```

8000 WRITE(14,16) PHASE
      CONTINUE
      CALL GETIME(IET)
      X=IET*.000026
      WRITE(6,99) X
      RETURN
      END

      SUBROUTINE PLOTTER
      DIMENSION X1PLOT(256), X2PLOT(256), X3PLOT(256), Y1PLOT(256), Y2PLOT(5
112), X4PLOT(512)
      READ(5,15) NDEC, NLAG, NSAMP, N, NREC
15  FORMAT(5I6)
      CALL SETIME
      REAL*4 XX/,
      M=4
      MLAG=90
      SMRT=6.2500
      DELS=SMRT/NLAG
      X3PLOT(1)=-2.0
      JLAG=NLAG/2
      DO 4001 J=1,512
      X4PLOT(J)=(J-1)/102.4
4001 CONTINUE
      DO 4000 I=1,NLAG
      X1PLOT(I)=(I-1)/SMRT
      X2PLOT(I)=(I-1)*DELS
      IF(I.EQ.1) GO TO 4000
      X3PLOT(I)=ALOG10(X2PLOT(I))
4000 CONTINUE
      CALL SCALE(X1PLOT, NLAG, 1, 5.0, 0.5, X1MIN, DX1)
      CALL SCALE(X2PLOT, MLAG, 1, 5.0, 0.5, X2MIN, DX2)
      CALL SCALE(X3PLOT, JLAG, 1, 5.0, 0.5, X3MIN, DX3)
      IF(N0.EQ.-1) GO TO 29
      REWIND 11
      REWIND 12
      READ(11,16) (Y1PLOT(J), J=1, NLAG)
      READ(11,16) (Y1PLOT(J), J=1, NLAG)
16  FORMAT(128A4)
      CALL SCALE(Y1PLOT, NLAG, 1, 7.00, 0.5, Y1MIN, DY)
      CALL PLOTS
      CALL PLOT(-10.0, 12.0, -3)
      CALL PLOTE
      CALL PLOTS
      CALL PLOTE
      CALL PLOT(.75, 0.0, -3)
      CALL PLOTE
      CALL PLOTS

```



```

CALL PLOT(0.0,0.0,-3)
CALL AXIS(0.78,2.0,XX,M,7.0,90.0,Y1MIN,DY)
CALL PLOT(0.78,2.0,XX,-4,5.0,0.0,X1MIN,DX1)
CALL PLOT(0.78,2.0,-3)
CALL LINE(X1PLOT,Y1PLOT,NLAG,1,1)
CALL SYMBOL(0.5,-0.5,0.14,TIME LAG IN SECONDS',0.0,19)
CALL SYMBOL(0.0,-1.0,0.14,PHASE',0.0,5)
CALL SYMBOL(-0.5,0.5,0.14,TEMPORAL AUTO CORRELATION',90.0,25)
CALL PLOT(-0.78,16.0,-3)
CALL PLOTE
CALL PLOTS
CALL PLOT(-10.0,12.0,-3)
CALL PLOTE
CALL PLOTS
CALL PLOT(-75.0,0,-3)
CALL PLOTE
READ(12,16) (Y1PLOT(J),J=1,NLAG)
READ(12,16) (Y1PLOT(J),J=1,NLAG)
CALL SCALE (Y1PLOT,NLAG,1,7.00,0.5,Y1MIN,DY)
CALL PLOTS
CALL PLOT(0.0,0.0,-3)
CALL AXIS(0.78,2.0,XX,-4,5.0,0.0,X1MIN,DX1)
CALL AXIS(0.78,2.0,XX,M,7.0,90.0,Y1MIN,DY)
CALL PLOT(0.78,2.0,-3)
CALL LINE(X1PLOT,Y1PLOT,NLAG,1,1)
CALL SYMBOL(0.5,-0.5,0.14,TIME LAG IN SECONDS',0.0,19)
CALL SYMBOL(0.0,-1.0,0.14,WAVE HEIGHT',0.0,11)
CALL SYMBOL(-0.5,0.5,0.14,TEMPORAL AUTO CORRELATION',90.0,25)
CALL PLOT(-0.78,16.0,-3)
CALL PLOTE
READ(11,16) (Y1PLOT(J),J=1,NLAG)
DO 3840 KK=1,NLAG
Y1PLOT(KK)=10.0*ALOG10(Y1PLOT(KK))
CALL SCALE (Y1PLOT,MLAG,1,7.00,0.5,Y1MIN,DY)
CALL PLOTS
CALL PLOT(0.0,0.0,-3)
CALL AXIS(0.78,2.0,XX,-4,5.0,0.0,X2MIN,DX2)
CALL AXIS(0.78,2.0,XX,M,7.0,90.0,Y1MIN,DY)
CALL PLOT(0.78,2.0,-3)
CALL LINE(X2PLOT,Y1PLOT,NLAG,1,1)
CALL SYMBOL(0.5,-0.5,0.14,FREQUENCY',0.0,9)
CALL SYMBOL(0.0,-1.0,0.14,PHASE HAMMING',0.0,13)
CALL SYMBOL(-0.5,0.5,0.14,POWER SPECTRUM LEVEL (DB)',90.0,25)
CALL PLOT(-0.78,16.0,-3)
CALL PLOTE
READ(12,16) (Y1PLOT(J),J=1,NLAG)
DO 3841 KK=1,NLAG
Y1PLOT(KK)=10.0*ALOG10(Y1PLOT(KK))

```



```
// SPACE=(CYL,(4,1))  
//GO.SYSIN DD *
```


COMPUTER PROGRAM 4: COMPUTE COHERENCE AND CROSS SPECTRAL PHASE ANGLE

```

C      DATA MUST BE SAMPLED AT EQUAL INTERVALS OF DT
C      IF NFLAG1=0, AUTOSPECTRA.....IF NFLAG1=1
C      NTS= NUMBER OF TIME SAMPLES
C      MLAG = NUMBER OF TIME LAGS
C      DT = TIME INCREMENT
C      DHZ = FREQUENCY SPACING
C      DM = 1/(2*TM)
C      TM = DT*MLAG
C      FBHZ = LOWEST FREQUENCY (HZ)
C      FBHZ = 1/(2*TM) 1/(2*MLAG*DT)
C      FEHZ = HIGHEST FREQUENCY OF INTEREST (HZ)
C      FEHZ = NIQUEST FREQUENCY = 1/(2*DT)
C      CALX1 = CALIBRATION FACTOR FOR TIME SERIES F1
C      CALX2 = CALIBRATION FACTOR FOR TIME SERIES F2
C      H = WATER DEPTH (METERS)
C      X2 = DEPTH OF WAVE PRESSURE TRANSDUCER BELOW SURFACE

C      DIMENSION F1(1300), F2(1300)
C      DIMENSION PHI(511), TAU(511), AX(2048), A(256), SPHI(256), APHI(256),
C      1PHN(256), BX(2048), PHN2(511), PHN1(256), B(256), CSPEC(513), QSPEC(513)
C      2, RESPF(513), PER(513), PHASE(513), COHER(513), FREQ(513), CYCL(513), SPE
C      3C(513), SPE2(513), GAR(512), DFREQ(512)
C      REAL*8 ITITLE(12), ITITEL(12), ITITIL(12), ITITLI(12), ITITLA(12),
C      1ITITAL(12), ITITL(12)
C      REAL*4 LABEL/4H PM/, LABEL2/4H PM/, LABEL2/4HVVHT/, LABEL3/4HEND
C      1 /
C      REAL*4 LABEL1/4H XX /, LABEL4/4HVVHT/, LABEL5/5HPHASE/
C      REAL*4 LABEL6/4HCCOR/
C      96 FORMAT(2I6)
C      98 FORMAT(7H NTS = ,I6//,8H MLAG = ,I6//,6H DT = ,F9.5//,6H DHZ= ,F10
C      1.8//, FBHZ = ,F10.8//, FEHZ = ,F12.8//, CALX1 = ,F10.8//,
C      2, CALX2 = ,F10.8//, H = ,F10.3//, X2 = ,F10.3//)
C      99 FORMAT(2I6,3F10.8)
C      101 FORMAT(4X,10H FREQUENCY,4X,15H AUTO-SPECTRUM1,3X,15H AUTO-SPECTRUM
C      12,3X,12H CO-SPECTRUM,2X,14H QUAD-SPECTRUM,3X15H WAVE PERIOD ,
C      2, PHASE , COHERENCE,/)
C      102 FORMAT(4X,F8.5,7X,E13.7,5X,E13.6,5X,E13.6,3X,F10.5,3X,
C      1F10.5,3X,F10.5)
C      103 FORMAT (9X,49H SMOOTHED(PARZEN WINDOW) ENERGY SPECTRAL DENSITY
C      1//)
C      104 FORMAT(3X,10H (CYC/SEC), 6X,7H M2/HZ)
C      105 FORMAT (10X,24H ENERGY SPECTRAL DENSITY//,5X,10H FREQUENCY,5X,13H
C      1 SPECTRUM)
C      106 FORMAT (5X,F10.5,6X,E12.6)
C      107 FORMAT(5X,F10.6,6X,F10.6,6X,F10.6)
C      COSPECTRA

```



```

WRITE(6,200) (ITITEL(I),I=1,12)
WRITE(6,98) NTS,MLAG,DI,DHZ,FBHZ,CALX1,CALX2,H,X2
C BAND WIDTH FREQUENCIES OF TOTAL ENERGY FLUX- CMIN,CMAX
CMIN = 0.0
CMAX = 2.5
PI=3.14159265
FB = FBHZ*2.0*PI
FE = FEHZ*2.0*PI
DF = DHZ *2.0*PI
FMIN = 2.0*PI*CMIN
FMAX = 2.0*PI*CMAX
C CALCULATING PERIOD AND FREQUENCY ARRAYS
NREQ=(FE-FB)/DF+0.1
DO 14 N=1,NREQ
  XN=N
  FREQ(N)=(XN-1.0)*DF+FB
14 CYCL(N) = FREQ(N)/(2.0*PI)
  PER(1) = 0.0
  DO 15 N = 2,NREQ
15 PER(N) = 1.0/CYCL(N)
C COMPUTING POWER SPECTRUM FIRST TIME SERIES.
C
C READING IN FIRST TIME SERIES F1 AND DETRENDING
REWIND 4
NREAD=5
DO 3000 IN=1,NREAD
  READ(4,16) (AX(K),K=1,2048)
  J=0
  DO 100 I=1,2048,8
    J=J+1
    A(J)=AX(I)
    CONTINUE
100 WRITE(8,18) (A(K),K=1,256)
3000 CONTINUE
4322 DO 4322 IM=1,3
  READ(4,16) (GAR(K),K=1,512)
  DO 3001 JN=1,NREAD
    READ(4,16) (BX(K),K=1,2048)
    J=0
    DO 308 I=1,2048,8
      J=J+1
      B(J)=BX(I)
308 B(J)=BX(I)
3001 WRITE(9,18) (B(L),L=1,256)
      REWIND 8
      REWIND 9
18 FORMAT(2(128A4))
16 FORMAT(4(128A4))

```



```

INT=1
DO 19 JJ=1,NREAD
MINT=INT+255
READ(8,18) (F1(I),I=INT,MINT)
19 INT=INT+256
CALL TREND(F1,NTS,DT,CALX1)
CALL AVER(F1,NTS,DT)
WRITE(6,901)(F1(I),I=1,NTS)
C CALCULATING AUTO-CORRELATION FUNCTION
21 DO 10 M=1,MLAG
SUM=0.0
NMAX=NTS-M+1
DO 8 I=1,NMAX
NN=M+I-1
8 SUM=SUM+F1(I)*F1(NN)
XNMAX=NMAX
XX=M-1
TAU(M)=XX*DT
PHI(M)=SUM/XNMAX
PHN(M)=PHI(M)/PHI(1)
10 CONTINUE
ANORM=PHI(1)
C APPLYING LAG WINDOW
CALL HAMM(MLAG,PHI)
C FOURIER INTEGRAL TRANSFORMING AUTO-CORRELATION FUNCTION
MLAGM1=MLAG-1
XMLAG=MLAG
46 DO 50 N=1,NFREQ
SUM=0.5*(PHI(1)+PHI(MLAG)*COS(FREQ(N)*TAU(MLAG)))
C1=COS(FREQ(N)*DT)
S1=SIN(FREQ(N)*DT)
CC=1.0
SC=0.0
DO 49 M=2,MLAGM1
CT=CC*C1-SC*S1
ST=SC*C1+CC*S1
CC=CT
SC=ST
49 SUM=SUM+PHI(M)*CC
50 SPECT(N)=SUM*2.0/XMLAG
C SPECTRAL VALUES -- A*A/DHZ*DHZ ( AMPLITUDE SQUARED/HZ)
C ROUTINE TO CALCULATE THE VARIANCE BY SUMMING THE AREA UNDER THE SPECTRUM
SUM=0.0
DO 650 N=1,NFREQ
650 SUM=SUM+SPECT(N)
WRITE(6,651) SUM
WRITE(6,798) PHI(1)
IF(NFLAG1) 743,743,744

```



```

744 CONTINUE
C COMPUTING POWER SPECTRUM SECOND TIME SERIES.
C
C READ 2ND TIME SERIES F2 AND DETRENDING
READ(9,18) (F2(I),I=1,NTS)
WRITE(6,901) (F2(I),I=1,NTS)
CALL TREND(F2,NTS,DT,CALX2)
CALL AVER(F2,NTS,DT)
WRITE(6,806)
C CALCULATING AUTO-CORRELATION FUNCTION
DO 70 M=1,MLAG
SUM=0.0
NMAX=NTS-M+1
DO 7 I=1,NMAX
NN=M+I-1
7 SUM=SUM+F2(I)*F2(NN)
XNMAX=NMAX
XX=M-1
TAU(M)=XX*DT
PHI(M)=SUM/XNMAX
PHI1(M) = PHI(M)/PHI(1)
70 CONTINUE
BNORM=PHI(1)
ABNORM=ANORM*BNORM
C APPLYING LAG WINDOW
CALL PARZ(MLAG,PHI)
C WRITE AND DRAW AUTO-CORRELATION FUNCTIONS
WRITE(6,112)
WRITE(6,107) (TAU(M),PHN(M),PHN1(M),M=1,MLAG)
CALL DRAW(256,TAU,PHN1,1,0,LABEL4,ITITLA,0.0,0.0,0.2,0.5,5,0,
1 LAST)
CALL DRAW(256,TAU,PHN,3-0,LABEL,ITITLA,0.0,0.0,0.2,0.5,5,0,
1 LAST)
C FOURIER INTEGRAL TRANSFORMING AUTO-CORRELATION FUNCTION
DO 71 N=1,NFREQ
SUM=0.5*(PHI(1)+PHI(MLAG)*COS(FREQ(N)*TAU(MLAG)))
C1=COS(FREQ(N)*DT)
S1=SIN(FREQ(N)*DT)
CC=1.0
SC=0.0
DO 79 M=2,MLAGM1
CT=CC*C1-SC*S1
ST=SC*C1+CC*S1
CC=CT
SC=ST
79 SUM=SUM+PHI(M)*CC
71 SPE2(N)=SUM*2.0/XMLAG

```



```

C ROUTINE TO CALCULATE THE VARIANCE BY SUMMING THE AREA UNDER THE SPECTRUM
SUM=0.0
DO 660 N=1,NFREQ
660 SUM=SUM+SPE2(N)
WRITE(6,651) SUM
WRITE(6,798) PHI(1)

C
C
C
C COMPUTING CROSS-CORRELATION FUNCTION.
20 MMT=2*MLAG-1
DO 5 M=1,MMT
AB=M-MLAG
MAB=ABS(AB)
IT=NTS-MAB
IF(M-MLAG) 1,1,2
1 IB1=MLAG-M+1
IB2=1
GO TO 3
2 IB1=1
IB2=M-MLAG+1
3 SUM=0.0
DO 4 I=1,IT
I1=IB1+I-1
I2=IB2+I-1
4 SUM=SUM+F1(I1)*F2(I2)
XIT=IT
PHI(M)=SUM/XIT
PHN2(M)=PHI(M)/SQRT(ABNORM)
TAU(M)=M-MLAG
5 PARZEN=TAU(M)*DT
XLAG = MLAG
XLAGH = XLAG/2.0-0.1
MLAGH1 = MLAGH + 1
DO 31 M=1,MLAGH
MM = M-1
R = MM
RM = R/XLAG
MA = MLAG+ MM
MB = MLAG - MM
UM = 1.0-6.0*RM*RM*(1.0-RM)
PHI(MA) = PHI(MA)*UM
PHI(MB) = PHI(MB)*UM
31 CONTINUE
DO 32 M = MLAGH1,MLAG
MM = M-1

```



```

R = MM
RM = R/XMLAG
RM1 = (1.0-RM)
MA = MLAG+MM
MB = MLAG-MM
UM = 2.0*RM1*RM1*RM1
PHI(MA) = PHI(MA)*UM
PHI(MB) = PHI(MB)*UM

32 CONTINUE
C FOURIER INTEGRAL TRANSFORMING THE CROSS-CORRELATION FUNCTION TO OBTAIN
C THE CROSS SPECTRUM
28 DO 30 M=1,MLAG
MM=M-1
MA=MLAG+MM
MB=MLAG-MM
30 SPHI(M)=PHI(MA)+PHI(MB)
APHI(M)=PHI(MA)-PHI(MB)
DO 40 N=1,NFREQ
SUM1=0.5*(SPHI(1)+SPHI(MLAG)*COS(FREQ(N)*TAU(MLAG)))
SUM2=0.5*(APHI(1)+APHI(MLAG)*SIN(FREQ(N)*TAU(MLAG)))
C1=COS(FREQ(N)*DT)
S1=SIN(FREQ(N)*DT)
CC=1.0
SC=0.0
DO 36 M=2,MLAGM1
CT=CC*C1-SC*S1
ST=SC*C1+CC*S1
CC=CT
SC=ST
36 SUM1=SUM1+SPHI(M)*CC
SUM2=SUM2+APHI(M)*SC
CSPEC(N)=SUM1/XMLAG
40 QSPEC(N)=SUM2/XMLAG
WRITE(6,110) (TAU(M),PHN2(M),M=1,MLAG)
WRITE(6,103)
WRITE(6,101)
WRITE(6,104)
C CALCULATING THE PHASE SPECTRUM
DO 17 I=1,NFREQ
PHASE(I) = ATAN( QSPEC(I)/ CSPEC(I))*180.0/3.1416
IF( CSPEC(I).LT.0.0)PHASE(I) = PHASE(I) + 180.0
IF(PHASE(I).GT.180.0) PHASE(I) = PHASE(I)-360.0
C CALCULATING THE COHERENCE SPECTRUM
COHER(I)=(QSPEC(I)*QSPEC(I) + CSPEC(I)*CSPEC(I))/
1 (SQRT(SPEC(I)*SPEC(I))*SPE2(I)*SPE2(I))
17 CONTINUE
IF(NFLAGP) 741,741,742

```



```

742 CONTINUE
741 MFREQ=2*NFREQ
DO 13 N=1,MFREQ
  XM=N
  13 DFREQ(N)=(XM-1.0)*DF/(2.0*PI)
C
C WRITING AND DRAWING SPECTRA
C
DO 51 N=1,NFREQ
  SPEC(N)=10.0*ALOG10(SPEC(N))
  51 SPEC2(N)=10.0*ALOG10(SPEC2(N))
  WRITE(6,102)(CYCL(M),SPEC(M),SPEC2(M),CSPEC(M),QSPEC(M),PER(M),
    1 PHASE(M),COHER(M),M=1,NFREQ)
C PLOT SPECTRA AS A FUNCTION OF FREQUENCY.
CALL DRAW(041,CYCL,SPEC2,1,0,LABEL2,ITITLE,0.1,0.000,0,0,0,0,5,4,
  *0, LAST)
CALL DRAW(041,CYCL,SPEC,3,0,LABEL2,ITITLE,0.1,0.000,0,0,0,0,5,4,
  *0, LAST)
C PLOT PHASE ANGLE AS A FUNCTION OF FREQUENCY.
CALL DRAW(041,CYCL,PHASE,0,0,LABEL,ITITLE,0.1,200.0,1,0,2,0,5,2,
  *0, LAST)
C PLOT COHERENCE AS A FUNCTION OF FREQUENCY.
CALL DRAW(041,CYCL,COHER,0,0,LABEL,ITITLE,0.1,1.0,0,0,0,0,5,1,0,
  * LAST)
CALL DRAW(511,DFREQ,PHN2,0,0,LABEL6,ITITLE,0.0,0.0,0,0,0,0,5,5,0,L
  *AST)
  11 CONTINUE
GO TO 999
C
743 CONTINUE
WRITE(6,107)(TAU(M),PHN(M),M=1,MLAG)
WRITE(6,105)
WRITE(6,106)(CYCL(M),SPEC(M),M=1,NFREQ)
CALL DRAW(435,TAU,PHN,0,0,LABEL,ITITLE,0.0,0.0,2,0,2,0,6,8,1,
  1 LAST)
CALL DRAW(100,CYCL,SPEC,0,0,LABEL,ITITLE,0.1,0.0002,0,0,0,0,6,3,
  10, LAST)
999 STOP
END

SUBROUTINE TREND(FX,NTS,DT,CALXX)
  DIMENSION FX(NTS)
C CALIBRATION RECORD
C COMPUTING THE LINEAR TREND
  FNTS = NTS
  SUMF = 0.0

```



```

101 DO 101 I=1,NTS
    SUMF = SUMF + FX(I)
    SUMF1 = 0.0
DO 102 I=1,NTS
    XI = I
102 SUMF1 = SUMF1 + XI*FX(I)
    XNM1 = NTS-1
    XNPI = NTS+1
    XM = (1.0/DT)*(12.0*SUMF1/(FNTS*XNM1*XNPI)-6.0*SUMF/(XNM1*FNTS))
    B = SUMF/FNTS-XM*XNPI*DT/2.0
    FMEAN = SUMF/FNTS
    WRITE(6,9) FMEAN,XM,B
9   FORMAT (3X,8H MEAN = ,F10.5,3X,9H SLOPE = ,F10.5,3X,13H INTERCEPT
1= ,F10.5//)
DO 103 I=1,NTS
    XI = I
103 FX(I) = FX(I) - (B+XM*XI*DT)
    RETURN
END

SUBROUTINE SMD(MD,X1,X2,NFREQ)
DIMENSION X1(MD),X2(MD)
DO 1 N=1,MD
    NA=N+MD
    NN=NFREQ-N+1
    NB=NN-MD
X2(NN) = 0.25*(X1(1)+X1(NA))+0.5*X1(N)
1 X2(NN) = 0.5*(X1(NN)+X1(NB))
3 MB=MD+1
5 ME=NN-1
    NA=N+MD
    NB=N-MD
2 X2(N)=0.25*(X1(NA)+X1(NB))+0.5*X1(N)
    RETURN
END

C
SUBROUTINE HAMM(MLAG,PHI)
HAMM SUBROUTINE HAMMING LAG WINDOWS THE AUTO-CORRELATION FUNCTION
DIMENSION PHI(MLAG)
PI = 3.14159265
XMLAG = MLAG
DO 31 M=1,MLAG
    R = M
UM = 0.54 + 0.46*COS(PI*R/XMLAG)
PHI(M) = PHI(M)*UM

```



```

31 CONTINUE
RETURN
END

SUBROUTINE AVER (FX,NTS,DT)
C SUBROUTINE FOR CALCULATING TURBULENT INTENSITY, URMS
C
DIMENSION FX(NTS)
U2=0.0
SUMU2=0.0
DO 151 I=1,NTS
U2 = FX(I)*FX(I)
SUMU2 = SUMU2 + U2
151 CONTINUE
FNTS = NTS
U2 = SUMU2/FNTS
URMS = SQRT(U2)
WRITE(6,152) U2,URMS
152 FORMAT (3X,6H H2 = ,F10.5,3X,8H HRMS = ,F10.5,5H M )
COMPUTING AVERAGE PERIOD, T
COUNTS THE TOTAL ZERO UP-CROSSINGS
USUM = 0.0
K = 1
68 N = K
69 N = N+1
IF(FX(N)) 73,69,69
73 K=N
71 K = K+1
IF(FX(K))71,71,80
80 USUM = USUM + 1.0
IF(NTS-K) 83,83,68
83 T = FNTS*DT/USUM
82 WRITE(6,82) T
FORMAT (3X,18H AVERAGE PERIOD = ,F10.5,4H SEC//)
RETURN
END

SUBROUTINE PARZ(MLAG,PHI)
C PARZ SUBROUTINE PARZEN FILTERS AUTO-CORRELATION FUNCTION
C
DIMENSION PHI(MLAG)
XMLAG = MLAG
MLAGH = XMLAG/2.0-0.1
MLAGH1 = MLAGH + 1
DO 31 M=1,MLAGH
MM = M-1

```



```

R = MM
RM = R/XMLAG
UM = 1.0-6.0*RM*RM*(1.0-RM)
PHI(M) = PHI(M)*UM
31 CONTINUE
DO 32 M = MLAGH1,MLAG
MM = M-1
R = MM
RM = R/XMLAG
RM1 = (1.0-RM)
UM = 2.0*RM1*RM1*RM1
PHI(M) = PHI(M)*UM
32 CONTINUE
RETURN
END
//GO.FT06F001 DD SYSOUT=A,SPACE=(CYL,(6,1))
//GO.FT04F001 DD DISP=(OLD,KEEP),UNIT=2311,DSNAME=RUF SR2.FILE38,
// VOLUME=SER=SYS005
//GO.FT08F001 DD JUNIT=SYSDA,DSNAME=F2614.CHAN1A,
// DCB=(RECFM=FB,LRECL=1024,BLKSIZE=2048),DISP=(NEW,PASS),
// SPACE=(CYL,(4,1))
//GO.FT09F001 DD JUNIT=SYSDA,DSNAME=F2614.CHAN2A,
// DCB=(RECFM=FB,LRECL=1024,BLKSIZE=2048),DISP=(NEW,PASS),
// SPACE=(CYL,(4,1))
//GO.SYSIN DD *

```


BIBLIOGRAPHY

1. Wilson, Wayne D., "Extrapolation of the Equation for the Speed of Sound in Sea Water," Journal of the Acoustical Society of America, v. 34, No. 6, p. 866, June 1962.
2. Leroy, C.C., "Development of Simple Equations for Accurate and More Realistic Calculation of the Speed of Sound in Seawater," Journal of the Acoustical Society of America, v. 46, No. 1, p. 216-226, June 1968.
3. Rautmann, Jurgen, Sound Dispersion and Phase Fluctuations in the Upper Ocean, Thesis, Naval Postgraduate School, Monterey, 1971.
4. Meyer, E. Skudrzyk, Sound Absorption and Sound Absorbers in Water, NAV SHIPS 900.164, v. 1, 1 December 1950.
5. Chernov, Lev A., Wave Propagation in a Random Medium, Dover Publications, Inc., 1967.
6. Enochson, L.D., and Otnes, R.K., Programming and Analysis for Digital Time Series Data, The Shock and Vibration Center, United States Department of Defense, 1968.
7. Bendat, J.S., and Pierson, A.G., Measurement and Analysis of Random Data, John Wiley and Sons, Inc., 1958.
8. Albers, V.M., Underwater Acoustics Handbook, The Pennsylvania State University Press, 1960.
9. Deven, C., Jr., Survey of Thermal, Radiation, and Viscous Damping of Pulsating Air Bubbles in Water, Journal of the Acoustical Society of America, v. 31, December 1959, p. 1654-1667.
10. Glotov, V.P., Kolobaeu, P.A., and Nenimin, G.G., Investigation of the Scattering of Sound by Bubbles Generated by an Artificial Wind in Sea Water and the Statistical Distribution of Bubble Sizes, Soviet Physics-Acoustics, v. 7, Apr. Jun 1962, p. 341-345.
11. Buxcey, S., McNeil, J.E., Marks, R.H., Jr., Acoustic Detection of Microbubbles and Particulate Matter Near the Sea Surface, Thesis, Naval Postgraduate School, Monterey, Calif., 1965.

INITIAL DISTRIBUTION LIST

	No. Copies
1. Defense Documentation Center Cameron Station Alexandria, Virginia 22314	2
2. Library, Code 0212 Naval Postgraduate School Monterey, California 93940	2
3. Commander, Naval Ship Systems Command Attn: Mr. Woodie L. Thompson Department of the Navy, Code PMS 302 Washington, D.C. 20360	1
4. Commander, Naval Ship Systems Command Attn: Mr. Alfred P. Franceschetti Department of the Navy, Code PMS 302-4 Washington, D.C. 20360	2
5. Dean of Research Administration Naval Postgraduate School Monterey, California 93940	1
6. Professor H. Medwin, Code 61Md Department of Physics & Chemistry Naval Postgraduate School Monterey, California 93940	10
7. Assoc. Professor W.W. Denner, Code 58Dw Department of Oceanography Naval Postgraduate School Monterey, California 93940	1
8. Asst. Professor E.B. Thornton, Code 58Tm Department of Oceanography Naval Postgraduate School Monterey, California 93940	1
9. Assoc. Professor N.E. Boston, Code 58Bb Department of Oceanography Naval Postgraduate School Monterey, California 93940	1
10. Asst. Professor G. Garrettson, Code 61Gr Department of Physics & Chemistry Naval Postgraduate School Monterey, California 93940	1

- | | | |
|-----|--|---|
| 11. | LCDR James R. Fitzgerald
Box 1667
Naval Postgraduate School
Monterey, California 93940 | 1 |
| 12. | Professor Peter C.C. Wang, Code 52Wf
Department of Mathematics
Naval Postgraduate School
Monterey, California 93940 | 1 |
| 13. | Mr. William Smith
Department of Physics & Chemistry
Naval Postgraduate School
Monterey, California 93940 | 1 |
| 14. | Director Acoustic Programs (Code 468)
Office of Naval Research
Department of the Navy
Arlington, Virginia 22217 | 1 |

DOCUMENT CONTROL DATA - R & D

(Security classification of title, body of abstract and indexing annotation must be entered when the overall report is classified)

1. ORIGINATING ACTIVITY (Corporate author)

Naval Postgraduate School
Monterey, California 93940

2a. REPORT SECURITY CLASSIFICATION

Unclassified

2b. GROUP

3. REPORT TITLE

Statistical Study of Sound Speed in the Inhomogeneous Upper Ocean

4. DESCRIPTIVE NOTES (Type of report and, inclusive dates)

Master's Thesis; December 1972

5. AUTHOR(S) (First name, middle initial, last name)

James R. Fitzgerald

6. REPORT DATE

December 1972

7a. TOTAL NO. OF PAGES

130

7b. NO. OF REFS

11

8a. CONTRACT OR GRANT NO.

b. PROJECT NO.

c.

d.

9a. ORIGINATOR'S REPORT NUMBER(S)

9b. OTHER REPORT NO(S) (Any other numbers that may be assigned this report)

10. DISTRIBUTION STATEMENT

Approved for public release; distribution unlimited.

11. SUPPLEMENTARY NOTES

12. SPONSORING MILITARY ACTIVITY

Naval Postgraduate School
Monterey, California 93940

13. ABSTRACT

The statistics of the fluctuations of the in-situ speed of sound in the upper ocean have been studied by analyzing the instantaneous phase difference of the output of two hydrophones separated by one meter for sounds of frequency 15 to 151 kHz. The experiment was conducted at 11 ft in water of depth 60 ft in low sea states at night. Comparison of the speed calculated from the time averaged phase difference, with the speed given by velocimeter or empirical relations, yielded differential speeds which deviate by 1 m/sec to 8 m/sec from the accepted values, for frequencies less than 100 kHz. Correlation and spectral analysis of the sound phase and ocean height fluctuations has shown the close relation between these two parameters. There is strong evidence of the presence and importance of bubbles in all of the results, particularly of a large population resonant in the frequency range 56.3 to 71.1 kHz (radius 50 to 60 microns). Evidence is presented to suggest that bubbles appear at the surface during internal wave activity at lower depths and that for sound frequencies near the bubble resonances the sound phase is strongly modulated by, and in phase with, the ocean wave height.

14

KEY WORDS

LINK A

LINK B

LINK C

ROLE

WT

ROLE

WT

ROLE

WT

Speed of sound

Dispersion

Phase fluctuations

Bubbles

Upper ocean

29 JUL 76
20 OCT 78

24342
25558

Thesis

138437

F478 Fitzgerald

c.1 Statistical study of
sound speed in the in-
homogeneous upper ocean.

29 JUL 76
20 OCT 78

24342
25558

Thes
F478
c.1

Thesis

138437

F478 Fitzgerald

c.1 Statistical study of
sound speed in the in-
homogeneous upper ocean.

thesF478

Statistical study of sound speed in the



3 2768 002 00208 1

DUDLEY KNOX LIBRARY